Garcia Center for Polymers at Engineered Interfaces

AT STONY BROOK UNIVERSITY

Summer 2015

"The program has no set time limits. Research is a lifelong experience and we hope to remain a resource to our students long after 'graduation'. "

The Garcia Center for Polymers at Engineered Interfaces was founded in 1996 and is named after the late Queens College professor Narciso Garcia, who was a pioneer in the integration of education and research. The Center focuses on the integration of materials research with tissue engineering, biomaterials, drug delivery systems, sustainable energy, nanocomposites, and recently, additive manufacturing. The Center also supports innovation through entrepreneurship and has multiple collaborations with industry and national laboratories, both in the US and abroad.
For information on the numerous programs that are available please see our website at:
http://polymer.matscieng.stonybrook.edu

The research scholar program offers the opportunity for high school teachers and students to perform research on the forefront of polymer science and technology together with the Garcia faculty and staff. Students work as part of focus research teams are taught to make original contributions of interest to the scientific community. In addition to entering national competitions, the students are encouraged to publish in refereed scientific journals , present their results at national conferences, and develop patents to protect their intellectual property.
Our goal is to convey to the students the excitement we enjoy daily in research and provide for them a supportive network within the scientific community. Research is a lifelong experience and we hope to remain a resource to our students long after "graduation".

Miriam Rafailovich and Jonathan Sokolov

FACULTY AND STAFF

Stephen Walker

Dennis Galanakis

Marcia Simon

Dilip Gersappe

Rebecca Isseroff

Dan Slep

Maya Endoh

Adriana Pinkas-
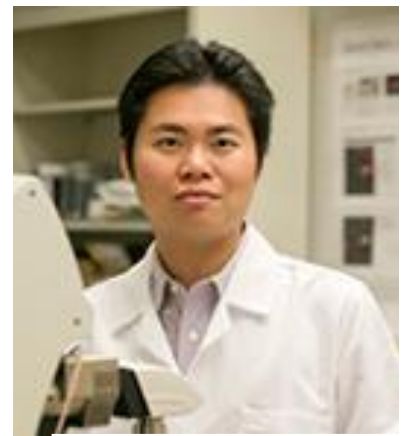
Tatsiana Mironava

Zoe Auletta

John Jerome

Ying Liu

Mengkun Liu
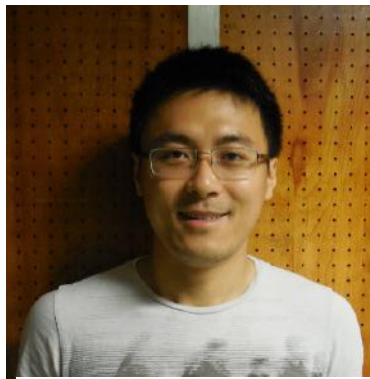

Stephen Tettelbach

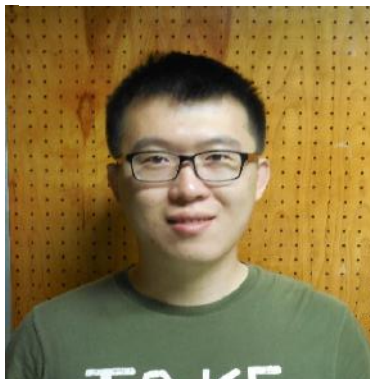Chung-Chueh (Simon) Chang

GRADUATE STUDENTS

Julia Budassi

Fan Yang

Na Hvun Cho

Yichen Guo

Kuan-che Feng

Hongfei Li

Juyi Li

Shan He

Yuan Xue

Clement Marmorat
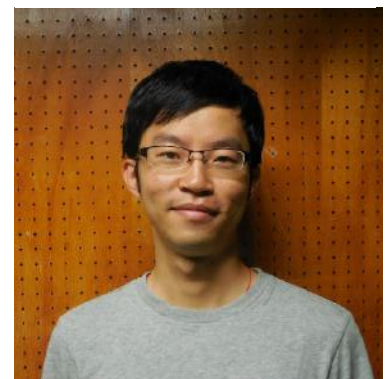
Kao Li

Yan Xu

Andrew Michaelson

Vincent Ricotta

Liudi Zhang

Jae Wha Yang

Yingjie Yu
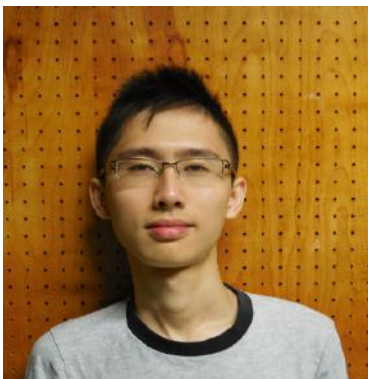
Ke Zhu
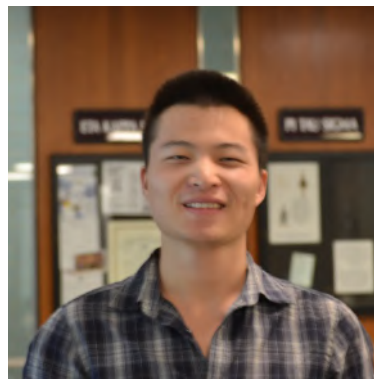
Zhenhua Yang
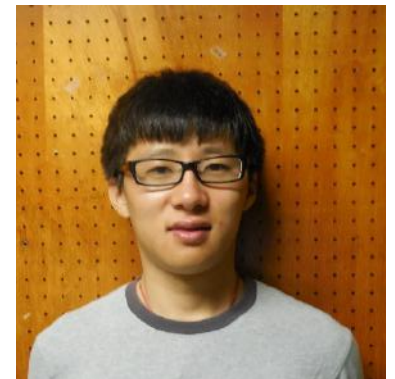
Xianghao Zuo

Research Experience for Undergraduates (REU)

Ellyn Anderson

Alyssa Auerbach

Ashley Bernstein

Veronica Burnett
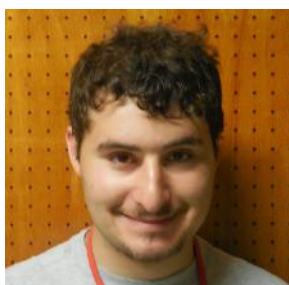
Gabriel Cecchini
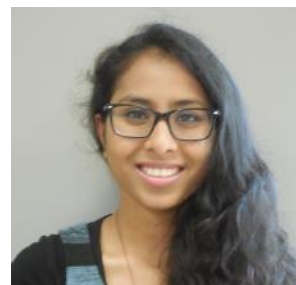
Sneha Chittababathini
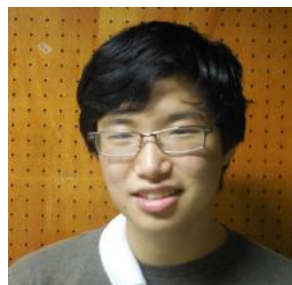
Jae Hee Cho
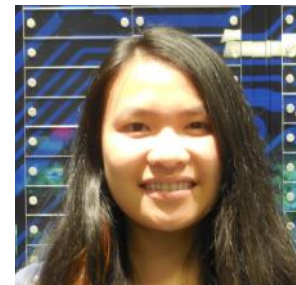
Jang Eunayo

Brianna Friedman

Aldina Goldberg

Naomi Javitt

Jaymo Kang
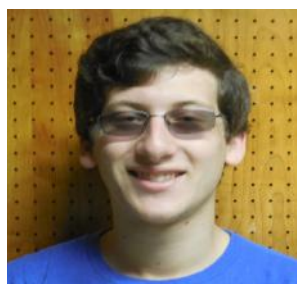
Steven Krim

Julia Landsberg
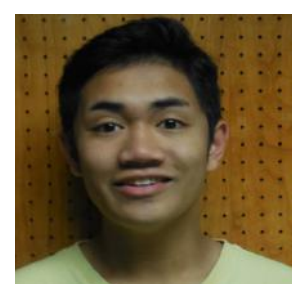
Matthew Limjoco
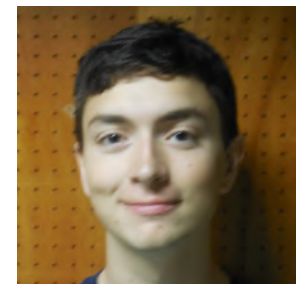
John Mele

Research Experience for Undergraduates (REU)
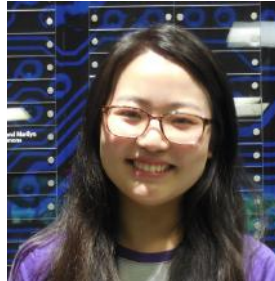
Tasnuva Moutushi   **Kim Nguyen**   **Jacob Plaut**   **Tara R. Schinasi**

Luke Shin   **Gurkirat Singh**   **Austin Wild**

Teachers (RET)

Gina Gabalski   Herb Weiss

High School Students

Jacob Abulencia

Andrew Adelhardt

Lee J. Blackburn

Sidharth Bommakanti

Daniel Chae

Arthur Chen

Eric Chen

Audrey C. Cheng

Tzippora Chwat

Dessie DiMino

Sean T. Donnelly

Robert J. Evans

David Fleschner

Justin Glickman
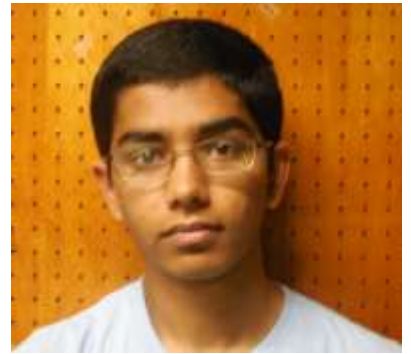
Rahul Gupta

Cameron Hanover
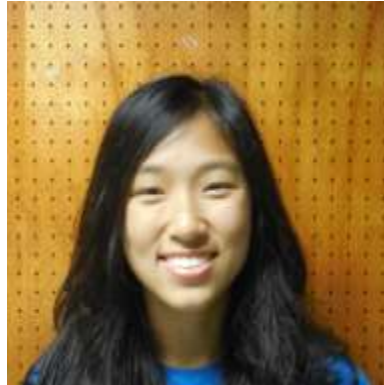
Connie He

David Herman

YingYan Ho

Jonathan J. Huang

Chiho Im

Effie W Jia
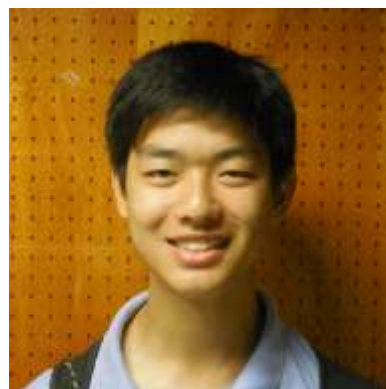
Jonathan Jow

Gabrielle Jung

Hyun Jo Kim

Amanda Klestzick

Evan Lander

Hope Lee

Maho Koga

Walt B Leung

Alexander Li
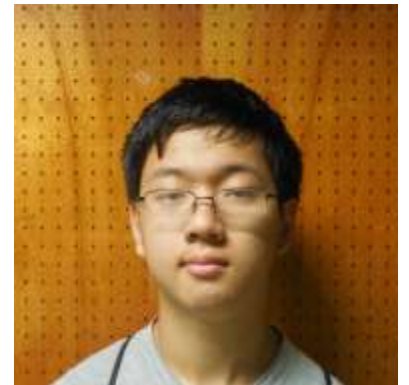
Thomas Li

Yanlin Li
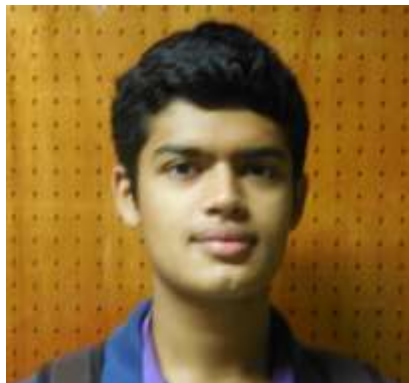
Aditya Mantri
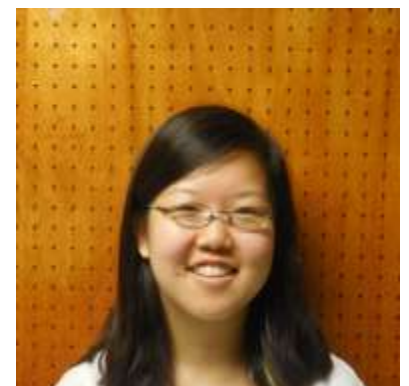
Michelle H. Mao

Bonnie H. Mendelson

Samuel J. Plaut
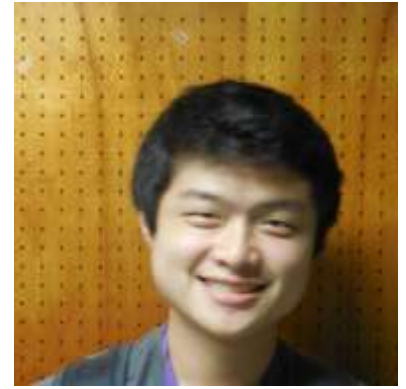
Kevin Qian

Brian Rhee

Kevin Sadhu

Samali A. Sahoo

Kunal Shah

Juliana Shenker

Jeremy Silverman

Arun Soni

Eva Spier

Arvind Sridhar

Yusha Y. Sun

Alan K. Tan
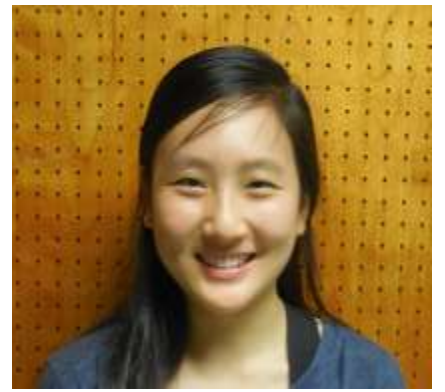
Natalie Tan

Kimberly A. Te

Andrew Z. Wang
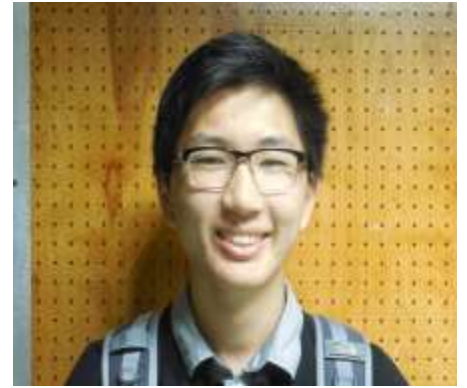
Andrew Y. Wang

Jeremy Wang

Abigail Wax

Alice Wu

Alice G. Wu

Sophia Wu

Yutong Xu
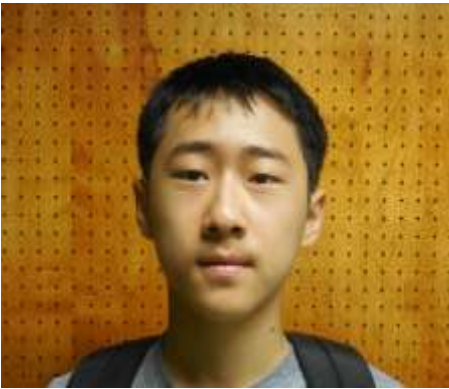
George Z. Yang

Richard Zhang

Xiaotian Zhang

Anthony Zheng

Simon X. Zhuang

Elaina Zodiatis

Andrew Zuckerman

Demian Zuric

Garcia MRSEC
Polymers at Engineered Interfaces
SUNY Stony Brook • Polytechnic University • CUNY • North Carolina State University

2015
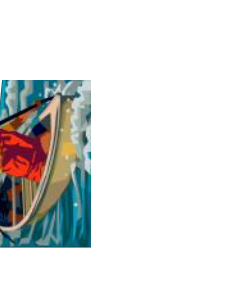
Summer Scholar Program Schedule of Activities

EVERY DAY STARTS WITH A GROUP MEETING

CHECK SCHEDULE DAILY!

	MONDAY	TUESDAY	WEDNESDAY	THURSDAY	FRIDAY
	6/29	6/30	7/1	7/2	7/3
Week of 6/29	**10:00 AM** General meeting **10:15 AM** Dr. Ann Marie Scheidt Welcome **10:30 AM** Dr. Srinivas Pentyala Dept. Anesthesiology Why do research? **11:30 AM** Dr. Dilip Gersappe Computational Design of Materials **12:30 PM** Lunch SAC **1:30 PM** Dr. Peter Brink Dept. Physiology & Biophysics, Sharks and Stem Cells **2:30** Mr. Herb Weiss Ethical Conduct in Science Research and Entering Science Competition Senior REU Meeting **3:30** Campus Facilities Tour/ Stony Brook ID Card Pictures (Bring personal ID with you)–Administration Building Lobby	**10:00AM** General meeting/Intro to Laboratory Statistics I **10:30 AM- 1:30 PM** Lab Safety Training w/ EH&S **1:30 PM** Lunch **2:00 PM** Dr. Steven Schwarz Fun puzzles, Reology, and the Physics of Thin film Processing **3:00 PM** Dr. Dennis Galanakis-Director SBU Blood Bank The science of blood **3:45 PM** Clement Marmorat The science of hydrogels **4:00 PM Mandatory training for REU and Grad student supervisors: Minor Protection Policy training**	**10:00 AM** General meeting Dr. Minkun Liu Nanolithogrphay with the AFM **10:30 AM** Library Resources and Intro to Excel Courses (2 Groups) **12:30 PM** Lunch **1:00 PM** Dr. Rina Tannenbaum Characterization with nanoscale Precision **2:00 - 4:00 PM** Facilities Tour: Hands on Safety Training /AFM, confocal, rheology, cell lab, Nanocomposites/flame retardant testing, safety demonstration with Simon (10 students per group) **4:00-6:00** (Optional) Poster Session--International Conference on Funcitonal Materials (Wang Center)	**10:00 AM** General meeting Welcome-Provost Assanis **10:15** Lab Safety Quiz **11:00 AM** Dr.**Richard Black** The Materials / Cell Interface (NYU/ Scotland) **12: 00 PM Lunch** **12:30 PM** Dr. Ping Liu Using DFT to model reactions **1; 10 PM** Dr. Dilip Gersappe Materials by Design **2:00 PM** Dr. Tatiana Mironova Nanotoxicology **2:40 PM** Dr. Jonathan Sokolov DNA research Ellipsometry: Hands on Measurements at the nanoscale.	7/3 Happy 4th of July

Week of 7/6

7/6
10:00 AM General Meeting

10:15 Nissim Garti
Engineering drug delivery vehicles

10:45 AM Dr. Allan Tannenbaum
Computational Biology for cancer Detection

11:45 AM Dr. Michael HadjiagyrouDept. Life Sciences, NYIT
Tissue Engineering~

12:30 PM Lunch

1:00 PM Dr. Stephen Tettlebach
Restoration of Peconic Scallops and Fisheries

2:00-4:00 PM Journal club presentations by students

7/7
10:00 AM General Meeting
Quizz do-over

10:30 AM Dr. Vijay Alreja
VJ Technologies
Analyzing materials with x-rays

11:30 AM Donna Tuminello
Intellectual Property

12:30 PM Lunch

1:00 PM Dr. Marcia Simon
Skin Biology and Physiology

2:00 PM Mrs. Rebecca Isseroff
The magic of graphene
Keeping a Lab Notebook
distribution of lab boxes

3:00 PM
Prof. Jon Sokolov
Experiment with coherent and incoherent light

7/8
10:00 AM General Meeting
Group Picture in Lobby

10:15 AM Spin Casting Lab

Distribution of schedules for individual groups

Students will follow schedule for each group.

Dr. Endohs lectures will be in room 143.

7/9
10:00 AM General Meeting

10:30 AM Spin Casting Lab cont.

1:30 PM   Calculations and work on reports

Preparation of results with REU and Grad students.

Two students from each group will be selected to present the results of the group this friday.

7/10
10:00 AM General meeting

Dr. Singh: Building a Blood vessel
10:15 Dr. Steven Walker: Microbiology

11:15-1:15 Reports from each of the seven groups on the results of the spin casting experiments

PIZZA Lunch–Hubkis of Plainview

2:00 Early Friday Dismissal

Bus leaves for BNL from SAC at 10 AM and returns at 2 PM.

BNL Summer Science Lab Tour On Sunday

summer sundays

Week of 7/13

7/13
10:00 AM General meeting
Dr. Sarafova: Dental Pulp Stem Cells

Selection of Projects

12:30 PM Lunch

4:00 pm **Game Night**
Softball

7/14
10:00AM General meeting

10:30-11:00 AM - **Gabor Balasz**
-
12:30 PM Lunch

7/15
10:00AM General meeting

10:15
12:30 PM Lunch

7/16
10:00AM General meeting

Field Trip

Long Island Aquarium & Exhibition Center

long island aquarium
+ butterflies, bugs & birds!

7/17
10:00AM General meeting

10:15 Dr. Marcus Abboud, DDS

Additive manufacturing in Dentistry

12:30 PM Pizza Lunch/Student presentations

2:00 PM Dismissal

Week	Mon	Tue	Wed	Thu	Fri
Week of 7/20	**7/20** **10:00 AM** General meeting **10:30 AM** WORK! **12:30 PM** Lunch	**7/21** **10:00 AM** General meeting **10:30 AM** WORK! **12:30 PM** Lunch	**7/22** **10:00 AM** General meeting **10:30 AM** WORK! **12:30 PM** Lunch	**7/23** **10:00 AM** General meeting **10:30 AM** WORK! **12:30 PM** Lunch **4:00 PM** Game Night Basketball	**7/24** **10:00 AM** General meeting **10:30 AM** WORK! **12:00 PM** Lunch
Week of 7/27	**7/27** **10:00 AM** General meeting **10:30 AM** WORK! **12:30 PM** Lunch Julia Byrd: Powerbridge	**7/28** **10:00 AM** General meeting **10:30 AM** WORK! **12:30 PM** Lunch	**7/29** **10:00 AM** General meeting **10:30 AM** WORK! **12:30 PM** Lunch	**7/30** **10:00 AM** General meeting **10:30 AM** WORK! **12:30 PM** Lunch	**7/31** **10:00 AM** General meeting **10:30 AM** WORK! **12:30 PM** Lunch BBQ
Week of 8/4	**8/3** **10:00 AM** General meeting CANOE TRIP!	**8/4** **10:00 AM** General meeting **10:30 AM** WORK! **12:30 PM** Lunch 6:30 PM Celtic Quest Fishing Trip	**8/5** **10:00 AM** General meeting **10:30 AM** WORK! **12:30 PM** Lunch	**8/6** 10: 00 AM Brooke Ellison Ethics in the STEM **10:30 AM** WORK! **12:30 PM** Lunch	**8/7** **10:00 AM** General meeting **10:30 AM** WORK! **12:30 PM** Pizza Lunch
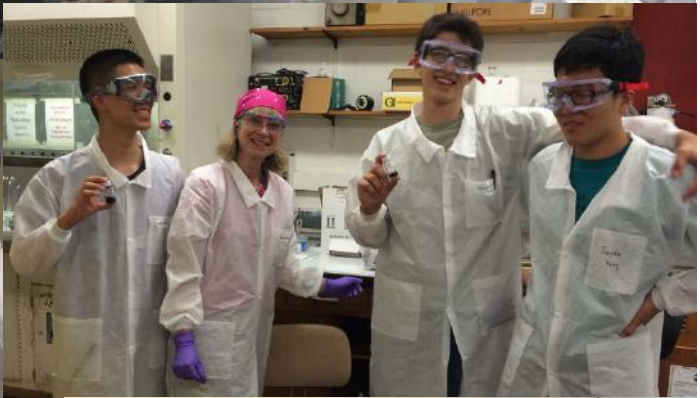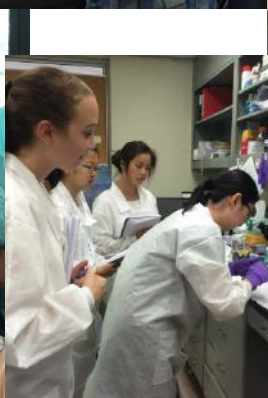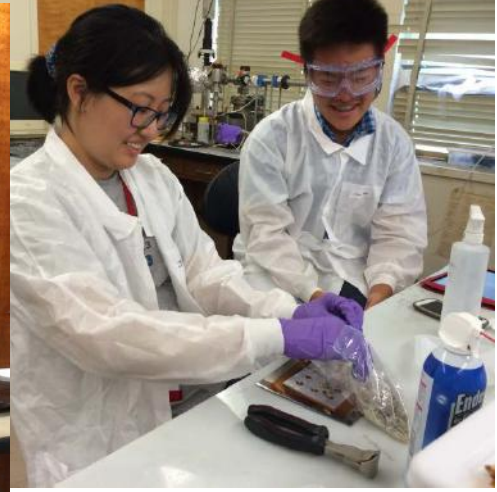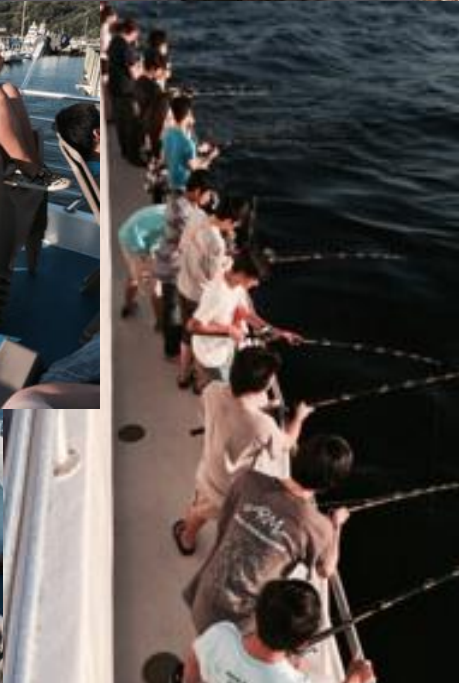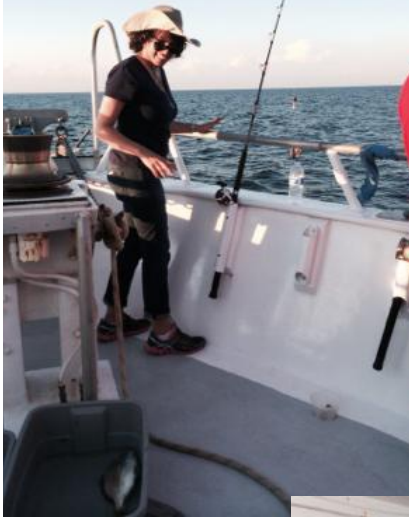
Nissequogue

Garcia Center for Polymers at Engineered Interfaces

AT STONY BROOK UNIVERSITY

The Garcia Center

Invites you to attend the

Annual Summer Symposium
of the
Research Scholars Program
On
Tuesday, August 11, 2015
at
10:00 AM - 1:00 PM
in the
Student Activities Center, Ballroom A

Introduction by: **Dr. Nadine Pernodet**

VP Skin Biology and Bioactives
Skin Biology & BioActives
R&D, ESTEE LAUDER COMPANIES

10:00 Coffee, Welcome, Student Musical Arrangements
10:15-10:25 Introduction by Dr. Pernodet
10:25-12:15 Student Presentations
12:15-1:30 Formal Luncheon (Catered by Wing Wan, W Hempstead, NY)

Garcia Center for Polymers at Engineered Interfaces

AT STONY BROOK UNIVERSITY

Symposium Program

10: 00   Coffee and Musical Arrangement: John Jerome, Julia Budassi, Students

10: 15   Introduction: **Dr. Nadine Pernodet**
              VP Skin Biology and Bioactives, R&D, ESTEE LAUDER COMPANIES

12: 30   Luncheon—*Wing Wan of West Hempstead*

I .Hydrogen Fuel Cell

Ashley Bernstein, Gurkirat Singh, Tasnuva Moutushi Stony Brook University
Gabriel Cecchini Rennsalear Polytechnic Institute

Gold-Alloy-Nanoparticles-Enhanced proton exchange membrane hydrogen fuel cell
Yanlin (Lydia) Li, The Hockaday School, 11600 Welch Road, Dallas, Texas

The effect of asymmetrically coated Nafion membrane faces on proton exchange membrane fuel cells' anode and cathode reactions
Richard Zhang, Redmond High School, Redmond, WA

Optimizing Microbial Fuel Cell Performance through a Single-Chamber Design and Macroporous Anodes
Kimberly Te, Manhasset High School, Manhasset, NY

Use of Varying Alloys of Gold in PEM Fuel Cells
Alex Rock South Side High School, Rockville Centre, NY

Incorporation of Platinum-Graphene Catalysts in Polymer Electrolyte Membrane Fuel Cell Electrodes for Increased Carbon Monoxide Tolerance
Lee Blackburn, Lawrence High School, Cedarhurst, NY

The Investigation of the Effects of Graphene Oxide on the Nafion Membrane in Polymer Electrolyte Membrane Fuel Cells
Roshan Patel Ward Melville High School, East Setauket, NY, **Brian Rhee** Half Hollow Hills High School East, Dix Hills, NY, **Kunal Shah** Syosset High School, Syosset, NY

Analyzing the Effects of Gold Nanoparticles Coated on Various Nafion Membranes for Improved Performance through the Catalysis of Carbon Monoxide Oxidation
David Herman Davis Renov Stahler Yeshiva High School For Boys, 700 Ibsen Street, Woodmere, NY, **Kevin Qian** Wayzata Senior High School, 4955 Peony Ln N, Plymouth, MN

Synthesis, Characterization, and Application of Noble Metal Alloy Nanoparticles
Xiaotian Zhang, Arun Soni Staples High School, 70 North Ave. Westport CT.

II. Organic Photovoltaics

Jaymo Kang, University of California, Berkeley

The Effects of PMMA and Graphene on P3HT/ PCBM Bulk Heterojunction Organic Solar Cells
Hope Lee, Woodbridge High School, Irvine, California

The Implementation of Polystyrene and Graphene in the Active Layer of PCDTBT:PCBM
Inverted Organic Solar Cells to Increase Energy Conversion Efficiency
Andrew Wang, Nikola Tesla Science, Technology, Engineering, and Mathematics (STEM) High School
Redmond, Washington
Effie Jia, Dougherty Valley High School, San Ramon, California

Integration of Multiple Donors and Graphene into SelfAssembled Organic Solar Cells to Increase Power
Conversion Efficiency
Audrey Cheng , Henry M. Gunn High School, Palo Alto, CA

Constructing Ordered Heterojunction Organic Solar Cells Using Selective Solvents to Improve
Morphology and Efficiency
Alexander Li Saratoga High School, Saratoga, CA
Alice Wu The Harker School, San Jose, CA

III. Dental Pulp Stem Cells

John Mele, Stony Brook University, Stony Brook, NY ;**Naomi Javitt** University of Maryland, MD
Adina Goldberg, City University of New York, NY; **Austin Wild,** Villanova University, Villanova, PA

The Effects of TiO2 Nanoparticles and LED Lights on Dental Pulp Stem Cells
Tzippora Chwat, Yeshiva University High School for Girls, Hollis, NY

The Role of Static Magnetic Fields on Biomineralization of Dental Pulp Derived Cells on Sulfonated
Polystyrene Films
Elaina Zodiatis Smithtown High School East, St. James, NY

The Effect of Surface Topography of 3D Printed PLA Scaffolds on Dental
Pulp Stem Cell Proliferation and Differentiation *in vitro*
Daniel Chae Thomas Jefferson High School for Science and Technology, Alexandria, VA
Sidharth Bommakanti Amador Valley High School, Pleasanton, CA
 Alan Tan Irvington High School, Fremont, CA

Effects of Topography and Composition of Electrospun P4VP Polymer Fiber on its Biocompatibility with
Dental Pulp Stem Cells
Amanda Klestzick, Sar High School Bronx, NY
Kevin Sadhu, Manhasset High School, Manhasset, NY
David Fleschner, HAFTR High School, Lawrence, NY

The Effect of LED Lights on Dental Pulp Stem Cells Plated on P3HT
Eva Spier SAR High School, Riverdale, NY

IV. Thrombosis and Angiogenesis
Sneha Chittabathini, Veronica Burnett Stony Brook University

Effect of Various Polymers on Endothelial Cell Adherence to Fibrinogen Coated Surfaces
Abigail Wax Harborfields High School, Greenlawn, NY
Juliana Shenker, Southside High School, Rockville Center, NY

An Investigation of the Interaction of Whole Plasma with Hydrophilic and Hydrophobic Surfaces
Michelle Mao Woodbury High School, 2665 Woodlane Drive, Woodbury, MN
Sophia Wu Lowell High School, 1101 Eucalyptus Drive, San Francisco, CA

Engineering A Blood Vessel Using Cultured Human Umbilical Vein Endothelial Cells And
Polydimethylsiloxane Substrates
Jacob Abulencia Half Hollow Hills High School West, Dix Hills
Bonnie Mendelson Yeshiva University High School for Girls, Holliswood, NY

V. Environmental Sustainability
Ginna Gabalski East Meadow HS **Jake Plaut** SUNY Binghamton

Determining the Properties of Polystyrene Fibers in Application to Prototyping Traps for the Common
Bedbug (*Cimex lectularius*)
YingYan Ho Texas Academy of Mathematics and Science, Denton, TX

Determining Optimal Concentration and Pigment Combinations for a Cream Which Can Physically
Impede the Feeding Mechanisms of Mosquitoes
Connie He, **Gabrielle Jung**, Half Hollow Hills High School West, Dix Hills, NY

Analysis of Peconic Bay Scallops
Cameron Hanover, Shawnee High School, 3333 Zurmehly Rd. Lima, Ohio

VI. Therapeutic Drugs and their Delivery
Jae Hee Cho, University of Texas at Austin and   **Heesu Shin** Cornell University

The Effect of a Fibronectin Derived Peptide on the Moduli and Migration of Dermal Fibroblasts
Samali Sahoo, The Harker School, San Jose, CA

Synthesis and Characterization of Food-Grade Microemulsions with Enhanced Bioavailability for
Nutraceutical and Drug Delivery Applications
Rahul Gupta Amador Valley HS, Pleasanton, CA,

Characterization of Graphene and its Derivatives Functionalized with Metal Nanoparticles on Bacteria
and Keratinocytes
Arthur Chen Lawrence High School, Cedarhurst, NY

VII. Nanocomposites
Tara Schinasi, Stony Brook University

Mechanical and Chemical Properties of Flame Retardant Biodegradable Nanocomposites
Thomas Li High Technology High School, Lincroft NJ
Aditya Mantri Columbus North High School, Columbus, IN

Engineering and characterization of novel, non-halogen, flame-retardant, biodegradable nanocomposites
Simon Zhuang, Dublin Jerome High School, Dublin, OH
Robert Evans, Division Avenue High School, Levittown, NY

 Gas Permeability of HDPE and LDPE Nanocomposites
Justin Glickman HAFTR High School, Cedarhurst, NY
Sam Plaut Rambam Mesivta High School, Lawrence, NY

Compatibilization of Immiscible Polymer Blends Using Graphene
Evan Lander Plainview-Old Bethpage John F. Kennedy High School, Plainview, NY

VIII. Nanotoxicology
Briana Friedman, Stern College Branch of Yeshiva University

Toxicology of RDP-mixed Polymers on Human Dermal Fibroblast Cells
Walt Leung Piedmont Hills High School, San Jose, CA

Cytotoxic Effects of TiO_2 Nanoparticle Exposure on Adipose-derived Stromal Cell Susceptibility to Bacterial Infection
Oliver Xu Edina High School, 6754 Valley View Road, MN 55439
Natalie P. Tan, Herricks High School, 100 Shelter Rock Road, New Hyde Park, NY 11040
Jeremy Silverman South Side High School, 140 Shepherd Street, NY

Effect of cell donor age on the cellular response to nanoparticle exposure
Hyun Jo Kim St. Paul's School, 325 Pleasant Street Concord, New Hampshire 03301
Andrew Adelhardt Paul D. Schreiber High School, 101 Campus Drive, Port Washington, New York

IX. DNA
Alyssa Auerbach, Stern College for Women at Yeshiva University **Won Park**, Stony Brook University

Novel DNA Sequencing: Comparison of 4 types of NEB buffers to desorb DNA molecules from PMMA surfaces
George Yang, BASIS Scottsdale High School[1], Scottsdale, AZ

Synthesis of an Ideal Silane Surface for DNA Adsorption and Desorption
Sean Donnelly, South Side High School

Combing and Removing DNA from Coated Silicon Wafers.
Demian Zuric, Ward Melville High School, East Setauket NY

X. Computational Analysis
Julia Landsberg, Queens College

Computer-Aided Diagnosis of Breast Lesions from Ultrasound Images
Andrew Zuckerman, The Wheatley School, Old Westbury, NY
Alice Wu, Half Hollow Hills West, Dix Hills, NY

Lattice Boltzmann Modeling of Coupled Diffusion in Transdermal Drug Delivery
Jonathan Jow, Phillips Academy, Andover, MA

Molecular Dynamics Simulations of Hydrogels in Drug Delivery
Jonathan Huang, University High School, Irvine, CA
Andrew Wang, Taipei American School, Taipei, Taiwan

XI. Hydrogels
Steve Krim, Stony Brook University
Ellyn Anderson, NYU- Poly

Synthesis and Analysis of Novel, Biocompatible, and Biomimetic Nano Graphene Oxide doped Cross-Linked Hydrogels for Drug Delivery in Squamous Carcinoma
Arvind Sridhar, Bellarmine College Preparatory, San Jose, CA

Optimization of Fluorescent Gelatin-based Hydrogels for Analysis of Fibroblast Cell Migration and Cell Traction Forces
Maho Koga, Ward Melville High School, East Setauket NY

3D Printed Hyaluronic Acid Scaffolds
Dessie DiMino, Garden City High School Garden City, NY

XII. Sensors
Matthew Limjoco Cornell University

Design Of Molecularly-Imprinted Potentiometric Sensors For Early Blood-Based Detection Of Fibrosis
Yusha Sun A&M Consolidated High School , College Station, TX
Chiho Im Choate Rosemary Hall, Wallingford, CT

Fabrication and Optimization of a Potentiometric Biosensor via pH and Concentration Analysis for the Detection of Hemoglobin
Anthony Zheng, Westview High School, OR
Jeremy Wang, Syosset High School, NY

Surface Characterization and Engineering of Materials with Electronic Phase Transitions.
Eric Chen, Aragon High School, San Mateo, CA
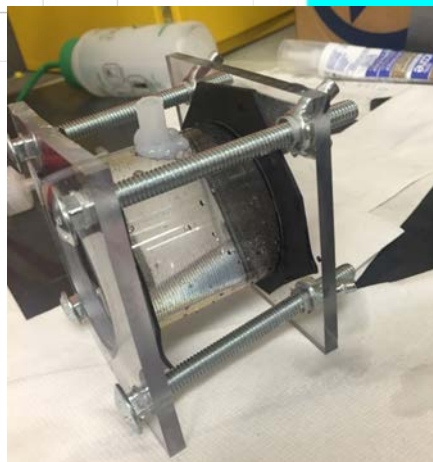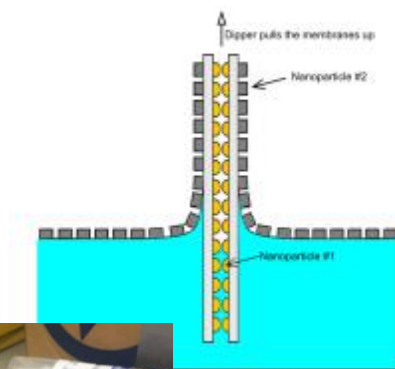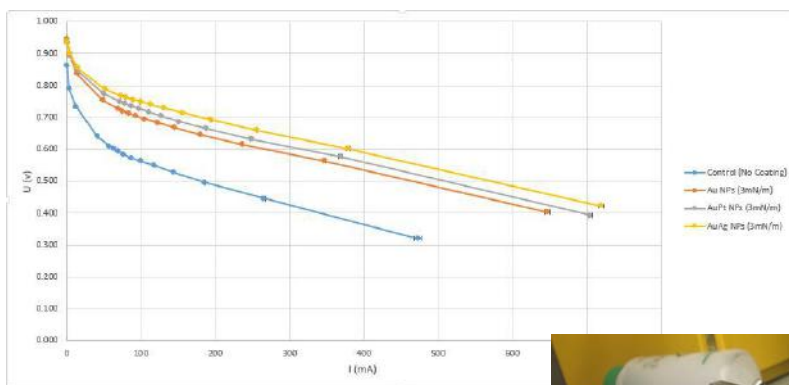**Aditya Cowsik,** Clayton High School, Clayton, Mo

Session 1   Hydrogen Fuel Cells

Hong Fei Li: Graduate Supervisor

Ashley Bernstein, Gurkirat Singh, Tasnuva Moutushi
Stony Brook University
Gabriel Cecchini Rennsalear Polytechnic Institute

Gold-Alloy-Nanoparticles-Enhanced Proton Exchange Membrane Hydrogen Fuel Cell

Author: Yanlin (Lydia) Li[*]; Mentors: Hongfei Li[#], Miriam H. Rafailovich[#]
[*]The Hockaday School, 11600 Welch Road, Dallas, Texas 75229; [#]Department of Materials Science and Engineering, State University of New York at Stony Brook, Stony Brook, New York 11794

Proton exchange membrane hydrogen fuel cells are an attractive source of green, renewable energy, but their low power output efficiency caused by CO poisoning has hindered their commercial application.[1] Platinum loaded on the electrodes catalyzes the decomposition of hydrogen gas into protons and electrons at the cathode. A Nafion membrane between the electrodes allows protons to pass to the cathode, while the electrons produce a current by going through an external wire to the cathode, where protons and electrons combine with oxygen to form water. CO gas, which is often the impurity contained in industrially produced hydrogen and can also be produced within the fuel cell through the reverse water-gas shift reaction, builds up around the Pt catalyst and reduces the current, therefore lowering fuel cell performance.[2, 3] Motivated by results from previous studies showing that gold nanoparticles exhibited high catalytic activity for CO oxidation, we investigated the effects of gold-alloy nanoparticles on the efficiency of PEM hydrogen fuel cells in this experiment.[4, 5]

Hydrophobic, thiol-functionalized gold nanoparticles, gold-silver nanoparticles, and gold-platinum nanoparticles were synthesized through the Brust Method.[6] We used a Langmuir–Blodgett trough to deposit the aforementioned nanoparticles onto Nafion membranes at various target pressures. We put each of the gold-alloy coated Nafion membranes into a single-stack fuel cell kit and tested its performance, recording the corresponding voltage and current produced and calculated the power at fifteen different resistances.

The highest power output for all types of gold-alloy NPs was observed at the target pressure of 3mN/m and hydrogen gas flow rate of 80ccm (25℃, 1 atm). From Figure 1 (a), we can see that the presence of AuAg and AuPt nanoparticles improved the fuel cell performance. As shown by Figure 1 (b), AuAg-coated membrane increased the maximum power by 93.2% over the uncoated membrane and by 16.3% over the membrane coated with pure gold; AuPt-coated membrane increased the maximum power by 80.5% over the uncoated membrane and by 8.67% over the membrane coated with pure gold. Similar results were observed when the cathode was connected to pure oxygen. Therefore, gold-alloy NPs are very effective (more so than pure-gold NPs) in increasing PEM fuel cell efficiency.
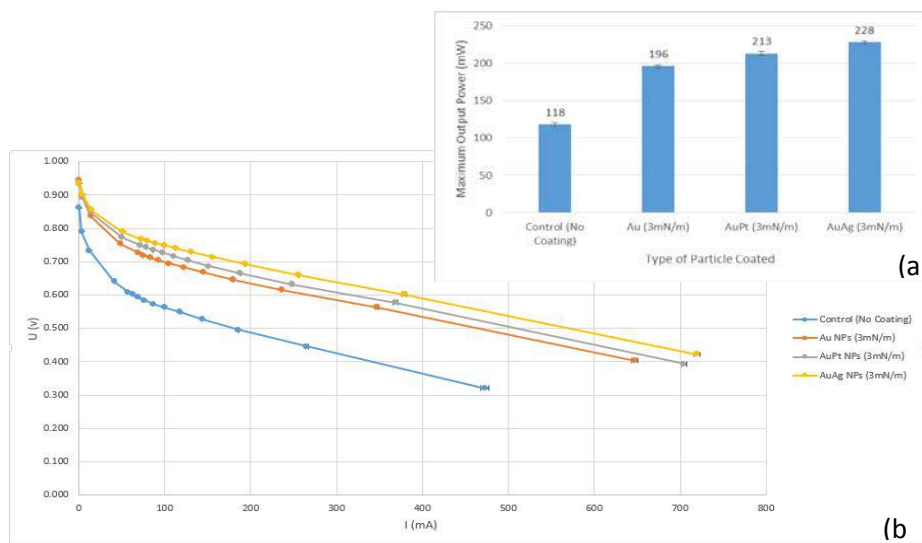
Figure 1. (a) Performance comparison for PEMFCs using AuAg, AuPt, Au, and uncoated membranes, under hydrogen flow rate of 80 ccm and cathode free air. (b) Maximum output power comparison.

We hypothesize that this increase is caused by a process similar to those previously studied by Green et al and by Li et al: the activation energy of CO oxidation through the water-gas shift reaction is significantly lowered at gold-alloy nanoparticle monolayer perimeter sites attached to the Nafion membrane.[1, 5] A beneficial future study is perform density functional theory calculations to understand the reaction mechanism.

References:

1. Li, H.; Pan, C.; Zhao, S.; Liu, P.; Zhu, Y.; Rafailovich, M. H. Gold nanoparticles-enhanced proton exchange membrane (PEM) fuel cell. Submitted to *Proc. Natl. Acad. Sci. U.S.A.*
2. Janssens, Ton V. W., et al. Insights into the reactivity of supported Au nanoparticles: combining theory and experiments. *Top Catal.* 2007, *44*(1-2), 15-26.
3. Kreur, K. D. On the development of proton conducting polymer membranes for hydrogen and methanol fuel cells. *J. Membrane Sci.* 2001, *185*, 29-39.
4. Haruta, M. Gold as a novel catalyst in the 21st century: preparation, working mechanism and applications. *Gold Bull.* 2004, *37*(1-2), 27-36.
5. Green, I. X.; Tang, W.; Neurock, M.; Yates, J. T., Jr. Insights into Catalytic Oxidation at the Au/TiO₂ Dual Perimeter Sites. *Acc. Chem. Res.* 2014, *47*(3), 805-815.
6. Brust, M.; Walker, M.; Bethell, D.; Schiffrin, D. J.; Whyman, R. Synthesis of thiol-derivatised gold nanoparticles in a two-phase liquid-liquid system. *J. Chem. Soc., Chem. Commun.* 1994, 801-802.

The effect of asymmetrically coated Nafion membrane faces on proton exchange membrane fuel cells' anode and cathode reactions

Richard Zhang, Redmond High School, Redmond, WA
HongFei Li, Stony Brook University, Stony Brook, NY
Dr. Miriam Rafailovich, Stony Brook University, Stony Brook, NY

Effective clean energy alternatives to petroleum and coal-based fuels are becoming more and more important to research and develop. One such alternative is hydrogen fuel cell technology. A longstanding and highly promising type of hydrogen fuel cell is the proton exchange membrane fuel cell (PEMFC), where a polymer membrane (PEM) fulfils the purpose of an electrolyte, transporting protons from the anode to the cathode while blocking gas permeation. The specific membrane ubiquitous as a PEM is known as Nafion®, a sulfonated Teflon®. Previous research has shown that coating the Nafion membrane with monolayers of certain nanoparticles, such as gold alloys, boosts the efficiency and power output of PEMFCs. It is hypothesized that these nanoparticles help prevent gas poisoning from carbon monoxide, and may also catalyze the anode and cathode oxidization reactions[2]. However, most previous research has coated both the anode and cathode-facing sides of the membrane with the same nanoparticle. This makes it impossible to compare the different effects of one nanoparticle or another on the separate cathode and anode reactions. Differentiating the Nafion coating on the anode and cathode sides by coating asymmetrically will reveal more specifics about the cathode and anode reactions.

The goal of this research is to see if asymmetrically coated Nafion membranes with different nanoparticle coatings each side have distinguishable effects on the anode and cathode reactions of the fuel cell. This demands a significantly different approach for preparing the membranes. Usually, Nafion membranes are coated symmetrically with a single nanoparticle using a Langmuir Blodgett Trough (L-B) with a simple procedure. The membrane is dipped into the L-B, the nanoparticle is spread across the surface of the L-B and held at a target surface pressure, and the membrane is slowly lifted out of the L-B, thus coating it with the nanoparticle at the target pressure. On the other hand, to coat only one side, two membranes are placed together with no gap in between and dipped into the L-B. The nanoparticle is spread and the membranes are lifted the same way a single membrane is lifted, effectively resulting in two membranes each coated on only one side. To coat asymmetrically, the L-B trough is reset and the two single-sided membranes are then flipped so that now the uncoated sides are facing outwards and the coated sides are facing inwards. A second nanoparticle is spread and the membranes are lifted again, finally ending up with two membranes that are both asymmetrically coated (Figure 1).
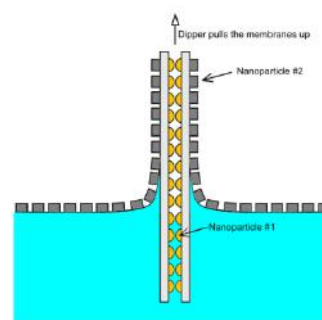
Figure 1: Diagram of Asymmetrical Coating with the L-B Trough

Four single sided membranes and two asymmetrically coated membranes were coated and tested, each with 80ccm pure H_2 flow on the anode side and air flow on the cathode end. These six include two Nafion 117 membranes coated single-side with AuNPs at 3mN/m and AuPdNPs at 5mN/m, two Nafion 115 membranes with the same single side coating, and a Nafion 117 and Nafion 115 asymmetrically coated with AuNPs at 3mN/m and AuPdNPs at 5mN/m. The target surface pressures of 3mN/m and 5mN/m for AuNPs and AuPdNPs, respectively, were selected after those nanoparticles were analyzed using the L-B's Isotherm curve test, to find the correct surface pressure to reach monolayers of Au and AuPd.
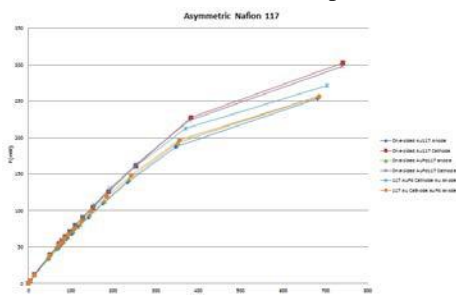
Figure 2: Graph of Results

Each of the six membranes was tested twice within a single stack fuel cell to show distinct effects of the nanoparticles at the cathode and anode ends alone. The single-sided coatings served as controls, and showed that the nanoparticles performed significantly better at the cathode ends than the anode ends, suggesting that they may somehow purify free air or positively catalyze the cathode reaction more than the anode reaction. The asymmetrically coated membranes' performance fell in between that of the single-sided ones, suggesting that two nanoparticle coatings may hinder rather than compound each other's catalysis on the cathode and anode ends if applied simultaneously (Figure 2). Further research could explore oxidization, additional membranes, and additional asymmetric coating combinations.

_____

[1]Jalani, N.H. (2006). Development of Nanocomposite Polymer Electrolyte Membranes for Higher Temperature PEM Fuel Cells (Doctoral dissertation). Retrieved from Worcester Polytechnic Institute Publications.
[2] Green, I., Tang, W., Neurock, M., Yates, J. T. Jr. (2013). Insights into Catalytic Oxidization at the Au/TiO_2 Dual Perimeter Sites. Accounts of Chemical Research 2014; 47 (3): 805-815.

Optimizing Microbial Fuel Cell Performance through a Single-Chamber Design and Macroporous Anodes

Kimberly Te[1], Gurkirat Singh[2], Dr. John Jerome[3], Dr. Miriam Rafailovich[4]

1) Manhasset High School, Manhasset, NY 11030 2) Stony Brook University-SUNY, Stony Brook, 11794 3) Department of Mathematics, Suffolk Community College, Selden, NY 11784 4) Department of Materials Science and Engineering, Stony Brook University, Stony Brook, NY 11794

Increasing fossil fuel consumption and its resulting greenhouse gas emissions cause a need for a clean renewable energy source. Microbial fuel cells (MFCs) offer a solution to this energy and environmental issue. MFCs are a bioelectrochemical technology that produces energy through the reduction-oxidation reactions of organic matter, such as wastewater, via microbes as catalysts. In addition to energy production, MFCs can be simultaneously used for remediation due to the microbial oxidation of the fuel source. Studies show MFCs can facilitate wastewater treatment, oil spill cleanup, and organic pollutant remediation. However, MFCs are not ready for commercial applications due to relatively low power density and high-cost materials. Therefore, the purpose of this study was to develop a cost-effective and electrically efficient MFC through the use of a single-chamber design and anodic modifications.

Traditional MFCs employ a two-chamber design with a proton exchange membrane (PEM) separating the anode and cathode compartments. Issues with traditional MFCs include the need to regularly replace the electron acceptor and insufficient reoxidation by oxygen. By using a single-chamber air cathode design, oxygen in the air provides an abundant and passive electron acceptor. In this study, the MFC was constructed from polycarbonate to create a cylindrical chamber. Air cathodes were prepared with a carbon base layer, 4 polytetrafluoroethylane diffusion layers, and a Pt/C catalyst layer, and had one side exposed to air for passive oxygen transfer. Anodes were submerged in the anodic solution (Luria Broth, anaerobic bacteria from Manhasset Bay, and Phosphate Buffer). This design provided a more compact and economical MFC.

Functioning as the site for microbial interactions, the anode must be conductive, biocompatible, and chemically stable in its solution. In this study, it was hypothesized that increased surface area would improve MFC electrical performance. Different anodes were prepared based on modifications of material, porosity, and coating. Uncoated carbon cloth, a microporous material, functioned as the control. Polyurethane foam and carbonized loofah sponges were prepared to have macropores ($>\mu$m) and sputtered with gold. Cyclic voltammetry, scanning electron microscopy, Raman spectroscopy, and X-ray photon spectroscopy will be collected to assess electrical performance, biofilm growth, and properties on the anode.
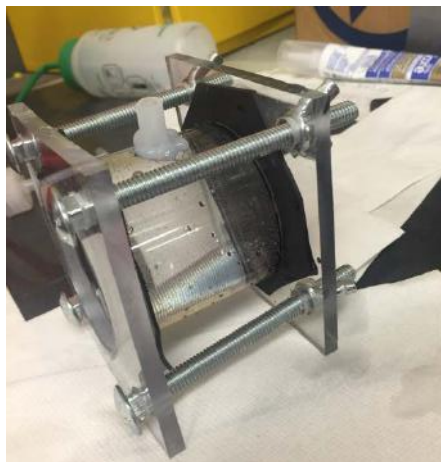
Figure 1: Image of single-chamber air cathode MFC (Taken by author).

References:
1) Xie, Xing. "Graphene-Sponges as High-Performance Low-Cost Anodes for Microbial Fuel Cells." *Energy & Environmental Science* (2012): n. pag. The Royal Society of Chemistry, 2012. Web.
2) Yuan, Yong. "Nanostructured Macroporous Bioanode Based on PolyanilineModified Natural Loofah Sponge for High-Performance Microbial Fuel Cells." *Environmental Science and Technology*. Guangdong Institute of Eco-environmental and Soil Sciences, 2013. Web. <pubs.acs.org/est>.

Use of Varying Alloys of Gold in PEM Fuel Cells

Alex Rock South Side High School, Rockville Centre, NY, 11570

   The purpose of this project was to explore the usefulness of PEM fuel cells. PEM, or proton exchange membrane cells, use a Nafion membrane to catalyze the reactions between hydrogen and oxygen. A fuel cell consists of an anode, an electrode, a membrane, another electrode, and a cathode. Hydrogen gas is poured into the anode, and this gas is ionized and separated into a proton and an electron. These ions travel across the membrane and react with oxygen, and form water as a byproduct. When the ions and oxygen bond to form water, chemical energy is released. This chemical energy is transformed into electrical energy and harvested by the cell. However, in this reaction, carbon monoxide is released as a byproduct. This carbon monoxide poisons the membrane, significantly impacting its effectiveness. Herein lies the purpose of our research. By coating the Nafion membrane with alloys of gold such as gold-silver, we aimed to decrease poisoning and increase efficiency of the cell. These alloys act as catalysts, and speed up the reactions of the ions and decrease waste.

   We tested Nafion membranes coated with varying alloys of gold. We used Gold-Silver, Gold-Platinum, and Gold Palladium. These alloys were coated onto the membrane to increase efficiency in the cell. In order to
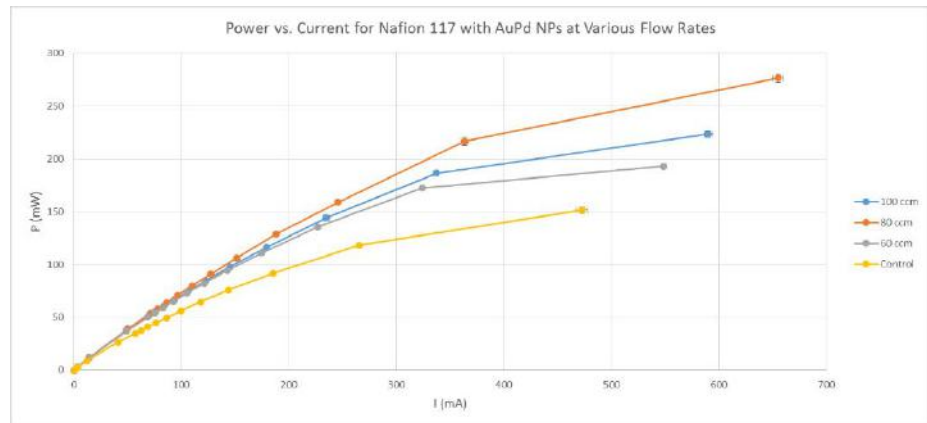
Figure 1: Power v current graph comparing the output of the control and the AuPd membrane.

coat the membrane, we used a Langmuir Blodgett trough. This machine uses clean deionized water When a PEM fuel cell operates, it produces CO as waste. This waste poisons the cell and decreases efficiency. We found that the Gold-Silver membrane was the most efficient. We tested the cell by using a voltmeter and ammeter, and calculated the power using the statistics we obtained. We measured the different powers at increasing resistances. As seen in figure 1, the optimal AuPd coated membrane was approximately twice as effective as the control. The various three different lines for the AuPd represent different flow rates of Hydrogen gas, which is the amount of gas supplied to the fuel cell. A flow rate of 80 ccm was the most efficient. The highest flow rate did not produce the highest power output. The Gold-Silver had the highest power output of all the membranes, which leads to the conclusion that this alloy provided the strongest protection against CO poisoning.

1. Loyselle, Patricia; Prokopius, Kevin. "Teledyne Energy Systems, Inc., Proton Exchange Member (PEM) Fuel Cell Engineering Model Powerplant. Test Report: Initial Benchmark Tests in the Original Orientation". *NASA*. Glenn Research Center. Retrieved15 September 2011.

2. [Millington, Ben, Shangfeng Du, and Bruno G. Pollet. "The Effect of Materials on Proton Exchange Membrane Fuel Cell Electrode Performance." Journal of Power Sources 196.21 (2011): 9013-017. Web.].

Incorporation of Platinum-Graphene Catalysts in Polymer Electrolyte Membrane Fuel Cell Electrodes for Increased Carbon Monoxide Tolerance

Lee Blackburn[1], Jaymo Kang[2], Rebecca Isseroff[1], Hongfei Li[3], Molly Gentleman[3,] Miriam Rafailovich[3]

[1]Lawrence High School, Cedarhurst, NY 11516
[2]University of California - Berkeley, Berkeley, CA 94720
[3]SUNY Stony Brook Department of Materials Science and Engineering, Stony Brook, NY 11794

There is a rapidly increasing demand for clean, renewable and efficient sources of energy due to the diminishing supply and availability of fossil fuels. More significantly, carbon dioxide emissions from burning fossil fuels and non-renewable fossil fuels are contributing to the rise in average global temperature. A viable energy alternative could possibly be the polymer electrolyte membrane fuel cell (PEMFC). PEMFCs generally utilize the oxidation of pure H_2 gas to create electrical energy. PEMFCs could replace fossil fuels but exposure to carbon monoxide (CO) poisons its platinum (Pt) catalyst, reducing efficiency. In the past, platinum-ruthenium (PtRu) has been used as an alternative catalyst with higher CO tolerance, a similar mechanism is hypothesized to occur in Pt-Graphene. This project hypothesized that metal-functionalized partially reduced graphene oxide (prGO) catalysts would have much greater oxidation properties compared to platinum catalysts. The increased CO tolerance could be due to the rate-determining step being the diffusion of CO onto the catalyst surface as opposed to the reaction of oxygen with the graphene surface.

Graphene oxide (GO) was produced from powdered graphite through a modified Hummer's Oxidation. GO was then functionalized with different concentrations of platinum nanoparticles--.10mM, .15mM, and .20mM--derived from Potassium tetrachloroplatinate(II) (K_2PtCl_4), producing Pt-GO. Partial reduction with 10mM NaBH4 produced Pt-prGO in solution. Raman spectroscopy confirmed the functionalization and partial reduction of the Pt-prGO compared to other metalized
and non-metalized graphene samples (Fig. 1)

To apply the Pt-prGO solution onto the electrodes, a spray bottle was used to disperse a homogenous distribution of catalyst onto the electrode surface. However, as the original electrode (carbon cloth) was extremely hydrophobic, carbon cloth was exposed to UV-Ozone for 10 minutes and then soaked in ethanol for 5 minutes so that the Pt-prGO solution would adhere more readily to the electrode. After drying for 30 minutes, a homogenous layer of catalyst was procured on top of the electrode (Fig. 2).

In the future, we plan to test the fuel cell at 80°C, the operating temperature of the fuel cell. We also plan to use cyclic voltammetry to test the potential of the electrode. An AuPt-prGO electrode will also be tested.
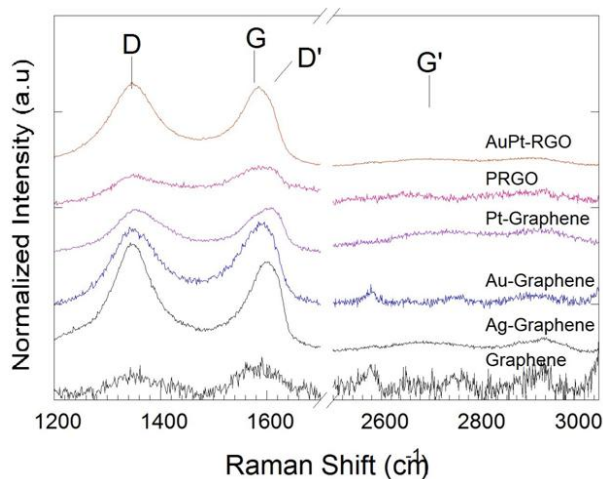
Fig. 1: Raman spectra of different graphene samples

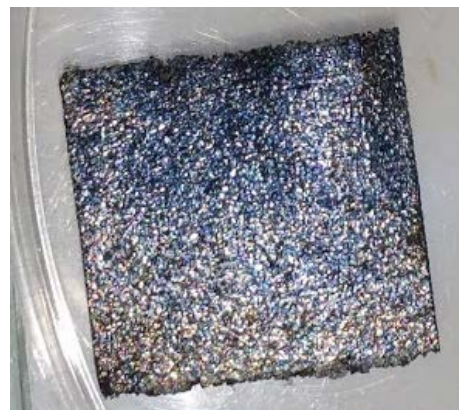**Fig. 2:** Homogenous dispersion of dried catalyst on a UV-Ozone + ethanol treated electrode.

Zhou, Yi-Ge, Jing-Jing Chen, Feng-bin Wang, Zhen-Huan Sheng, and Xing-Hua Shia. "A Facile Approach to the Synthesis of Highly Electroactive Pt Nanoparticles on Graphene as an Anode Catalyst for Direct Methanol Fuel Cells." Chemical Communications (2010): n. pag. Royal Society of Chemistry, 05 July 2010.

The Investigation of the Effects of Graphene Oxide on the Nafion Membrane in Polymer Electrolyte Membrane Fuel Cells

Roshan Patel (Ward Melville High School, East Setauket, NY)

Brian Rhee (Half Hollow Hills High School East, Dix Hills, NY)

Kunal Shah (Syosset High School, Syosset, NY)

Ashley Bernstein (Stony Brook University, Stony Brook, NY) , **Gabriel Cecchini** (Rensselaer Polytechnic Institute, Troy, NY), **Tasnuva Moutushi** (Stony Brook University, Stony Brook, NY)

Hongfei Li, Miriam Rafailovich (Dept. of Materials Sciences, Stony Brook University, NY)

Polymer electrolyte membrane fuel cells (PEMFC) provide a promising source of alternative energy on the industrial and private level[1]. Nonetheless, the full scale utilization of the PEMFC is limited by its production expense and inefficient power output. A major setback to the PEMFC's efficien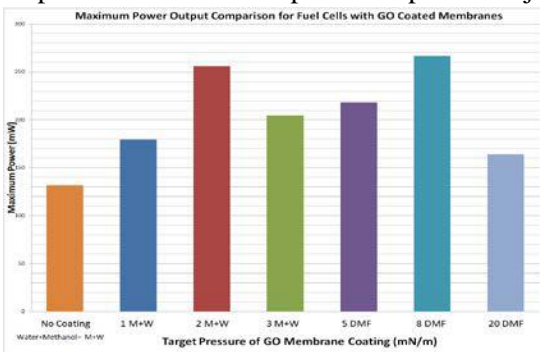cy is the poisoning of the catalysts that are located on the electrodes[2]. Recently, Graphene Oxide (GO), with its fortuitous functional groups, has shown potential in increasing the self humidification and proton conductivity of the Nafion membrane, the standard polymer electrolyte used in PEMFC. However, the effect of its presence on the surface of the Nafion membrane is unknown and requires further investigation. The purpose of this study is to ascertain the effect of Graphene Oxide on the surface of the Nafion membrane, specifically looking at whether it mitigates the effect of this CO poisoning or assists in the dissociation of hydrogen at the anode.

GO was at first prepared in a 1 mg/mL solution using a one to five ratio of water/methanol as the solvent. Upon assessment of the unfavorable qualities of the combination of water and methanol as a solvent, another GO solution was created using dimethylformamide (DMF) as a solvent. Subsequently, a Langmuir - Blodgett Trough (KSV 5000) was used to obtain isothermal curves for both the DMF and Water/Methanol solutions of graphene oxide. These isothermal curves assisted in choosing coating pressures that were believed to create a monolayer on the Nafion membrane - believed to be the most optimal particle configuration to maximize efficiency. Pressures of 5 mN/m, 8 mN/m, and 10 mN/m were chosen for the graphene oxide dissolved in DMF, and pressures of 1 mN/m, 2 mN/m, and 3 mN/m were chosen for the graphene oxide dissolved in water methanol.

Figure 2 Maximum Output Power measured by H-Tec PEMFC kit using free air as the cathode feed gas.
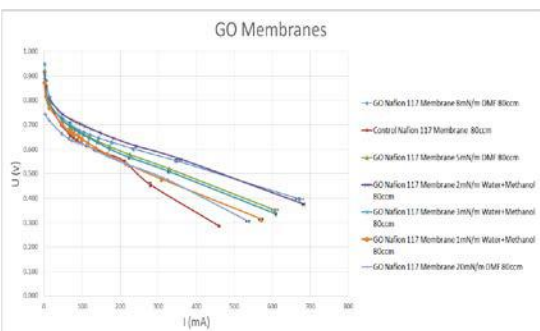

Figure 1 Graph displaying voltage vs. current curve for different target pressures and solutions, measured by the H-Tec PEMFC kit using free air as the cathode feed gas.

After the Nafion membranes, six in total, were coated with the graphene oxide at their chosen pressures, they were put in an H-Tec Fuel Cell, where the power output of the modified membranes were quantified using a multimeter. The target pressure that produced the highest maximum power output was the DMF solution at an 8mN/m target pressure at $\Omega 0$ (Figure 1, Figure 2). With a maximum power output of 267 mW, this was a 102% increase over the uncoated control membrane. The second highest power output was the Water / Methanol solution at a 2mN/m target pressure at $\Omega 0$ (Figure 1, Figure 2). With a respectable maximum power output of 256 mW, this was a 94% increase over the uncoated control membrane. Further research would focus on GO's effects on possibly minimizing CO poisoning. In addition, the mechanism at which GO increases the efficiency of the PEMFC's maximum power output will be investigated by coating only one side of the Nafion 117 membrane. By doing so, the capabilities of the GO in either aiding with H_2 dissociation or minimizing CO poisoning will be clear.

[1]Murphy OJ, Hitchens GD, Manko DJ (1994) High power density proton-exchange membrane fuel cells. J Power Sources 47(3): 353-368.

[2] Lee SJ, Mukerjee S, Ticianelli EA, McBreen J. Electrocatalysis of CO tolerance in hydrogen oxidation reaction in PEM fuel cells. Electrochim Acta 1999;44:3283-93.

Analyzing the Effects of Gold Nanoparticles Coated on Various Nafion Membranes for Improved Performance through the Catalysis of Carbon Monoxide Oxidation

David Herman*, Kevin Qian◦, Hongfei Li+, Miriam H. Rafailovich+

*Davis Renov Stahler Yeshiva High School For Boys, 700 Ibsen Street, Woodmere, NY 11598, United States
◦Wayzata Senior High School, 4955 Peony Ln N, Plymouth, MN 55446, United States. +Department of Materials Science and Engineering, State University of New York at Stony Brook, Stony Brook, New York 11794-2275,

Hydrogen Fuel Cells are an attractive alternative energy source due to their environmentally safe emissions and relatively high efficiencies. However, one of the major problems with direct hydrogen fuel cells is the poisoning of the platinum catalysts in the electrodes, which serve to catalyze both the oxidation of hydrogen gas and the reduction of oxygen gas. The *water gas shift reaction:* $CO + H_2O \rightarrow H_2 + CO_2$ is an equilibrium reaction that leads to the accumulation of Carbon Monoxide, which binds to the active sites of the platinum catalyst, preventing the hydrogen from oxidizing in the catalyst site. Thus, CO inhibits the performance of the fuel cell, and lowers the value of fuel cells[1].

Proton Exchange Membranes or Polymer Electrolyte Membranes (PEM) in fuel cell allow for the passage of protons between the anode and cathode while remaining impermeable to gases and electrons. One of the most common PEM substances is Nafion, a registered product of DuPont, which is a sulfonated tetrafluoroethylene (teflon) based fluoropolymer-copolymer. Nafion membranes come in different types, mainly varying in thickness. Gold nanoparticles have been found in previous research to have the potential to be used as effective catalysts for the oxidation of CO[2]. In this paper, we will discuss the effects of gold nanoparticles coated on different nafion membranes and their performance.

We determined the optimal target pressure for coating AuNP's after finding the isotherm curve, which was determined to be 3 mN/m. Various Nafion membranes (Nafion 117, 115, and 212) were tested at various flow rates (40, 60, 80, 100, and 120 ccm), with several gases (pure Hydrogen gas with free air on cathode-side, hydrogen gas with pure oxygen on cathode-side, and CO poisoned gas). Coating the nafion membrane involved the Langmuir

Figure 1. Experimental data on the effects of gold nanoparticles on Nafion 117, and data from an uncoated Nafion 117 at various flow rates.

Blodgett trough (referred to as LB-Trough). By controlling the pressure of gold nanoparticles on the surface of the water inside the trough, we were able to create a monolayer. When lifting the nafion membranes from below the water's surface, the particles are applied and thereby coated onto the membrane.

Figure 1 illustrates the improved performance with the addition of gold nanoparticles. Nafion 117 was used for measurement, one membrane was left uncoated for the control while the other was coated with AuNP's at a target pressure of 3 mN/m. Each membrane was tested at several flow rates: 60, 80, and 100 ccm. The optimal flow rate was found to be at 80ccm, and the gold coated membrane had a 38% greater output than the non-coated membrane. The other two Nafion membranes were tested, and each yielded similar results: gold coated membranes result in a higher power output than non-coated membranes, demonstrating that gold nanoparticles can have the potential to be used in a variety of applications.

[1].J.C. Amphlett, R.M. Baumert, R.F. Mann, B.A. Peppley, P.R. Roberge, A. Rodrigues, "The Effect of Carbon Monoxide Contamination on Anode Efficiency in PEM Fuel Cells", Royal Military College of Canada (1993).

[2]. Green, Isabel X., Wenjie Tang, Matthew Neurock, and John T. Jr. Yates. "ChemInform Abstract: Insights into Catalytic Oxidation at the Au/TiO2 Dual Perimeter Sites." *ChemInform* 45.21 (2014): n. pag. Web. 16 July 2015.

Synthesis, Characterisation, and Application of Noble Metal and Noble Metal Alloy Nanoparticles to Proton Exchange Membrane (PEM) Hydrogen Fuel Cells for Enhanced Catalytic Activity

Xiaotian Zhang,[a] Arun Soni,[a] Hongfei Li,[b] Miriam Rafailovich,[b] Tatsiana Mironava[b]

[a] Staples High School, 70 North Ave. Westport, CT 06880
[b] Stony Brook University, Department of Materials Science and Engineering, Stony Brook, NY 11794

Nanoparticles have a growing list of applications in science and industry[1]. In this project, we synthesised noble metal nanoparticles and alloy nanoparticles using a modified Brust method. We synthesised Au, AuAg, AuPt, Ag, PtAg, Pt, AuPt 1:6, AuPt 6:1, AuPt 1:3, and AuPt 3:1. We performed Transmission Election Microscopy, UV-Visible Spectroscopy, and Zeta Potential measurements on the particles for characterisation. Most particles measured by TEM are around 4 nm, while Ag is 27 nm and PtAu 6:1 is 12 nm. Zeta Potential measurements revealed negative charges and good stability on our particles, with a -84.66 mV zeta potential on the AuAg particles. Particles were coated onto Proton Exchange Membrane (PEM) hydrogen fuel cells to test catalytic activity. We found that the AuAg particles have the greatest enhancement on catalytic activity: compared to the control [117] Nafion membrane with no nanoparticle coating, the AuAg coated [117] Nafion membrane resulted in a 36% increase in current, a 27% increase in voltage, and a 73% increase in power at zero resistance. The enhanced performance of AuAg compared to PtAg is most likely caused by the presence of Au in AuAg catalysing the CO → CO_2 reaction, while the Pt part of the catalyst in PtAg gets poisoned by CO. Future work could involve synthesising new particles with different ratios of Au and Ag.
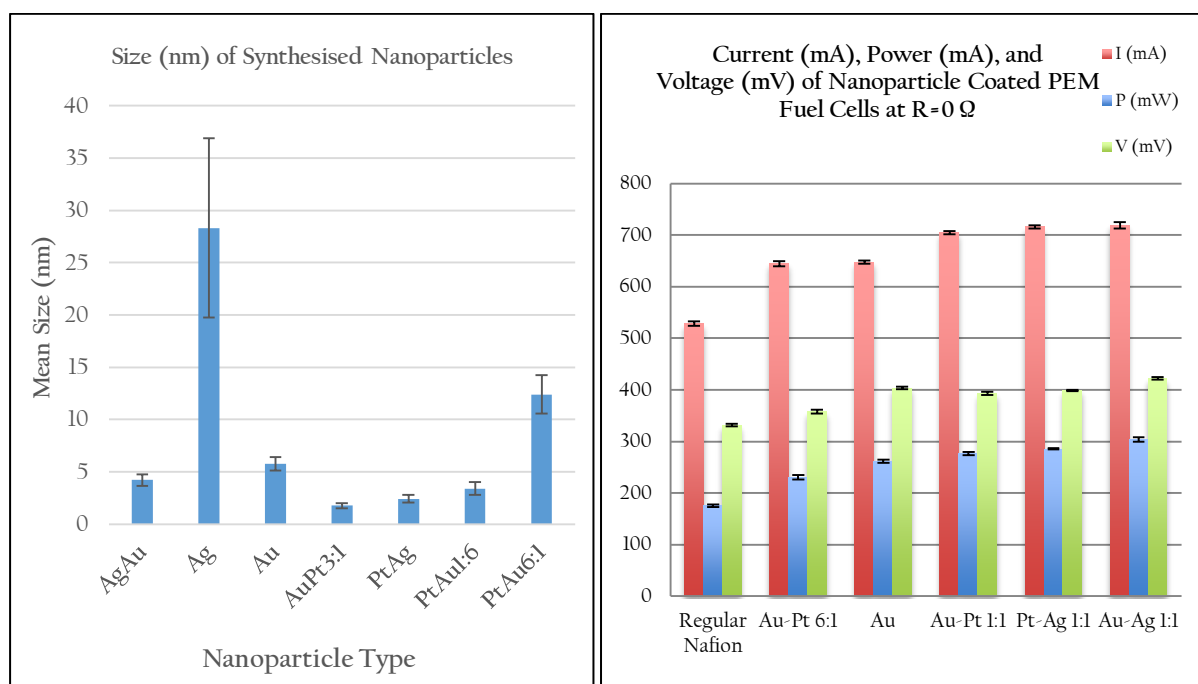
Fig 1. Measured Sizes of synthesised nanoparticles.   Fig 2. Catalytic Activity measurements of PEM fuel cells.

1 Stark, W. J., Stoessel, P. R., Wohllebenb, W. and Hafnerc, A. (2015). Industrial applications of nanoparticles. *Chem. Soc. Rev.*, 2015, 44, 5793—5805.

Session 2   Organic Photovoltaics

Zhenhua Yang: Graduate Supervisor

Jaymo Kang, University of California, Berkeley: REU
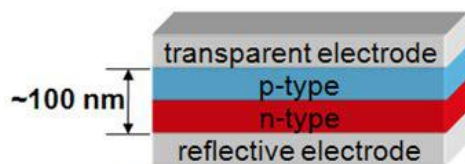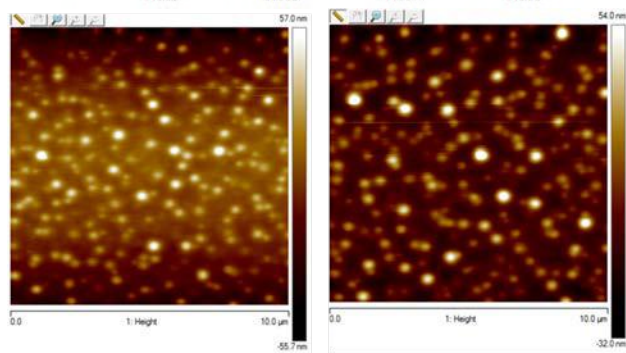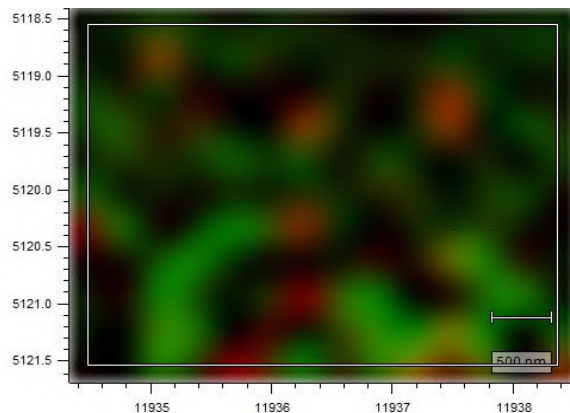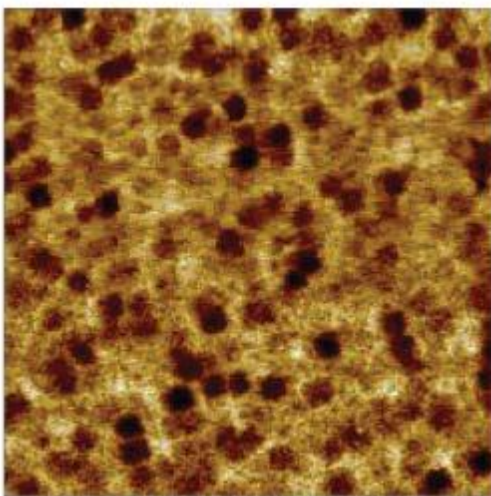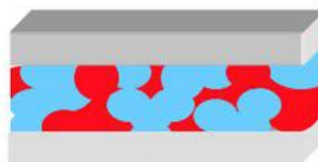
(a) Planar heterojunction   (b) Random heterojunction   (c) Ordered heterojunction

The Effects of PMMA and Graphene on P3HT/ PCBM Bulk Heterojunction Oragnic Solar Cells

Hope Lee[1], Zhenhua Yang[2], Crisleine Saleri[2], Dr. Miriam Rafailovich[2]
[1]Woodbridge High School, Irvine Californica, 92604
[2]Department of Material Science and Engineering, Stony Brook University, Stony Brook, NY, 11794

It is undeniable that the world is facing an inevitable and upcoming energy crisis. One of the most powerful solutions to this quandary would be to efficiently harness the near inexhaustible energy of the sun. However, even though conventional silicon solar cells have been reported to reach an upper limit of 29% efficiency[1], these cells have certain major drawbacks including the cost, thickness, and opaqueness of the cells[2]. As such, organic solar cells utilizing photovoltaic polymers have become a recent development.

The type of organic solar cell studied was inverted bulk heterojunction (BHJ) cells. In a BHJ solar cell, the electron donor material and electron acceptor material are mixed directly in the active layer in attempt to increase surface contact between the two phases and thus facilitate charge flow[3]. P3HT and PCBM, both photovoltaic polymers, served as the electron donor and acceptor respectively.

For this study, the composition of the active layer was altered by adding various amounts of PMMA and graphene. First a set of samples with PMMA to P3HT to PCBM ratios (in mg/mL) of 0:20:20, 5:20:20, and 10:20:20 were created. Each sample had a volume of 0.5mL. Efficiency was tested using an IV tested. The greatest efficiency tested was 2.51% with a 5:20:20 ratio. Using an AFM, morphology images are generated for each sample and average contact angles calculated: for 0:20:20, an average of 2.26 degrees; for 5:20:20, 36.85 degrees; and for 10:20:20, 21.27 degrees.

Then utilizing the 5:20:20 ratio, a set of samples, one with additional graphene added and one without were created. IV tests and AFM scans were performed (Figure 1). The efficiencies were 1.79% on average for the sample without and 1.45% on avergage for that with graphene. The contact angles were on average 6.066 degrees for the sample without and 5.723 degrees for the sample with graphene.

With such analysis of the morphology and efficiency, one can gain a better understanding of which factors significantly impact the efficiency of these organic solar cells and therefore in which ways this relatively new technology can be improved.
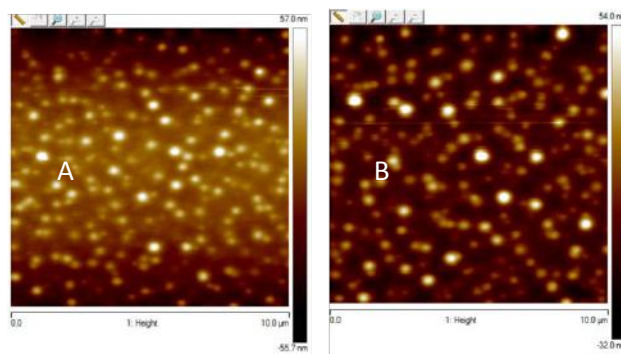
Figure 1: Above are AFM images characterizing the morphology of the solar cell surfaces. (A) demonstrates a solar cell sample that has no graphene added. (B) demonstrates a solar cell sample that has graphene added. AS the morphology is similar, one can conclude that the addition of graphened does not affect PMMA created self-organized structure that is desired.

[1] Blakers, Andrew, Ngwe Zin, Keith R. McIntosh, and Kong Fong. "High Efficiency Silicon Solar Cells." High Efficiency Silicon Solar Cells. Elsevier, n.d. Web. 06 Aug. 2015.

[2] Goetzberger. "Crystalline Silicon Solar Cells." SpringerReference (2011): n. pag. ICTP. Web.

[3] Scharber, M. C., and N. S. Sariciftci. "Efficiency of Bulk-heterojunction Organic Solar Cells." Efficiency of Bulk-heterojunction Organic Solar Cells. Elsevier, Dec. 2013. Web. 06 Aug. 2015.

The Implementation of Polystyrene and Graphene in the Active Layer of PCDTBT:PCBM Inverted Organic Solar Cells to Increase Energy Conversion Efficiency

Andrew Wang [1], Effie Jia [2], Zhen-Hua Yang [3], Crisleine Saleri [3],and Miriam Rafailovich [3]

[1] Nikola Tesla Science, Technology, Engineering, and Mathematics (STEM) High School, Redmond, Washington 98053

[2] Dougherty Valley High School, San Ramon, California 94582

[3] Department of Materials Science, Stony Brook University, Stony Brook, New York 11794

Rising demand for energy and the growing concern over the effect of fossil fuels on global climate change have necessitated the further development of renewable energy technology. Photovoltaics (PV) offer a form of passive energy generation and versatility due to the different types of PV systems available ranging from flexible organic thin film systems to more rigid inorganic crystalline systems. Organic solar cells optimized for higher Power Conversion Efficiency (PCE) through the modification of the polymer active layer are one type of engineered PV solutions[1].

Polystyrene (PS) and Graphene in the active layer and thin film spin speed were first studied as influential variables to the system. Polystyrene is utilized to alter the polymer morphology of the active layer by changing the structure from a Bulk Heterojunction (BHJ) structure to an Ordered Heterojunction (OHJ) (see Figure 1) structure which offers increased surface area for electron and hole transfers to occur[2]. Graphene is used as an addition to the electron acceptor polymer in the active layer in order to facilitate electron transport by lowering electrical resistance and providing alternate pathways. A standard device was fabricated utilizing PCDTBT and PCBM (electron donor and acceptor) in a predetermined ratio through dissolution in Chlorobenzene (CB) and spin casted at two different speeds, 2000 and 3000 rpm[3]. Polystyrene was added to new device solutions in even increments and spun at 3000 rpm to extrapolate a relationship between concentration of PS and PCE. Due to its low solubility in CB, Graphene was then added to new device solutions containing the optimal amount of PS in a constant amount while the amount of PCBM was manipulated. Data was then collected regarding PCE, Short Circuit Current (J_{SC}), Open Current Voltage (V_{OC}), and Fill Factor (FF).
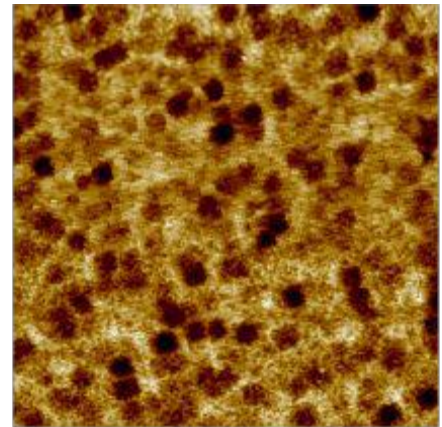
Figure 1:
AFM image of PCDTBT:PS (4:4) washed with Chlorobenzene indicates "column" structures found at the circular dark regions indicating removed polystyrene.

The engineered PV cells were compared primarily through their PCE. The first parameter tested was the effect of thin film spin speed on PCE, where data collected indicated that a speed of 3000 rpm and thus a thinner film (confirmed via SEM) resulted in a higher PCE of 1.915%. The following tested parameter was the effect of PS on PCE, where data collected indicated that a concentration of 2 mg/mL of PS corresponded to a PCE of 2.365%, the highest PCE of the concentrations tested. Furthermore, the final parameter tested was the effect of Graphene on PCE, where data collected indicated that the addition of graphene increased PCE to 2.523%. Collectively, the changes studied resulted in an overall increase in efficiency of 31.72%, bringing efficient organic solar PV systems to the forefront of energy production technologies.

References

[1] "Efficiency of Bulk-heterojunction Organic Solar Cells." *Science Direct*. N.p., Dec. 2013. Web.

[2] Etzold, Fabian. "Ultrafast Exciton Dissociation Followed by Nongeminate Charge Recombination in PCDTBT:PCBM Photovoltaic Blends." *Research Gate* (2011): n. pag. Print.

[3] Movla, Hossein. "Influence of Active Region Thickness on the Performance of Bulk Heterojunction Solar Cells: Electrical Modeling and Simulation." *Research Gate*. N.p., 7 Nov. 2013. Web.

Integration of Multiple Donors and Graphene into Self-Assembled Organic Solar Cells to Increase Power Conversion Efficiency

Audrey Cheng, Henry M. Gunn High School, Palo Alto, CA, 94036
Crisleine Saleri, **Zhenhua Yang**, and **Dr. Miriam Rafailovich**, Stony Brook University, Stony Brook, NY, 11794

With the growing energy crisis, solar power is a viable alternative to current fossil fuel-based technologies. The organic solar cell is one of the most promising technologies in bringing about low cost energy production and offers many unique benefits, including flexibility, semitransparency, low manufacturing costs, and integration into a variety of products[1]. A major limitation in these devices, however, is the relatively narrow spectrum over which these cells can harvest light energy. A multiple donor and acceptor system was tested to increase the efficiency of organic photovoltaics.

To form columnar structures within the active layer to increase device performance, polystyrene (PS) was added into the mixture of electron donor and acceptors[2]. The main electron donor used was Poly[*N*-9′-heptadecanyl-2,7-carbazole-*alt*-5,5-(4′,7′-di-2-thienyl-2′,1′,3′- benzothiadiazole)] (PCDTBT), as it has been shown to give better efficiencies and longer lifetimes to solar cells. Various amounts of Poly(3-hexylthiophene-2,5-diyl) (P3HT), a photoactive polymer found commonly in organic solar cells, were added into the active layer. Phenyl-C61-butyric acid methyl ester (PCBM) and graphene were used as electron acceptors.

All solar cells were constructed in the inverted structure and were tested under 100 mW/cm^2 AM 1.5G illumination. A spin speed of 2000 rpm during spincasting of the active layer was found to be most effective in creating solar cells with higher efficiencies. From the various ratios of P3HT tests, the device with a P3HT:PCDTBT:PS:PCBM blend of 1.2:4:2:12 showed the highest efficiency of 2.07%. It was observed that adding P3HT to the system lowered the efficiency compared to a blend without P3HT. This decrease could be caused by the the inability of P3HT to mix efficiently with PCDTBT. Adding graphene significantly increased the cell efficiency to 3.37% in the device with a P3HT:PCDTBT:PS:PCBM: Graphene blend of 1.2:4:2:12:0.1. Graphene could have possibly compatibilized the electron donors or helped the PCBM to aggregate favorably within the active layer, leading to a 62.8% increase in efficiency in the solar cells.

AFM images were taken of the cells (Figure 1). The features in the active layer were too small to resolved clearly so selective solvents will be used to dissolve one component of the active layer and the morphology will be observed in more detail. Contact angle and roughness data were taken from each sample.

Further work involves UV-Vis and Raman spectroscopy to elucidate in detail the effect of the additives to the structure of the active layer. Additional ratios of P3HT and graphene will also be tested.
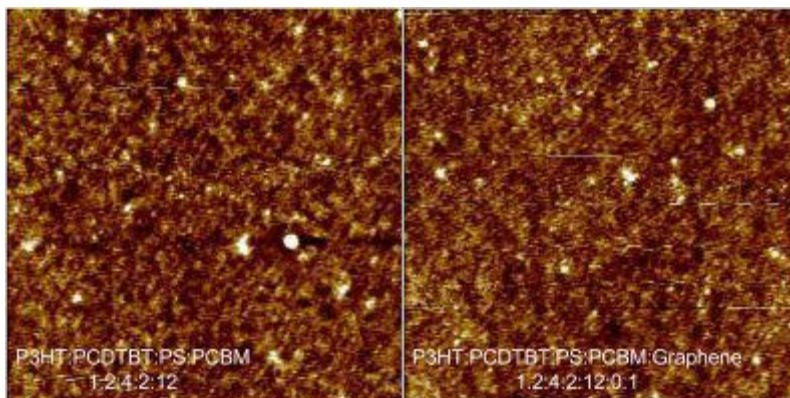
Figure 1. AFM images of the active layer in solar cells.

References
[1] M.C. Scharber, N.S. Sariciftci. "Efficiency of bulk-heterojunction organic solar cells." Progress in Polymer Science 38.12 (2013):1929-1940.
[2] Pan, Cheng, Hongfei Li, Bulent Akgun, Sushil K. Satijia, Yimei Zhu, Di Xu, Joseph Ortiz, Dilip Gersappe, and Miriam H. Rafailovich. "Enhancing the Efficiency of Bulk Heterojunction Solar Cells via Templated Self-Assembly." Macromolecules 46.5 (2013): 1812-1819.

Constructing Ordered Heterojunction Organic Solar Cells Using Selective Solvents to Improve Morphology and Efficiency

Alexander Li[1], Alice Wu[2], Zhenhua Yang[3], Crisleine Saleri[4], and Miriam Rafailovich[3]

[1] Saratoga High School, Saratoga, CA 95070 [2] The Harker School, San Jose, CA 95129 [3] Department of Materials Science, SUNY Stony Brook, Stony Brook, New York 11790 [4]

Organic solar cells offer the benefits of cheap, environmentally friendly, and easy-to-manufacture solar cells. P3HT-PCBM bulk heterojunction solar cells are the current standard for organic solar cells with efficiencies of over 5%.[1, 2] , but their lack of ordered structure results in lower efficiencies. Recent papers have found that adding polystyrene (PS) to the active layer creates columnar nanostructures that provide more direct pathways for charge.[3, 4] Our work aims to use the nanostructures created by PS to increase the interfacial area and charge transport abilities of planar heterojunctions to ultimately improve the power conversion efficiency (PCE). In addition, we introduce another photoactive polymer, Poly[N-heptadecanyl-2,7-carbazole-alt-5,5-di-2-thienyl- benzothiadiazole] (PCDTBT), which has been shown to increase PCE, into the standard mixture of [6,6]- Phenyl C61 butyric acid methyl ester (PCBM) and Poly(3-hexylthiophene-2,5- diyl) (P3HT).

We began with a 25% PS to P3HT solution for our active layer because Vohra et al. found that to be the ratio with the highest efficiency.[3] However, Atomic Force Microscope (AFM) imaging of our thin film morphology, shown in Figure 1.a, revealed the pores to be larger and more irregular than that of Vohra et al. Thus, we decreased our ratio to 15% PS to P3HT. AFM imaging, shown in Figure 1.b, confirmed that the new ratio created smaller and more regular pores that matched the AFM images of 25% PS in Vohra et al.[3]
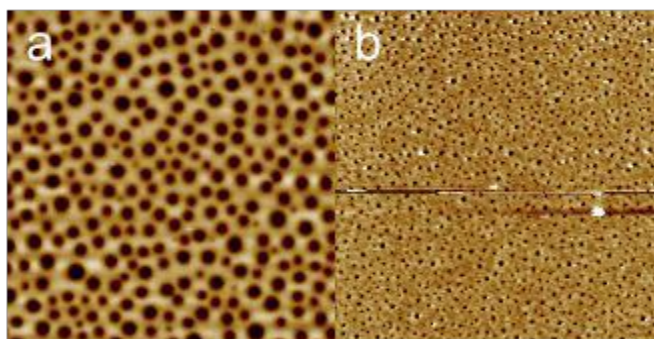

Figure 1. Atomic Force Microscope image of acetone-washed (a) 15:5 P3HT:PS thin film and (b) 17:3 P3HT:PS thing film.

The structure with the highest PCE was found to be as follows. Overall, we used an inverted solar cell structure. To construct the active layer, we began by spin casting a P3HT:PS solution with a concentration of 17:3 mg/mL in chlorobenzene onto TiO_2 coated ITO glass. Then, we immersed the resulting devices in acetone, a good solvent for PS but a poor solvent for P3HT, for 30 minutes to remove the non-photoactive PS. We spin casted either an 8 mg/mL PCBM solution or an 8:0.05 mg/mL PCBM:PCDTBT solution in dichloromethane, a poor solvent for P3HT, onto the P3HT pattern to fill in the holes left by PS.

Our solar cells demonstrated significant phase separation, as shown in Figure 1. The P3HT:PCBM solar cells exhibited an efficiency of 1.73% with a J_{SC} of 8.15 mA/cm² and a fill factor of 0.447, while the P3HT:PCBM:PCDTBT solar cells exhibited an efficiency of 1.26% with a J_{SC} of 6.50 mA/cm² and a fill factor of 0.407. The lower fill factor may be explained by greater exciton recombination brought by the addition of PCDTBT. Future work includes examining the efficiency of exciton dissociation, as well as finding new solvents to increase the concentration of PCDTBT that can be used.

[1] M. Reyes-Reyes, K. Kim and D. L. Carroll, *Appl. Phys. Lett.*, 2005, **87**, 083506.

[2] W. Ma, C. Yang, X. Gong, K. Lee and A. J. Heeger, *Adv. Funct. Mater.*, 2005, **15**, 1617–1622.

[3] V. Vohra, M. Campoy-Quiles, M. Garriga, and H. Murata, *J. Mater. Chem.*, 2012, **22**, 20017.

[4] C. Pan, H. Li, B. Akgun, S. K. Satijia, Y. Zhu, D. Xu, J. Ortiz, D. Gersappe, and M. H. Rafailovich, *Macromolecules*, 2013, **46**, 1812-1819.

Session 3:   Dental Pulp Stem Cells

Kuan-che Feng, Vincent Ricotta, Linxi Zhang : Graduate Supervisors

John Mele, Stony Brook University ;**Naomi Javitt** University of Maryland; **Adina Goldberg,** City University of New York; **Austin Wild,** Villanova University, **Villanova, PA : REUs**
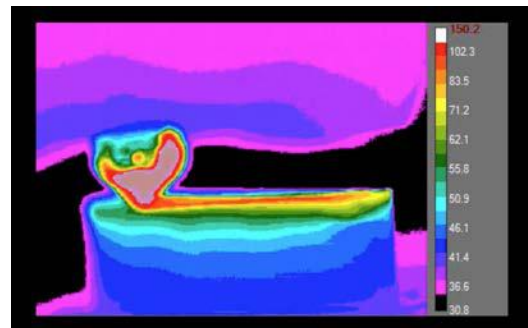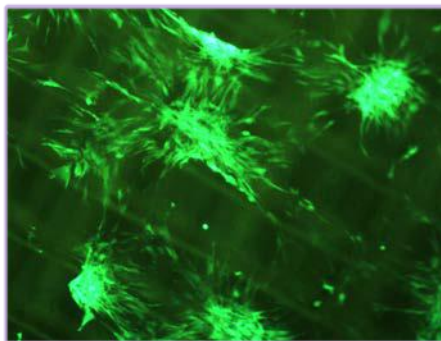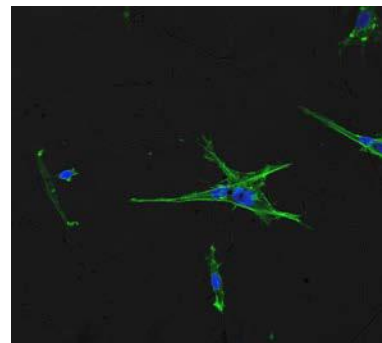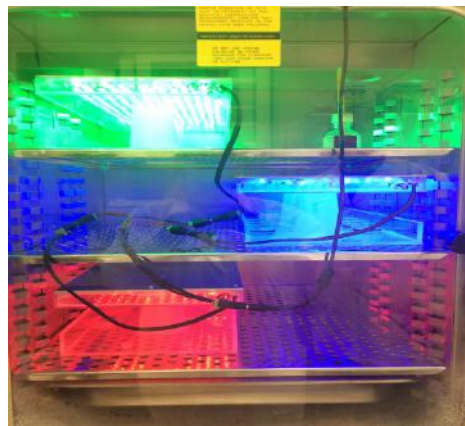
The Effects of TiO2 Nanoparticles and LED Lights on Dental Pulp Stem Cells

Tzippora Chwat, Yeshiva University High School for Girls, Hollis, NY 11423
Vincent Ricotta, Stony Brook University, Stony Brook, NY 11790
Austin Wild, Villanova University
Jae Cho, Boston University

Stem cells are of interest due to their potential to be used for tissue regeneration. Dental Pulp Stem Cells (DPSCs) specifically are interesting because they are easy to access with low morbidity, clonogenic, highly proliferative, and capable of regeneration. Understanding factors that could improve DPSCs' growth and differentiation rates could assist in the creation of new treatments to aid in tissue repair. [1] [2]

Many factors can affect the rates of proliferation and differentiation in DPSCs. One such factor is lights. Previous studies have shown the various effects of lights on the growth of cells. Specifically, blue light is known to retard cell proliferation while red and green lights are known to improve growth rates. Red LED lights have been shown to specifically promote differentiation of DPSCs for tissue repair. [3] [4]

Titanium Dioxide is a widely used nanoparticle, which may be found as an additive as a white pigment and food colorant, as well as in sunscreens and cosmetics. Nanoparticles are known to be more toxic to cells as size decreases due to their increased surface area, chemical reactivity, and ability to penetrate cells. Still the cytotoxicity of TiO_2 is considered relatively negligible compared to other nanoparticles. TiO_2 is also a known photocatalyst. It has been used for water and air purification. When exposed to UVA light, TiO_2 expresses antibacterial properties. However, little has been done to investigate its effects with other lights.

Figure 1. Proliferation of DPSCs with TiO2 Nanoparticles and LED Lights

The affects of the additions of blue, green, and red LED lights, as well as TiO2 nanoparticles on growth and differentiation of human DPSCs were investigated. Additionally, cells were grown on tissue culture plastic under each light and no light to serve as controls [Figure 2]. Cells were counted using a hemocytometer on days 1,2,3 and 8 [Figure 1]. The lights had expected effects as the blue slowed proliferation, while red and green promoted cell growth. However, cells with TiO2 nanoparticles, which is expected to be toxic to cells, grew more than cells without the nanoparticle in their media.

Additional research will include looking at the cells with a confocal microscope, SEM, Raman Spectroscopy, qRT-PCR, and AFM to determine the morphology of the cells grown under different conditions.

Figure 2. Set up of DPSCs and lights in incubator.

[1] Riccardo d'Aquino, Gianpaolo Papaccio, Gregorio Laino, Antonio Graziano. "Dental Pulp Stem Cells: A Promising Tool for Bone Regeneration". Stem Cell Rev 4:21–26. February 2008.

[2] S. Gronthos, M. Mankani, J. Brahim, P. Gehron Robey, S. Shi. "Post Natal Human Dental Pulp Stem Cells in Vitro and in Vivo". PNAS 13625-13630. December 5, 2000.

[3] Masayuki Ohara, Yuzo Kawashima, Osamu Katoh and Hiromitsu Watanabe. "Blue Light Inhibits the Growth of B16 Melanoma Cells." Jpn. J. Cancer Res. 93, 551–558, May, 2002

[4] M.J. Holder, M.R. Milward, W.M. Palin, M.A. Hadis and P.R. Cooper. "Effects of Red Light-emitting Diode Irradiation on Dental Pulp Cells." J DENT RES 2012 91: 961

[5] Jia Ran-Gurr, Alexander S.S. Wang, Chien Hung-Chen, Kun-Yan Jan. "Ultrafine titanium dioxide particles in the absence of photoactivation can induce oxidative damage to human bronchial epithelial cells." Toxicology 213 (2005) 66–73. 2015.

The Role of Static Magnetic Fields on Biomineralization of Dental Pulp Derived Cells on Sulfonated Polystyrene Films

Elaina Zodiatis[1], Vincent Ricotta[2], Dr. Miriam Rafailovich[2]
[1]Smithtown High School East, St. James, NY 11780, [2]Department of Material Sciences and Engineering, Stony Brook University, Stony Brook, NY 11790,

Current endodontic research focuses on the proliferation, differentiation, and biomineralization of dental pulp stem cells (DPSCs) in vitro[1]. Due to their accessibility, high proliferation rate, and multi-potential differentiation, DPSCs are ideal for tissue engineering and regeneration[2]. This study examines the ability of static magnetic fields (SMF) and Poly(Styrene-co-4-styrene sulfonic acid) (SPS) to induce DPSC differentiation.

SPS was spuncast at thickness of 17 nm (170 Å). DPSCs were plated on both these SPS coated silicon wafers and tissue culture plastic (TCP), with and without the presence of the static magnetic field of strength 150 mT.

After counting cells during the first three days of incubation, cell proliferation of the different DPSC samples was calculated (Figure 1). The smaller cell proliferation rate of SPS samples could be contributed to the cells beginning to differentiate.

Atomic force microscopy showed higher relative modulus for SPS+SMF, suggesting differentiation of cells (Figure 2). In the future, we plan on conducting SEM, Raman, qRT-PCR, AFM, and confocal in order to determine differentiation of DPSCs.

Figure 1: Cell Proliferation Days 1-3
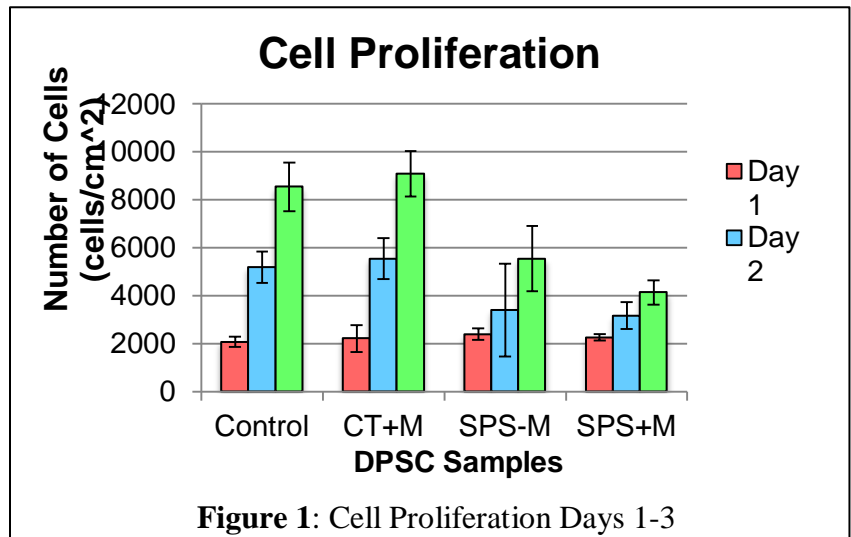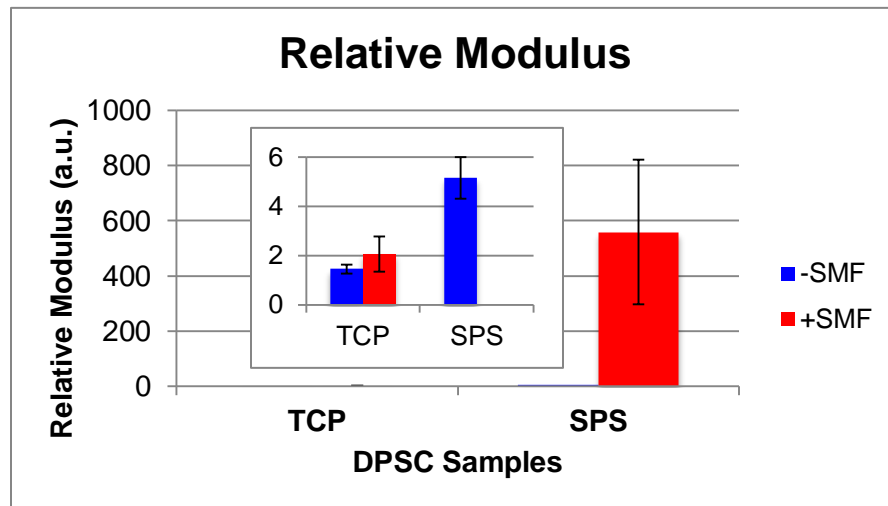

Figure 2: Cell Relative Modulus of DPSC Samples with and without SMF

[1]Bronckaers, A.; Hilkens, P.; Fanton, Y.; Struys, T.; *Angiogenic Properties of Human Dental Pulp Stem Cells*. 2013, PLOS ONE. 8 (8), 1-12.
[2]Gronthos, S.; Mankani, M.; Brahim, J.; Gehron Robey, P.; Shi, S.: *Postnatal human dental pulp stem cells (DPSCs) in vitro and in vivo*. 2000, PNAS. 97 (25), 13625–1363.

The Effect of Surface Topography of 3D Printed PLA Scaffolds on Dental Pulp Stem Cell Proliferation and Differentiation *in vitro*

Daniel Chae[1] ; Sidharth Bommakanti[2] , Alan Tan[3], Kuan-che Feng[4], Naomi Javitt[5], Adina Goldberg[4], Michael Cuiffo[4], Adriana Pinkas-Sarafova[4],Miriam Rafailovich[4], Sihana Rugova[6], Marcia Simon[6]

Thomas Jefferson High School for Science and Technology, Alexandria, VA 22312[1], Amador Valley High School, Pleasanton, CA 94566[2], Irvington High School, Fremont, CA94539[3], Dept of Mat Sci and Eng, SBU, Stony Brook, NY 11794[4], University of Maryland College Park MD [5] Dept. of Oral Bio and Path, SDM, Stony Brook, NY 11794

The use of 3D printers is a promising approach in the field of tissue regeneration. Molded polylactic acid (PLA) structures are FDA approved biodegradable materials that are commonly used in dental applications[1]. 3D printed PLA scaffolds are of high interest as they are cheaper than molded scaffolds for custom fitting, and may be generated with surface topographies that support tissue regeneration. With this in mind, we studied the growth and differentiation of dental pulp stem cells (DPSC) cultured on 3D printed scaffolds with checkerboard and line patterns compared to flat surfaces prepared by 3D printing, molding and spin casting of PLA[2,3]. DPSCs support dentin formation (mineralization of the extracellular matrix) during tooth development and repair and in vitro can undergo odontogenic/osteogenic differentiation with matrix mineralization. The human DPSC strain used was AV3-eGFP, a strain that was previously genetically engineered to express enhanced green fluorescent protein (eGFP) to allow detection by fluorescence microscopy. Biomineralization was monitored using 20μM xylenol orange.

The scaffolds used were either molded, spun cast, or produced by two different 3D printers: MB Replicator™ 2nd and 5th generation. The difference between the printers consists of different temperatures in the head (230° C for 2nd generation (230P) and at 215° C for 5th generation (215P) and speed of extrusion. The scaffolds were evaluated using differential scanning calorimetry (DSC) to measure the melting temperature, contact angle to measure hydrophobicity, and scanning electron microscopy (SEM) to measure topography. Thermal imaging was also used during scaffold production* (Figure 1E & 1F). Both SEM and contact angle showed statistically significant differences between the scaffolds from the two printers. SEM images indicated mixed nano and micropatterns. The 215P produced surfaces with unfused PLA filaments and sporadic rough patches, whereas the 230P produced surface lines that were fused and with a higher density of rough patches (Figure 1A & 1B). The contact angle of the scaffold produced with the 230P was greater than that produced with the 215P.

Figure A represents SEM imaging of the 3-D printed flat scaffold at 10% fill on the 230P while figure B is a 3-D printed flat scaffold at 10% fill on the 215P. Figure C represents flourescent microscopy of DPSCs on a 3-D printed flat scaffold at 10% fill on the 230P while Figure D is DPSCs on a 3-D printed flat scaffold at 10% fill on the 215P.
Figure E represents a thermal image of the 230P creating a flat pattern at 10% fill. Figure F shows the vertical temperature gradients of 230P and 215P, indicating similarity in the exponential slope.

To compare the ability of each scaffold to support DPSC growth and differentiation, samples were sterilized with ethylene oxide after which DPSCs were plated 10^4 cells/cm^2, in non-induction media (αMEM, 200 mM ascorbic acid, and 10 mM β-glycerol phosphate) and induction media (αMEM, 200 mM ascorbic acid, 10 mM β-glycerol phosphate, and 10 nm dexamethasone) and cells followed microscopically. As shown in Figure 1C and 1D, no differences in cell morphology were observed in cultures on the 215P and 230P scaffolds, although proliferation on the 215P produced surface appeared less than on the 230P produced surface. Further, three 3D printed designs were produced to assess the large-scale (micro & milli) pattern effects on cell growth. For these experiments replicate cultures were incubated with gentle shaking. As a positive control for mineralization, half of the samples were fed with media plus DEX a corticosteroid that is known to induce differentiation in DPSCs. We found higher proliferation rates on all scaffolds cultured with shaking. On day 9 post-plating, cell nodule formations (early differentiation sign), were observed in all 3D printed samples, although they were more abundant in cultures supplemented with DEX. No similar structures were found on spin cast samples. The end point analysis by confocal microscopy, SEM and RT-PCR for detection of osteogenic or odontogenic markers will be performed for evaluation of each scaffold.

[1]Tiziano Serra, Miguel A Mateos Timoneda, Josep A Planell & Melba Navarro (2013) 3D printed PLA based scaffolds, Organogenesis, 9:4,239244. [2] Grottkau, B. E., Purudappa, P. P., & Lin, Y. F. (2010). Multilineage differentiation of dental pulp stem cells from green fluorescent protein transgenic mice. *International journal of oral science* , 2 (1), 21.
[3] Kolind, K., Kraft, D., Bøggild, T., Duch, M., Lovmand, J., Pedersen, F. S., & Besenbacher, F. (2014). Control of proliferation and osteogenic differentiation of human dental pulp derived stem cells by distinct surface structures. *Acta biomaterialia* , 10 (2), 641650.
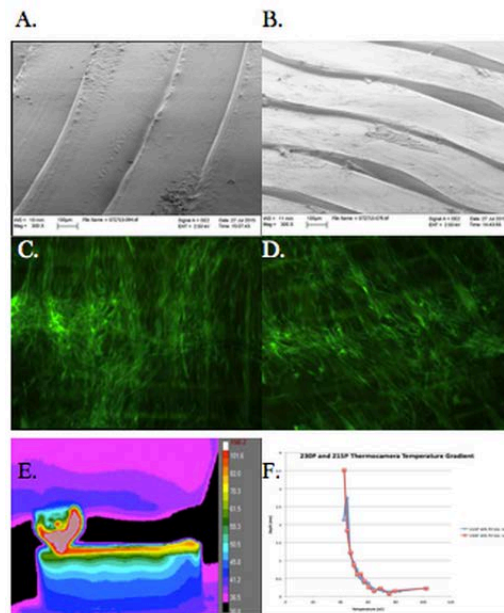
Effects of Topography and Composition of Electrospun P4VP Polymer Fiber on its Biocompatibility with Dental Pulp Stem Cells

Amanda Klestzick[1], Kevin Sadhu[2], David Fleschner[3], John Mele[4], Linxi Zhang[4]

[1]Sar High School Bronx, NY 10471   [2]Manhasset High School, Manhasset, NY 11030
[3]HAFTR High School, Lawrence, NY 11559   [4]Stony Brook University, Stony Brook, NY 11794

Many studies have shown that dental pulp stem cells (DPSCs) are a promising approach in tissue engineering and bone regeneration due to the easy access to collection sites [1]. The objective of this study was to examine the electrospun P4VP(Poly(4-Vinylpyridine)), P4VP/Graphene and P4VP/PCBM(Phenyl-C61 Butyric Acid Methyl Ester) fiber substrates and their interaction with DPSCs.

P4VP polymer solutions of varying concentrations—15wt%, 17wt%, 21wt%, 25wt%—were prepared by dissolving the respective P4VP in ethanol/DMF (5:1 weight ratio) mixture solvent. Two other sets of 17wt% and 25wt% P4VP solutions were also prepared and loaded with 3wt% graphene and 1.5wt% PCBM, respectively. Subsequently, a 70nm thin film was spincasted onto micro-coverglass to enhance fiber adhesion during the electrospinning process. Prepared polymer solutions were electrospun onto spincoated cover glass at 15kV and 5ul/min feeding rate. SEM, AFM and TEM were conducted to study the morphology and mechanical properties of the electrospun fibers. DPSCs were plated on the electrospun fiber substrates and examined by confocal microscopy after 1-day, 4-day and 7-day incubation.

SEM images showed that fiber diameter increases with increasing solution concentration. The morphology of the fibers was not altered by the presence of graphene or PCBM. TEM images concluded that the graphene and PCBM were successfully dispersed into the P4VP fibers. The AFM results showed that as P4VP fiber diameter increased, moduli decreased; when graphene was added, fiber moduli increased, and PCBM had no significant effect on fiber moduli. The confocal microscopy showed that the cell was elongated when placed on the electrospun fibers as seen in figure 1. Cell modulus was measured after 7-day incubation. As the cell diameter increased the moduli decreased, but when graphene and PCBM were added the cell moduli increased, which indicates that the cells can adjust their moduli to respond to the topographical and compositional changes in the fiber substrates.
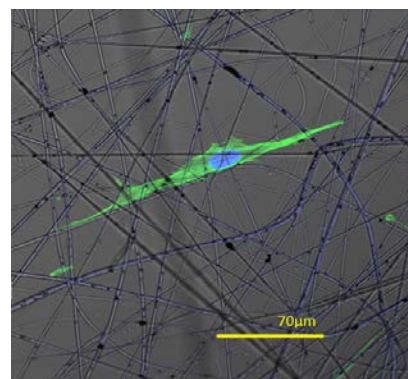
Figure 1. Elongated dental pulp stem cell on *P4VP*/graphene microfiber viewed through confocal microscopy.

We plan to determine the cell proliferation and doubling rate of DPSCs using the confocal microscopy images[2]. SEM with EDAX will be conducted after 28-day incubation to study the biomineralization of DPSCs on different substrates.

---

[1] d'Aquino, R., et al. (2008). "Dental Pulp Stem Cells: A Promising Tool for Bone Regeneration." Stem Cell Reviews 4(1): 21-26.

[2] Korzynska, Anna, Zychowicz, Marzena. (2008). "A Method of Estimation of the Cell Doubling time on Basis of the Cell Culture Monitoring Data." Biomedical Engineering 28(4): 75-82

The Effect of LED Lights on Dental Pulp Stem Cells Plated on P3HT

Eva Spier[1], Vincent Ricotta[2], Austin Wild[3], Jae Hee Cho[4], Marcia Simon[5], Miriam Rafailovich[2]
[1]SAR High School, Riverdale, NY [2]Dept. of Mat Sci & Eng, Stony Brook 11794 [3]Villanova University, Villanova, PA [4]Boston University, Boston, MA, [5]Dept of Oral Bio and Path, SDM, Stony Brook 11794

Dental pulp stem cells (DPSCs) are studied for their ability to regenerate dental tissue. Understanding factors that affect their growth and differentiation can help cells differentiate quickly, which is ideal for clinical use. Many factors can trigger the differentiation of the DPSCs. One potential stimulator is Poly(3-hexylthiophene-2,5-diyl) or P3HT, which is known for its efficiency in solar cells. P3HT is a photosensitizer, or a polymer that releases a photon when struck with light. P3HT absorbs green light the most, then blue light, then red light. Blue light has previously been shown to limit cell growth, while red has been shown to stimulate it. [1] [2]

The growth and differentiation of human DPSCs growing on P3HT under red, blue and green LED lights and no light were investigated. Cells were also grown on tissue culture plastic (TCP) under each color light and without light to serve as controls. The cells were counted using a hemocytometer at 4
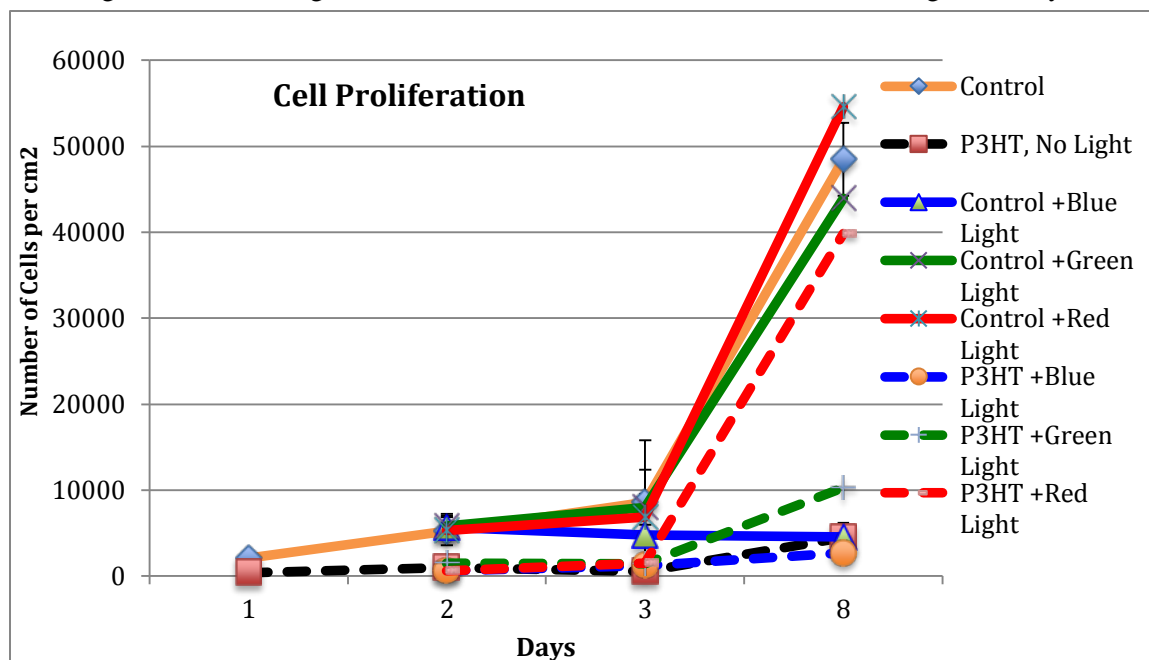

Figure 1: Graph of cell proliferation over 8 days

time points; days 1,2,3, and 8 [Figure 1]. After comparing each sample it was discovered that the cells on TCP with red light and those on the control had the largest number of cells, while the P3HT with red light was the most successful sample grown on P3HT. The cells behaved as expected under blue light conditions, and did not grow as rapidly as the other samples. P3HT seems to encourage the blue light's negative effect on cell growth. The P3HT under green light grew steadily the red light promoted a lot of growth. The point at which the cells began rapidly growing is unclear because on the time points chosen and will be further investigated in upcoming research.

Additionally future work will look at the cells under the Confocal, SEM, Raman, qRT-PCR, and the AFM to determine the properties of the DPSCs under each environment. These tests will help understand what type of cell the DPSCs differentiate into.

[1]Masayuki Ohara, Yuzo Kawashima, Osamu Katoh and Hiromitsu Watanabe. "Blue Light Inhibits the Growth of B16 Melanoma Cells." *Jpn. J. Cancer Res*. 93, 551–558, May, 2002
[2]M.J. Holder, M.R. Milward, W.M. Palin, M.A. Hadis and P.R. Cooper. "Effects of Red Light-emitting Diode Irradiation on Dental Pulp Cells." *J DENT RES* 2012 91: 961

Session 4:   Thrombosis and Angiogenesis

Liudi Zhang : Graduate Supervisor

Sneha Chittabathini, Veronica Burnett Stony Brook University
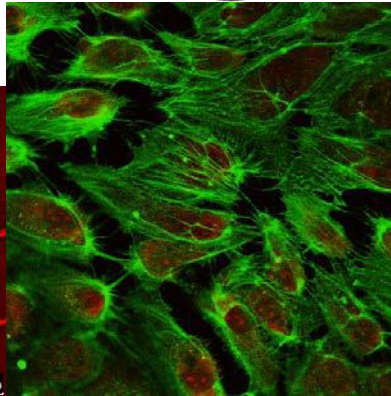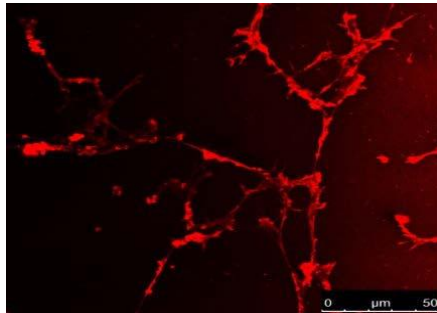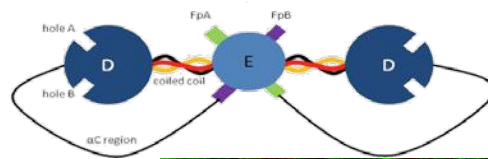
The Effect of Various Polymers on Endothelial Cell Adherence to Fibrinogen-Coated Surfaces

Abigail Wax[1], Juliana Shenker[2], Liudi Zhang[3], Dr. Miriam Rafailovich[3], Dr. Dennis Galanakis[3],
[1]Harborfields High School, Greenlawn, NY; [2]South Side High School, Rockville Centre, NY; [3]SUNY Stony Brook University, Stony Brook, NY

Fibrinogen is a protein found in blood plasma that has a significant role in both blood clotting and endothelialization, which is the adherence of endothelial cells to the linings of blood vessels through tight junctions (Tersteeg, C., et. al.)[1]. Fibrinogen is made up of two distal D regions and one central E region attached to one another by triple-stranded coiled-coil connectors. Fibrinogen also consists of two αC regions formed from the C-terminal portions of the Aα chains that extend from the D regions (Galanakis, D, et. al.)[2]. Due to the structure of an individual fibrinogen molecule, which includes a hydrophilic end - the αC chain region - and a hydrophobic end - the D and E regions - it was predicted and determined that fibrinogen would be able to form fibers on hydrophobic surfaces, since the attraction between the given hydrophobic surface and the D and E regions of the fibrinogen molecule would cause the αC chain to cleave, enabling multiple fibrinogen molecules to bind together. However, fibers would not be able to form on hydrophilic surfaces because those surfaces would attract the αC chain, therefore preventing multiple fibrinogen molecules to connect. Confocal microscopy proved the presence or absence of fibers on the hydrophobic and hydrophilic surfaces, respectively.

The goal of this work was to determine the best polymer surface to coat fibrinogen and whole plasma on so that endothelial cells would be best able to adhere to the fibrinogen. Polystyrene, Poly (4-vinylpyridine), and Poly (L-lactide) were spuncast onto silicon wafers, which were then coated with both pure fibrinogen, at concentrations of 0.1 and 4.0 mg/mL, and whole plasma, which includes fibrinogen along with other proteins normally found in blood. These surfaces were plated with HUVEC endothelial cells. The cells were allowed to proliferate and were o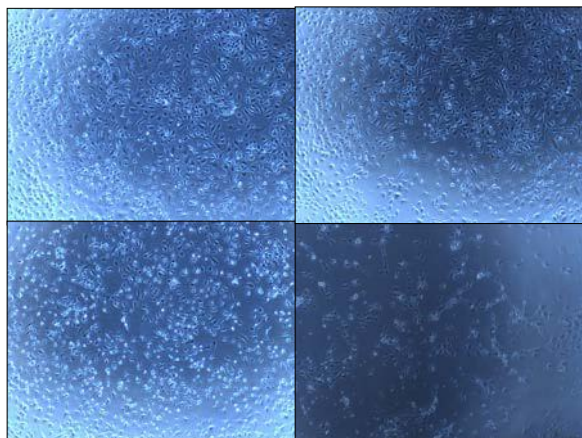bserved via optical microscopy at both 20 and 48 hours. These images show that cells were able to grow in the presence of fibrinogen [Figure 1]. However, cells plated on the PS whole plasma surfaces showed vascularization at 20 hours, but at 48 hours the cells were detaching from the surface and dying. The cause of this is unknown, but is predicted to be the enzymes found in whole plasma which may be reacting with the surfaces. Later, cells were fixed and both nuclei and tight junctions of the cells were stained for confocal microscopy. By imaging the cells with confocal, we will be able to observe the adherence of the endothelial cells to the fibrinogen.

Figure 1: Optical Microscope Images of cells at 48 hours on PLA fibrinogen (top left) and whole plasma (bottom left) and PS fibrinogen (top right) and whole plasma at 20 hours (bottom right).

We intend to continue research by exposing cells to Fibronectin, another protein in blood, and P12, a polymer, and by studying the effect that they have on fiber formation and cell adherence. Furthermore, there is great therapeutic potential by deducing the surface that best allows fibrinogen to form fibers and consequently attract cells – this certainly applies to cardiovascular stents, since it is vital to use surfaces that will not attract platelets, which would result in the formation of unnecessary and potentially dangerous blood clots, but rather attract endothelial cells.

[1]Tersteeg, C. et. al. "A fibronectin-fibrinogen-tropoelastin coating reduces smooth muscle cell growth but improves endothelial cell function."
Journal of Cellular and Molecular Medicine. (2012). 16 (9): 2117-2126.
[2]Galanakis, D, et. al. "Thromboelastographic phenotypes of fibrinogen and its variants: Clinical and non-clinical implications." *Thrombosis Research.* (2014). 133 (6): 1115-1123.

An Investigation of the Interaction of Whole Plasma with Hydrophilic and Hydrophobic Surfaces

Michelle Mao[1], **Sophia Wu**[2], **Liudi Zhang**[3]

[1]Woodbury High School, 2665 Woodlane Drive, Woodbury, MN 55125
[2]Lowell High School, 1101 Eucalyptus Drive, San Francisco, CA 94132
[3]Stony Brook University, Stony Brook, NY 11794

Coronary stents are used to expand arteries weakened from the buildup of plaque. However, depending on the properties of different stent surfaces, fibrinogen, a protein involved in blood clotting, can spontaneously form clots and render the stent useless. The self-assembly of fibrinogen should differ depending on the properties of the surface; fibrinogen is amphiphilic, and when the hydrophilic (alpha C) regions are exposed (on a hydrophobic surface), they link together to form fibers conducive to platelet binding. However, when the hydrophobic regions (gamma chains) are exposed (on a hydrophilic surface), the platelet-binding sites on the hydrophobic regions are also exposed, which is also conducive towards clot formation. This was true with pure fibrinogen and hydrophilic and hydrophobic surfaces; therefore, the purpose of this research is to observe how surfaces interact with fibrinogen present in whole plasma, a more physiologically relevant setting. Silicon wafers (approximately 1 cm x 1 cm) as well as glass substrates were spincasted with polystyrene (PS), polylactic acid (PLA), and poly(4-vinylpyridine) (P4VP). The surfaces were coated with different solutions (bovine serum albumin (BSA), purified fibrinogen, whole plasma, desalpha C fibrinogen), and incubated.

Thin film ellipsometry was used to find the thickness of the polymer surfaces, to characterize the materials used. Optical light microscopy was used to observe the surfaces, and the AFM was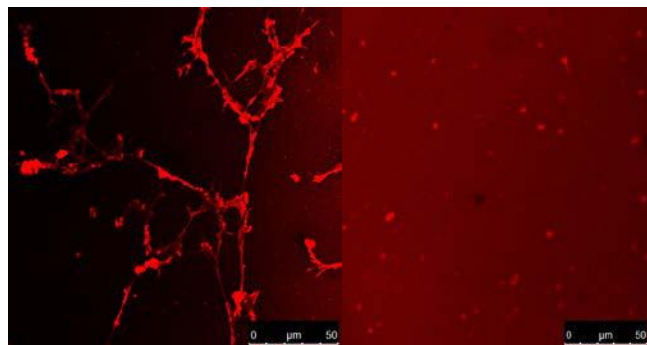 used to confirm the presence of fibers on the wafers. Confocal microscopy was used to image the different hydrophilic and hydrophobic regions of fibrinogen, fibers, and antibody stained cells (Figure 1). Antibody staining of the alpha C regions and gamma chains and AFM proved that hydrophilic regions of the fibrinogen were not attached to the surface of PS, a hydrophobic polymer, and vice versa, verifying the proposed model. In the future, we can study the competition between platelets and endothelial cells to bind to fibrinogen. If endothelial cells are able to bind to fibrinogen before platelets, it may prevent blood clot formation. Further research can lead to lower risk of spontaneous clot formation in stents for patients.

Figure 1. Confocal images of alpha chain antibody stained pure fibrinogen (concentration 4 mg/mL), PS on left and P4VP on right.

References

Koo, J., Galanakis, D., Liu, Y., Ramek, A., Fields, A., Ba, X., ... & Rafailovich, M. H. (2012). Control of anti-thrombogenic properties: surface-induced self-assembly of fibrinogen fibers. *Biomacromolecules*, *13*(5), 1259-1268.

Koo, J., Rafailovich, M. H., Medved, L., Tsurupa, G., Kudryk, B. J., Liu, Y., & Galanakis, D. K. (2010). Evaluation of fibrinogen self assembly: role of its αC region. *Journal of Thrombosis and Haemostasis*, *8*(12), 2727-2735.

Zhu, J., Lin, F., Brown, D. A., & Clark, R. A. (2014). A fibronectin peptide redirects PDGF-BB/PDGFR complexes to macropinocytosis-like internalization and augments PDGF-BB survival signals. *Journal of Investigative Dermatology*,*134*(4), 921-929.

Engineering A Blood Vessel Using Cultured Human Umbilical Vein Endothelial Cells And Polydimethylsiloxane Substrates

Jacob Abulencia[1], Bonnie Mendelson[2], Sneha Chittabathini[3], Veronica Burnett[3], Steven Krim[3], Dr. Gurtej Singh[3] and Dr. Miriam Rafailovich[3]

[1]Half Hollow Hills High School West, Dix Hills, NY; [2]Yeshiva University High School for Girls, Holliswood, NY; [3]Stony Brook University, Stony Brook, NY

Endothelial cells make up the inner layer of human blood vessels. The purpose is to engineer a full human blood vessel using human umbilical vein endothelial cells (HUVECs) which were cultured on a polydimethylsiloxane (PDMS) substrate. Several other hypotheses were tested, such as whether exposing the cultured cells to different concentrations of graphene tightened the junctions between the cells, the optimal ratio of base to cross-linking agent[1] of the PDMS to culture the cells on, and determining whether cells adhere to PDMS alone or if they needed another agent to stick. In order to create the vessel, a PDMS mold in the shape of a tube had to be created. This was accomplished by drawing blueprints for a Teflon mold and having it engineered by a professional. The PDMS substrates were made by mixing different concentrations of base and cross-linking agent. The cells were then cultured on small circles of solid PDMS. For the graphene, different concentrations of a graphene-phosphate buffered saline solution were mixed with the media for cell growth. Through the experiments, it was found that the optimal ratio of base to cross-linking agent in PDMS was ten to one. As for the cells adhering to the PDMS, they were not able to stick to the substrate. Therefore, an adhering agent is required to attach the cells to the PDMS.[2] For the graphene, it was not possible to tell whether it promoted tight junctions because all cells that were exposed to graphene died. Future work will be dedicated to working on culturing HUVECs on the curved surface of the created PDMS mold and testing the resulting cell tube's strength and elasticity.
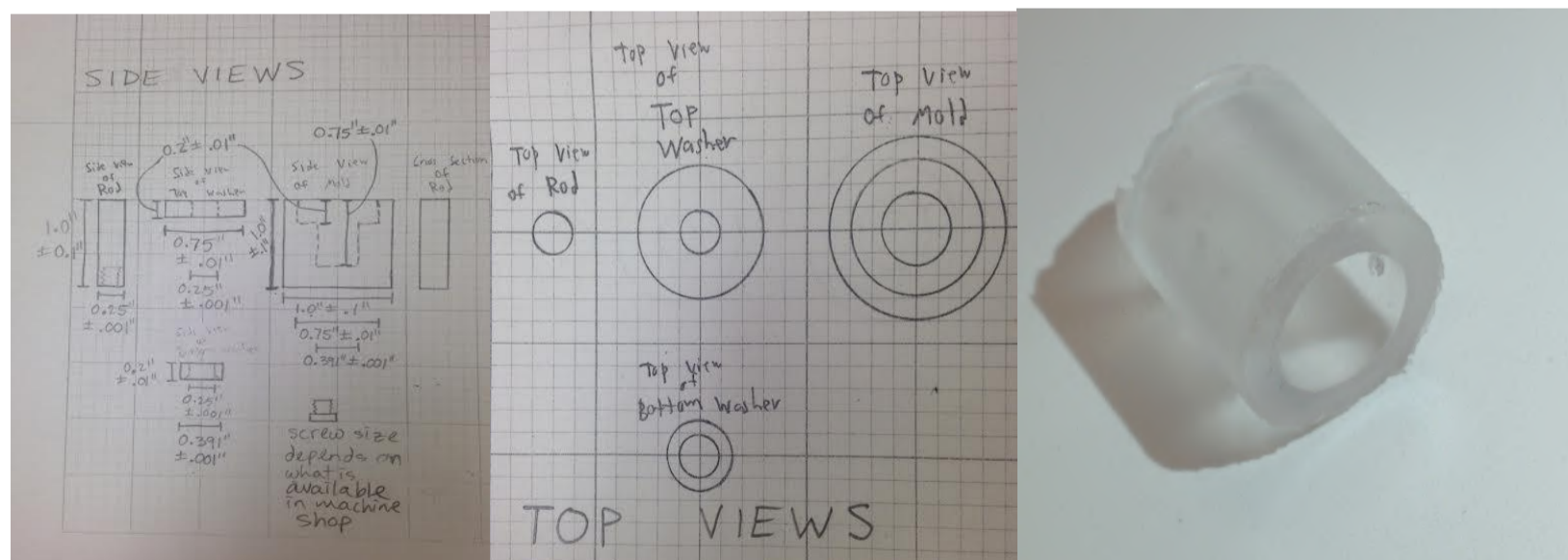

Figure 1. (From left to right) Drawing of a side view and a top view of teflon tubing to mold PDMS and the PDMS mold shaped by the teflon tubing.

References:

[1] Oldörp, Klaus (2013). Testing a Viscoelastic PDMS Standard in Oscillation. *Thermo Fisher Scientific.* Retrieved August 6, 2015, from www.thermoscientific.com

[2] Fuard, D., Tzvetkova-Chevolleau, T., Decossas, S., Tracqui, P., & Schiavone, P. (2008). Optimization of poly-di-methyl-siloxane (PDMS) substrates for studying cellular adhesion and motility. *Microelectronic Engineering,* 1289-1293. Retrieved August 6, 2015, from www.sciencedirect.com

Session 5: Environmental Sustainability

Harry Shan He : Graduate Supervisor

Ginna Gabalski East Meadow HS;
Jake Plaut SUNY Binghamton
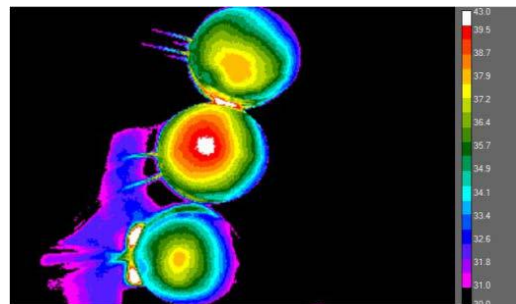
Determining the Properties of Polystyrene Fibers in Application to Prototyping Traps for the Common Bedbug (*Cimex lectularius*)

YingYan Ho[1], Jake Plaut[2], Harry Shan He[3], Dr. Miriam Rafailovich[3]

1) Texas Academy of Mathematics and Science, Denton, TX 76203 2) Binghamton University, Binghamton, NY 13902 3) Garcia MRSEC, Stony Brook University, Stony Brook NY 11790

The infestation of the common bedbug, *Cimex lectularius*, is an increasing global problem. Bedbugs have existed alongside humans for a long time. In the 1940-1950s the rise in popularity of insecticides and subsequent usage of DDT pushed bedbug populations down. In 1972, DDT was banned due to its toxic effects on biological communities. Since the 1980s, there has been a resurgence in chemically resistant bedbugs (particularly to pyrethroids, which have been chemically overused methods of eradicating bedbugs)[1]. As fully grown bedbugs are 5-7mm and about as thin as a credit card, they are very good at hiding in mattresses, luggages, walls, and dark crevices. They are hard to spot and even harder to treat. The increased amount of travelers and low awareness for the bedbug problem has contributed to the spread of their numbers across the world, including the US, Europe, Australia. While a wealth of commercialized products exists in the market today for trapping bedbugs such as glue traps, interceptors, CO_2 emitters, etc., they are still imperfect.

The purpose of this study was to produce a viable, more effective bedbug trap utilizing electrospun fibers. Electrospun polystyrene fibers have the potential to trap bedbugs; however, the fibers must be spaced far enough apart to allow the bedbug's leg to enter the fiber matrix, but close enough so that they can entangle the hair on a bedbug's legs as the bedbug moves. As the leg of a bedbug is approximately 40 microns wide and the space between hairs is approximately 25 microns, the fibers must create a spacing 50-60 microns wide.

The first part of creating this prototype, determining fiber properties, was executed by utilizing electrospun polystyrene fibers. 12%, 15%, and 18% polystyrene and recycled polystyrene solutions were prepared using tetrahydrofuran and dimethylformamide and were used for electrospinning fibers. Fiber properties were determined using AFM (relative shear modulus), DLS (zeta potential), optical microscopy (fiber diameter, fiber spacing), and SEM. Recycled polystyrene at 15% was found to be the most ideal solution to use for electrospinning, thanks to its production of "fluffy", loopy fibers, few beads, and ideal gap spacing, as versus to the straighter fibers produced by pure polystyrene (Figure 1).

The second part of this was constructing trap prototypes that would attract bedbugs. 6 different prototypes were drafted up in Layout, taking into account the affinity that *C. lectularius* has to vertical surfaces and shadows[2]. Several prototypes were constructed out of manila folders and then fibers were electrospun into their geometric nets. Future work involves testing bedbug's attraction to the traps and the time it takes for them to die with the traps.
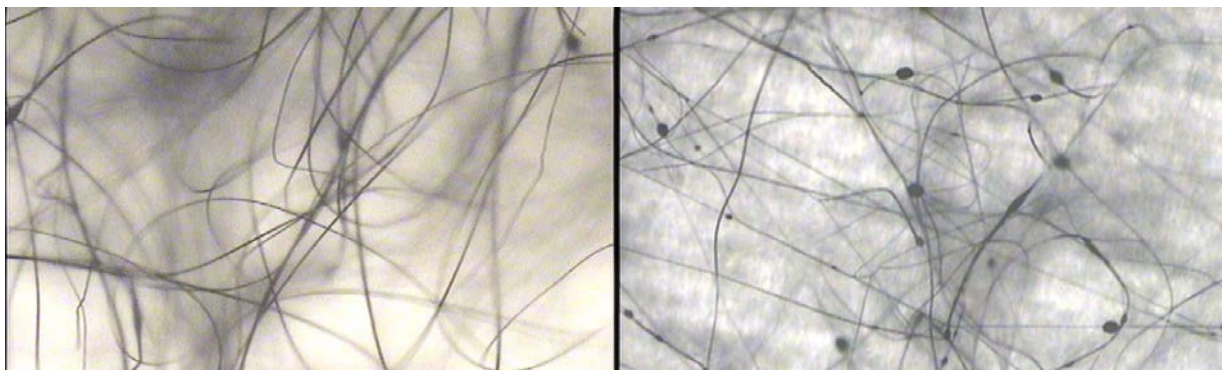

Figure 1: 15% RPS fibers electrospun onto Al (left); 15% PS fibers electrospun onto Al (right). 5x magnification

1. Wang, C., Singh, N., & Cooper, R. (2015). Field Study of the Comparative Efficacy of Three Pyrethroid/Neonicotinoid Mixture Products for the Control of the Common Bed Bug, Cimex lectularius. Insects, 6(1), 197-205. doi:10.3390/insects6010197

2. Singh N, Wang C, Cooper R (2015) Role of Vision and Mechanoreception in Bed Bug, Cimex lectularius L. Behavior. PLoS ONE 10(3): e0118855. doi:10.1371/journal.pone.0118855

Determining Optimal Concentration and Pigment Combinations for a Cream Which Can Physically Impede the Feeding Mechanisms of Mosquitoes
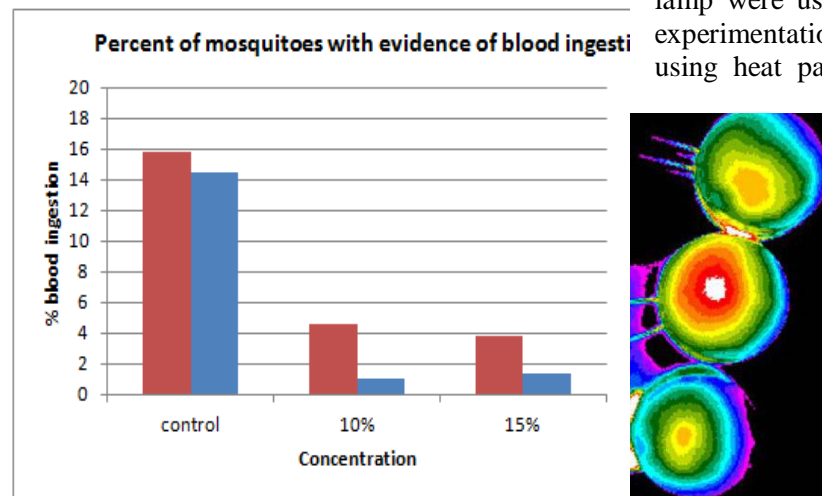
Connie He, Half Hollow Hills High School West, Dix Hills, NY 11746
Gabrielle Jung, Half Hollow Hills High School West, Dix Hills, NY 11746
Harry Shan He, Stony Brook University, Stony Brook NY 11790
Ginna Gabalski, East Meadow High School, NY 11554
Dr. Miriam Rafailovich, Stony Brook University, Stony Brook NY 11790

The World Health Organization approximates that between 300 and 500 million cases of malaria occur each year worldwide [1]. Mosquito bites contribute to the deaths of more than 1 million people every year. A majority of these deaths occur in tropical areas in the Southern Hemisphere, particularly Sub-Saharan Africa, and are particularly caused by malaria. Currently, the methods of repelling mosquitoes are either ineffective or hazardous to humans. Conventional mosquito repellents contain the chemical diethyl-meta-toluamide (DEET), which can cause headaches, nausea, dizziness, skin irritation, and rashes [2]. Metofluthrin is a chemical commonly used in battery-powered fans that has recently been discovered to possess neurotoxic properties. In order to repel these annoying, everyday pests and alleviate the global epidemic of malaria, a novel method of physically blocking the female mosquito's proboscis from penetrating through human skin was investigated.

The ultimate goal of our research was to synthesize a biologically compatible moisturizing cream that physically blocks the female mosquito's mouth, or proboscis. The proboscis contains two inner tubes known as the hypopharynx, which circulates saliva, and the labrum, which draws blood. Another parameter that was adjusted to optimize the cream was pH. The concentrations of red, black, and yellow pigments were adjusted to produce a cream that matches various human skin tones.

Female mosquitoes, *Aedes aegypti*, were released into a mosquito cage containing three bovine blood wells at 35-37°C, each treated with the same formulation. A heat incubation waver and nocturnal infrared lamp were used to heat the blood wells. During experimentation, temperature was maintained using heat patches. A thermo vision IR camera measured the temperature gradient throughout each blood well. The mosquitoes were allowed to attempt to probe and feed from the blood wells for 20 minutes. The whole cage was placed in the freezer afterwards to kill the mosquitoes. Mosquitoes were then examined under the optical microscope to observe for evidence of blood ingestion as well as to study the anatomical structure of the mosquitoes. The total number of mosquitoes which showed evidence of blood ingestion was recorded. mosquitoes, as shown in Fig. 1.

Figure 1: Left:Percent of mosquitos who have ingested blood from uncoated membranes (control) and those coated with our formulation. (Patent pending) Right: Thermal scan of membranes

References: 1. Hardy, Jay. The Most Deadly Animals: Mosquitoes - Anopheles and Malaria(n.d.): n. pag. Web. 2. Robbins, P. J., & Cherniack, M. G. (1986). Review of the biodistribution and toxicity of the insect repellent- diethyl- - toluamide (DEET). Journal of Toxicology and Environmental health, 18(4), 503-525.

Analysis of Peconic Bay Scallops

Cameron Hanover, Shawnee High School, 3333 Zurmehly Rd. Lima, Ohio 45806; Dr. Stephen Tettelbach, Long Island University Post, 720 Northern Blvd. Brookville, NY 11548; Chelsea Miller, Long Island University Post, 720 Northern Blvd. Brookville, NY 11548

In 1985, the first of several occurrences of harmful "brown tides" took place in the Peconic Bay and Great South Bay of Long Island. These blooms of harmful algae were caused in part due to high levels of organic nitrogen in the waters. These algal blooms were particularly devastating to the populations of hard clams and Atlantic Bay scallops that live in these areas. Despite decades of restoration efforts, scallop populations have only made a mild recovery. This study explored the composition of the scallop shells to see if there was a correlation in strength between the scallops raised in hatcheries and those collected from the wild.

During this study, the first test that was run was thermogravimetric analysis (TGA), which was used to determine the organic to inorganic ratio of mass in the shells. The scallop shells used were those collected from the hatchery, which were then separated according to color and placed into the TGA instrument. The results of this test are shown in Figure 1, which demonstrates that all three colors have approximately a 50:50 ratio of
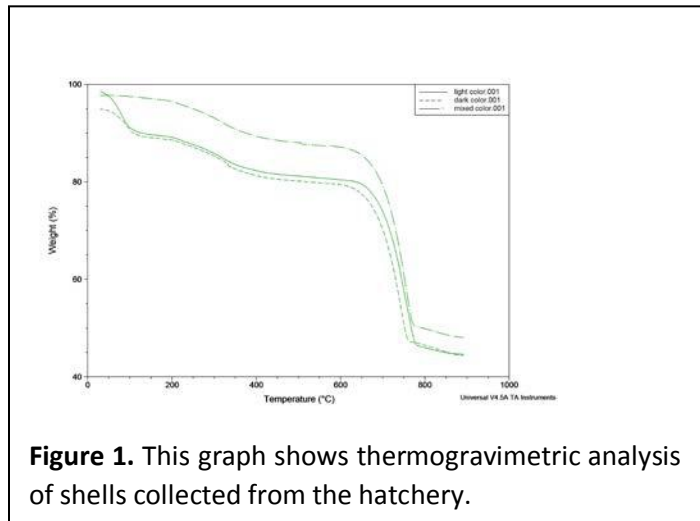

Figure 1. This graph shows thermogravimetric analysis of shells collected from the hatchery.

organic to inorganic matter. Next, several shells were ground up into a fine powder and analyzed using x-ray diffraction. The results of this test showed that the shells are primarily calcite, which is consistent with known results. A scanning electron microscope was also used to observe the shells, but showed no conclusive facts. Finally, compressive tests were run using an Instron machine in order to determine the strength of the scallop shells, as shown in Figure 2. The results from this series of tests show that the hatchery scallops are much weaker than the wild scallops, though the reason is unknown. Future planned tests include running a thermogravimetric analysis of the scallop shells collected from the wild, in order to determine if there are any differences in the organic to inorganic composition of the wild scallops.

Figure 2. Scallop shell being compressed in the Instron machine.

Session 6:   Therapeutic Drugs and their Delivery

Kao Li, Juyi Li : Graduate Supervisors

Jae Hee Cho, University of Texas at Austin;
Luke Heesu Shin Cornell University
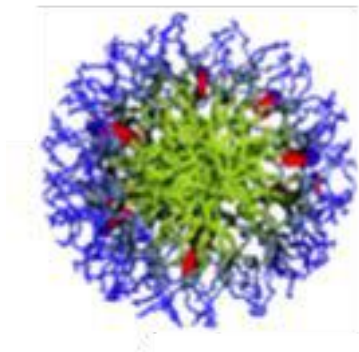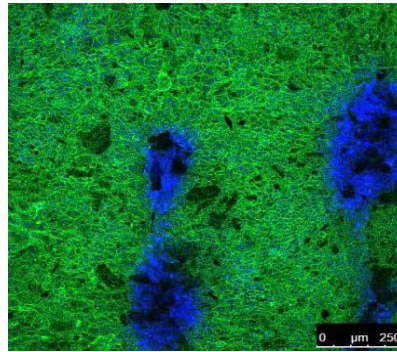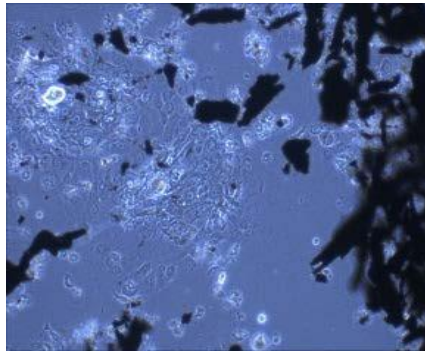
The Effect of a Fibronectin Derived Peptide on the Moduli and Migration of Dermal Fibroblasts

Samali Sahoo, The Harker School, San Jose, CA; Kao Li, Miriam Rafailovich, Department of Materials Science and Engineering, Stony Brook University, Stony Brook, NY, Richard Clark, Department of Dermatology, Stony Brook University, Stony Brook, NY
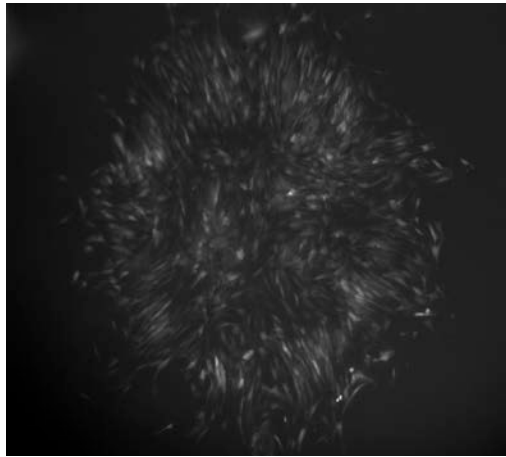
Figure 1: Dermal Fibroblasts in an Agarose Droplet Migrating Outwards
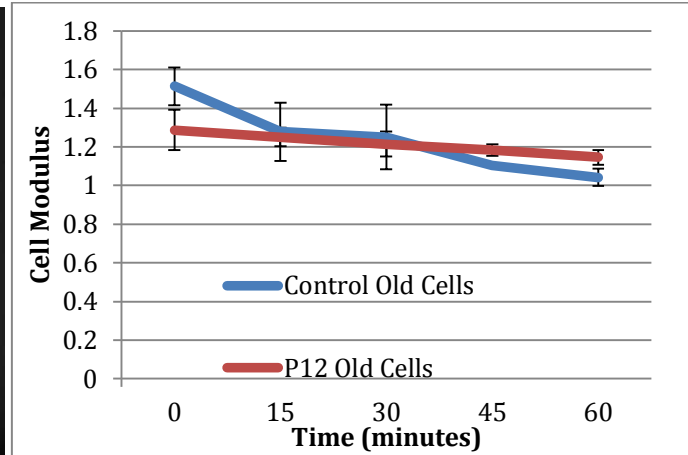

Figure 2: Cell Modulus of 84 year old cells measured with Atomic Force Microscopy

Fibronectin is a protein found in the extracellular matrix of cells, which is involved in cell adhesion and cell migration, which proves to be crucial in the body for wound healing especially burn victims.[1] P12, a polypeptide sequence derived from Fibronectin, has been shown to be able to bind to platelet-derived growth factor and thus promote tissue survival in burn injuries.[2] This experiment seeks to determine the effect of p12 on fibroblast moduli, which could determine the durability of fibroblasts, as well as migration, which would promote wound healing. P12 scrambled served to determine if a chemical conformation of p12 that would not bind to growth factor could have effects on fibroblasts.

Both young and old dermal fibroblasts were cultured in DMEM with 10% Fetal Bovine Serum and 1% Pen Strep. Cells were plated and P12 and P12 scrambled were added to the petri dishes to make a 10µM solution of the polypeptide. The moduli of the fibroblasts in two petri dishes containing each sample including two controls were measured using a soft tip with Atomic Force Microscopy. In order to measure cell migration, a solution of 30 mg/mL Polymethyl methacrylate dissolved in Toluene was spun-cast onto glass coverslips at 2500 rpm for 30 seconds. The coverslips were then heated in a vacuum oven at 130ºC for 3 hours to heat the PMMA past its glass transition temperature. The coverslips were coated with Fibronectin for 2 hours. Fibroblasts were then suspended in a 0.2% agarose gel and hardened for 10 minutes at 4ºC. The cell migration was measured using an optical microscope attached to a Nikon Camera shown in Figure 1. Initial data involving the young 31 year old cells showed that P12 greatly increased the cells' moduli. The P12 scrambled did not have a significant effect on the fibroblasts' moduli confirming the hypothesis that its chemical conformation would not bind with growth factor. Additionally, the data from Figure 2 of the 84 year old cells shows that P12 reduces the decrease of cells

moduli over time relative to the control. In the future, P12 should be cultured in a media in the absence of growth factor to confirm the mechanism by which P12 works.

---

[1] Lin, F., Zhu, J., Tonnesen, M. G., Taira, B. R., McClain, S. A., Singer, A. J., & Clark, R. A. F. (2014). Fibronectin peptides that bind PDGF-BB enhance survival of cells and tissue under stress. *The Journal of Investigative Dermatology*, *134*(4), 1119–1127. doi:10.1038/jid.2013.420

[2] Zhu, J., Lin, F., Brown, D. A., & Clark, R. A. F. (2014). A fibronectin peptide redirects PDGF-BB/PDGFR complexes to macropinocytosis-like internalization and augments PDGF-BB survival signals. *The Journal of Investigative Dermatology*, *134*(4), 921–929. doi:10.1038/jid.2013.463

Synthesis and Characterization of Food-Grade Microemulsions with Enhanced Bioavailability for Nutraceutical and Drug Delivery Applications

Rahul Gupta[1], Juyi Li[2], Nissim Garti[3], Marcia Simon[4], Miriam Rafailovich[2].

[1]Amador Valley HS, Pleasanton, CA, 94566; [2]Deptartment of Materials Science & Engineering, Stony Brook University, Stony Brook, NY 11794; [3]Casali Intitute of Applied Chemistry, The Hebrew University of Jerusalem, Jerusalem 91904, Israel; [4]School of Dental Medicine, Stony Brook University, Stony Brook, NY 11794

Microemulsions are optically clear, thermodynamically stable, isotropic dispersions of water, oil, and a surfactant which is normally accompanied with a cosurfactant. These fusions offer two distinct advantages over other drug/ nutrient delivery mechanisms such as cyclodextrins and polymer-based encapsulations: greatly increased bioavailability (O/W ME) and cost-effective synthesis.[1] Furthermore, microemulsions can be functionalized with dendrimers for specific cell targeting.[2] Microemulsion systems allow for increased absorption of drugs due to an enhancement of penetration through cellular membranes. Past research efforts have pointed to short-chain alcohols to avoid the use of surfactants but these compounds are customarily restricted from food products. Therefore, for microemulsions to be commercially viable, food-grade ingredients are of prime interest.

Previous work had shown that polysorbate 80, more commonly known as Tween 80, and propylene glycol form a microemulsion that can be infinitely diluted along the 70:30 dilution line. Initial testing of the physiochemical properties of this system was done. However, the determination of drug-solubilizing effects and toxicological work has not been previously completed. Curcumin (CUR), a lipophilic drug known for its anti-cancer properties, was used as a model hydrophobic substance. The size and size distribution of the unloaded and loaded microemulsions was determined through DLS. The particles were between 4 and 7 nm across, thereby facilitating permeability through natural barriers. Zeta potential measurements showed that the ME particles were neutral. Viscosity of the various dilutions of the unloaded ME's from 10 to 90% (w/w) revealed that the Winsor III phase occurs at 30% water levels.

Figure 1. Cell toxicity test of Tween 80 and PG based microemulsions with neonatal fibroblasts.
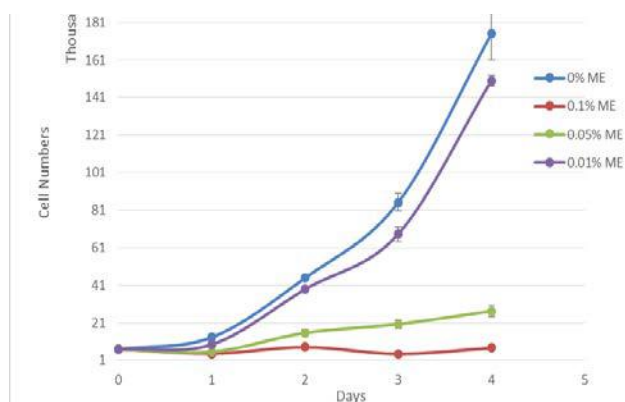

Of the potentially cytotoxic components of ME, the surfactant has been given the most attention due to its nonselective cell membrane destabilization. Therefore, cellular assays at different concentrations of Tween 80 were fed to the cells. Results showed that at 0.01% the Tween 80 is not significantly cytotoxic as the rate of growth is statistically similar (Figure 1). With this observation, an unloaded ME with this similar concentrations of Tween 80 were fed to the cells. Current assays are detecting the ability of the T80/PG ME's ability to carry curcumin to the cells. UV-Vis spectroscopy was employed to build a standard curve of curcumin and to determine the concentration of curcumin loaded in microemulsion.

The multifunctional properties of microemulsions arise from the surfactants ability to reduce noble metal salts and stabilize them into quantum dots. The inner oil phase further assists with this process. The synthesis of monodisperse coated gold nanoparticles whose size depends on the various easily changeable factors such as temperature and concentration was conducted as well. Preliminary analysis of these particles show sizes of appx. 30nm at room temperature synthesis. In addition, the coating of the AuNP's with the relevant drug is essential for imaging purposes.

[1]Talegaonkar S, Azeem A, Ahmad FJ, Khar RK, Pathan SA and Khan ZI. 2008. Microemulsions: A Novel Approach to Enhanced Drug Delivery. *Recent Pat Drug Deliv Formul*. **2**(3):238-57. [2]Nir I, Aserin A, Libster D, and Garti N. 2010. Solubilization of a Dendrimer into a Microemulsion. *J. Phys. Chem. B*. **114**(50):16723–16730.

Characterization of Graphene and its Derivatives Functionalized with Metal Nanoparticles on Bacteria and Keratinocytes

Arthur Chen[1], Jae Hee Cho[2], Rebecca Isseroff[3], Dr. John Jerome[4], Dr. Marcia Simon[5], Dr. Miriam Rafailovich[6]
Lawrence High School, Cedarhurst, 11516, Stony Brook University, Stony Brook, 11790

Graphene is a single layer of carbon atoms arranged in a hexagonal lattice structure, with the potential to revolutionize therapeutics. However, even though it has this potential, so little is known about how graphene and its derivations of graphene oxide (GO), reduced graphene oxide (RGO), and partially reduced graphene oxide (prGO) affect biological organisms, especially when functionalized with metal nanoparticles. Therefore, the goal of this project was to discover how graphene affects bacteria, specifically staphylococcus aureus (S. aureus), and klebsiella pneumoniae (K. pneumoniae) when functionalized with either silver or platinum particles. As well as how GO, prGO, RGO, and graphene affect both cancerous (SCC13) and non-cancerous (D33) keratinocytes. We hypothesize that graphene functionalized with silver nanoparticles will kill SCC13's, staph, and klebs since silver nanoparticles by itself has been proven to kill these things.

Graphene oxide was produced by a modified Hummer's method, and then functionalized with either silver or platinum nanoparticles, creating metallized-GO in solution. Reduction with $NaBH_4$ was used to produce metallized-RGO and metallized-(prGO) in solution. SEM confirmed the synthesis, reduction, dispersion, and functionalization. Confocal microscopy confirmed that Ag-graphene killed both S. aureus and K. pneumoniae while our other samples either had no effect on the bacteria or helped proliferate it. Confocal and optical microscopy also showed that Ag-graphene killed both the SCC's and the feeder cells (3T3's), while only killing the 3T3's for the D33's (Fig 1.). The other graphene samples either helped proliferate both types of cells, or made them unhealthy.

Future work will test the GO, prGO, and RGO samples with confocal microscopy and stain them with rhodamine to determine how many keratinocytes stayed attached to the tissue culture plastic.
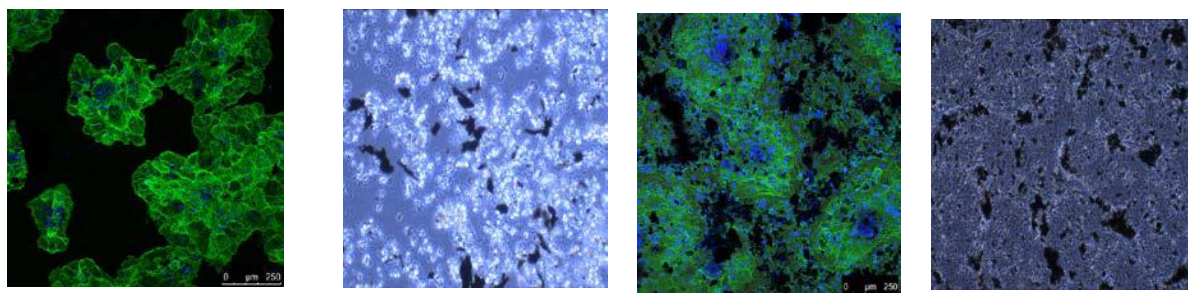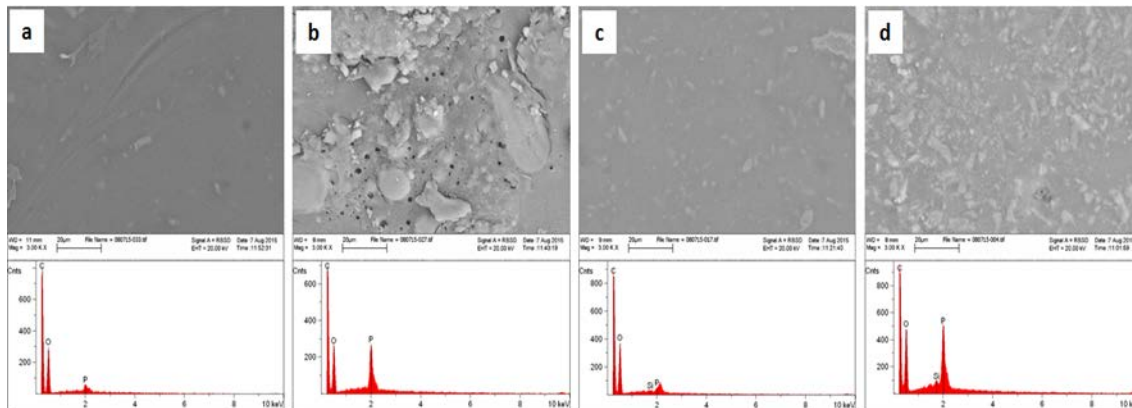

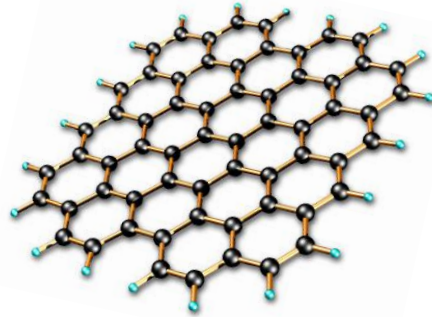Fig. 1: a) Confocal of Ag-Graphene. b) Optical of Ag-Graphene. c) Confocal of Pt-Graphene. d) Optical of Pt-Graphene

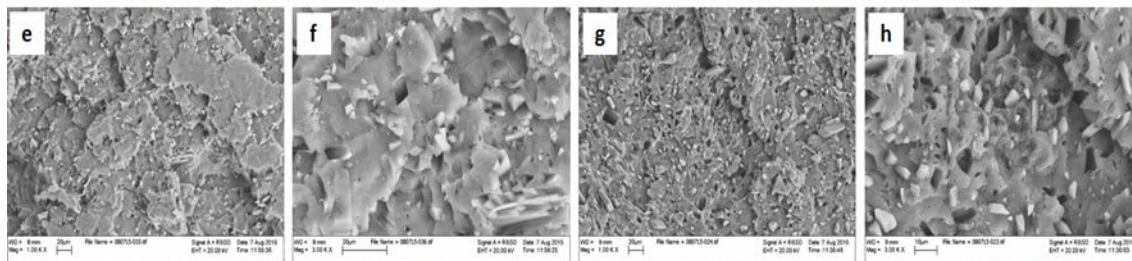# Session 7:   Nanocomposites

Yichen Guo, Yuan Xue, Xianghao Zuo : Graduate Supervisors

Tara Schinasi,
Stony Brook University

83PLA17MP: (a) Unburnt, (b) Burnt.   82PLA17MP1C-20A: (c) Unburnt, (d) Burnt.

83PLA17MP Fracture surface: (e) X1k, (f) X3k.   82PLA17MP1C-20A Fracture surface: (g) X1k, (h) X3k.

Mechanical and Chemical Properties of Flame Retardant Biodegradable Nanocomposites

Thomas Li[1], Aditya Mantri[2], Tara Schinasi,[3] Harry Shan He[3]

1. High Technology High School, Lincroft NJ 07738
2. Columbus North High School, Columbus, IN 47201
3. Stony Brook University, Stony Brook NY 11794

Previously, halogenated flame retardants were popular in fire prevention efforts. However, they have been shown to possess environmental and health hazards such as neurotoxicity that may result in death.[1] As a result, halogenated flame retardants have recently incurred bans across the world. Finding a safe and environmentally efficient flame retardant could offer potential in electronics and other plastic-based markets.

Combining the biodegradable polymers Polylactic Acid (PLA) and PBAT (Ecoflex), in an optimized ratio offers potential for a promising class of biodegradable polymer blends.[2] Resorcinol diphenyl phosphate (RDP) is used as the primary flame retardant in the polymer mixture, combined with micro-scale cellulose fibers in order to prevent dripping and ensure that it passes the UL-94 V0 test. Using the Izod Impact Test and the Instron Tensile Test, the different mechanical properties of Young's modulus of elasticity and toughness were analyzed at different concentrations of polymer ratios. Given the potential applications of polymeric flame retardants, the success of its impact toughness is vital to potential usage.[3] To determine the structural properties of the mixtures, FT-IR and cone calorimetry were utilized in order to begin investigation of the chemical mechanism of the flame retardant.

The results of the mechanical characterization of the polymer blends indicate that when the mass percentage of PLA in the polymer blend is near 30%, the impact toughness is maximized [Figure 1].
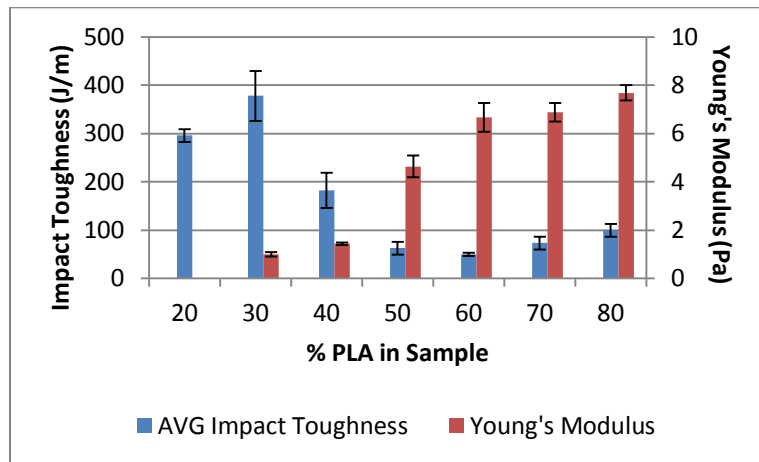
Figure 1: Impact toughness and moduli of PLA/PBAT blends

[1] Shaw, S. (2011). Halogenated Flame Retardants: Do the Fire Safety Benefits Justify the Risks? *Reviews on Environmental Health, 25*(4), 261-305.

[2] Campo, E. Alfredo. (2006). *The Complete Part Design Handbook.* Hanser.

[3] Jiang, L., Wolcott, M., & Zhang, J. (2006). Study of biodegradable polylactide/poly(butylene adipate-co-terephthalate) blends.*Biomacromolecules, 7*(1), 199-207.

# Engineering and characterization of novel, non-halogen, flame-retardant, biodegradable nanocomposites

Simon Zhuang, Dublin Jerome High School, Dublin, OH 43016; **Robert Evans**, Division Avenue High School, Levittown, NY 11756; **Yichen Guo**, Stony Brook University, Stony Brook, NY 11790

Polymers are used expansively around the world today for industrial and commercial purposes. Unfortunately, many polymers currently in use have several problems: they are not biodegradable and they burn easily. Flame retardants, which solve the latter problem, can pose new ones as well: halogen based flame retardants can be toxic.[1] Polylactic acid (PLA) is produced from biomass, and thus, is biodegradable. Melamine phosphate (MP) is a known halogen-free flame retardant and, when combined with nanoparticles, has been shown to be an effective flame retardant in various other polymers.[2]

To begin, the UL 94 flame test was conducted on pure PLA, confirming that PLA itself is not flame retardant. To determine the necessary MP concentration for flame retardancy, MP was mixed with PLA at concentrations ranging from 15% to 30%. Results show that at least 30% concentration of MP was necessary for the polymer to receive a grade of V_0. Next, the MP was reduced to 17% and a 1% of concentration of nanoparticle was added. Among graphene nanoparticles, halloysite nanotubes, and Cloisite C20A nanoclay, only C20A proved to be an effective additive in improving flame retardancy. Various concentrations of C20A and MP were then tested; the only sample to achieve V_0 flame retardancy was the sample of 82% PLA, 17% MP, and 1% C20A.

The mechanical properties of the newfound flame retardant samples were measured using the tensile test, impact test, DMA, and DSC. Tensile test results indicated that the modulus of each sample remained approximately equal. Results from the impact test, DMA, and DSC, on the other hand, all showed significant weakening with the addition of MP, but the addition of C20A increased the strength of the sample to approximately that of pure PLA. Therefore, due to decreased impact strength, the 70% PLA, 30% MP sample was eliminated as a viable option.

Figure 1 FTIR Results. Circled in red are missing MP peaks on the burnt sample
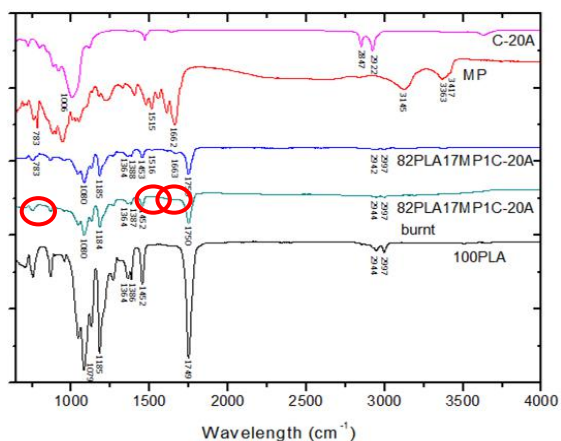
In order to determine the mechanisms by which the flame retardant nanocomposites work, several tests were performed. TGA confirmed the presence of a charring from phosphates, which protects the inside of the sample from thermal degradation. As shown in Figure 1, FTIR analysis demonstrates that melamine present in the unburnt sample no longer appears on the burnt sample: it becomes gaseous and lowers the oxygen availability. Finally, rheology results demonstrated that at 180°C, pure PLA demonstrates significantly lower viscoelastic properties in comparison to PLA with additives; MP and C20A increase viscosity and eliminate dripping during burning.

In the future, SEM imaging will be performed to examine the surface of the nanocomposites with C20A clay in comparison to pure PLA and the PLA and MP mixture. Other further research will include cone calorimetry testing, limit oxygen index testing, and TEM scanning to confirm the proposed mechanism and to understand more flame retardant mechanical properties. Possible applications for the flame retardant polymer include electronics casings to prevent fires caused from overheating, 3D printing filament to create flame retardant molds, and utensils for barbeque use.

References

[1]Rahman, F., Langford, K., Scrimshaw, M., Lester, J. (2001), Polybrominated diphenyl ether (PBDE) flame retardants. *Science of the Total Environment*, 275(1-3), (1-17).

[2]Si, M., Araki, T., Ade, H., Kilcoyne A. L. D., Fisher, R., Sokolov, J., Rafailovich, M. (2006), Compatibilizing Bulk Polymer Blends by Using Organoclays. *Macromolecules, 39, 4793-4801.*

Gas Permeability of HDPE and LDPE Nanocomposites

Justin Glickman HAFTR High School, Cedarhurst, NY 11516
Sam Plaut Rambam Mesivta High School, Lawrence, NY 11559
Xianghao Zuo Material Science Department, Stony Brook University

A popular way to change polymers' mechanical strengths and gas barrier properties is to add various nanoparticles, such as nano-clays into them. This project involves making various blends of polymers, clay nanoparticles, and graphene in order to try to optimize the gas permeability of our material to the limit that we desire. Our optimum gas permeability is as close to zero as possible, since what we are trying to make a material that can be used in food packaging, for example, and we don't want any air going in and out of the package. We used two different main polymers, HDPE (High Density Polyethylene) and LDPE (Low Density Polyethylene). We blended these polymers with various amounts of 20A, RDP, and Na^+ nano-clays, and C750 graphene. Each nanocomposite's gas permeability and tensile strength was tested, but only the HDPE samples were tested for impact strength because the LDPE would not break when tested.

The results of the gas permeability test for the HDPE indicate that the RDP and 20A nano-clays were the most effective in inhibiting gas flow through the polymer, and maintaining an aspect ratio that fits one of the curves in Nielsen's model of predicted trends in aspect ratio as a result of changes in volume fraction. The Na^+ nano-clay and the C750 graphene were ineffective at increased quantities with varying aspect ratios as seen in the graph (Figure 1). The impact results for the HDPE samples show that the HDPE + C-RDP samples, when the amount of nano-clay is increased, the impact strength remains roughly the same, which indicates that the RDP clay does not disrupt the crystalline structure of the base polymer

Figure 1: Gas permeability of HDPE nanocomposites as a relation of volume fraction to aspect ratio

(Figure 2). The RDP clay proved to be a better additive to the polymer than the 20A clay when accounting for both the gas permeability and the impact strength due to both its grea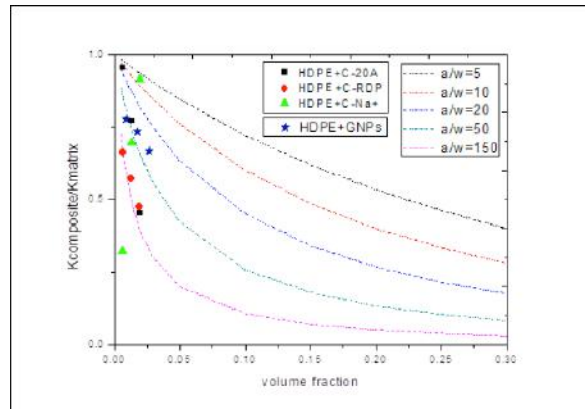ter immediate effect on the speed at which the gas passed through the samples, as well as its impact strength not suffering at increased concentrations of nano-clay. To further determine that the RDP clay did not disrupt the crystalline structure, we did a DSC (Differential Scanning Calorimetry) test to determine both the melting point, and more importantly the crystallinity. We determining through calculation that the crystallinity remained approximately the same, further indicating that the RDP clay did not in fact disturb the crystal structure of the HDPE. In the future we would like to test the HDPE with greater amounts of RDP clay in order to determine whether the gas permeability data will continue to follow the curve predicted by Nielsen's model, and if the crystalline structure will remain unaffected at higher concentrations, as well as compile the data acquired from the LDPE samples.
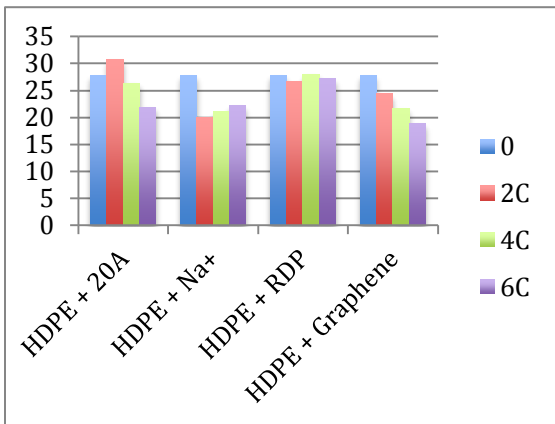

Figure 2: Impact Strength data showing the average impact strength in J/M (N) as a function of different nanoparticle concentrations in HDPE

References:

Amit Arora and G.W. Padua; *Review: Nanocomposites in Food Packaging;* Journal of Food and Science Vol. 75 Nr. 1, 2010 R43-R49

G. Choudalakis, A.D. Gotsis*; Permeability of polymer/clay nanocomposites: A review*; European Polymer Journal 45 (2009) 967-984

Compatibilization of Immiscible Polymer Blends Using Graphene

Evan Lander[1], Yuan Xue[2], Dr. Miriam Rafailovich[2]
[1]Plainview-Old Bethpage John F. Kennedy High School, Plainview, NY
[2]Dept. of Material Science and Engineering, Stony Brook University

Polymer blends have been one of the most prolific areas of polymer technology in the past five decades. They are used for a host of applications, ranging from the development of new, enhanced materials to recycling. Most polymer blends are immiscible, where the polymers do not mix with each other and the resultant blends have weak mechanical and thermal stability.[1] The most common approach to this problem is by the use compatibilizers, molecules that adhere the phases together and stabilize the blend. In this two-year study, the compatibilizing potential of the novel substance graphene is determined. The first phase of the study involved measuring the contact angle between the polymers in a thin film and calculating the Gibb's Free Energy of the blend systems. . Graphene decreased the contact angle and made the free energies negative, thereby making the systems prefer miscibility over phase-separation. The second phase of the study involves several characterization techniques (Transmission Electron Microscopy, Dynamic Mechanical Analysis, IZOD Impact, Tensile, and SEM) that will give further insight regarding graphene's compatibilization mechanism and implications.

The results confirmed graphene's effectiveness as a compatibilizer. TEM (only done for PS/PMMA) showed the graphene segregated to the PS phase; however, when 5% filler was added, the graphene moved to the interface (as shown in figure 1). Also, as more graphene was added, the domain size of the PS droplet decreased. These results allowed us to conclude that graphene at the interface is the reason for the blend's enhanced mechanical properties. The IZOD impact test (done only for EVA/HDPE blend) showed an increasing impact strength when more graphene was added and increased up to 50% with a 15% filler (as shown in figure 2). The tensile test showed that the modulus and ultimate tensile strength increased as more graphene was added, no matter what the ratio; the strain energy decreased as the material became more brittle. DMA showed storage modulus increases for both blends, especially when the blend had a 15% filler, as well as transition glass temperature increases in the PS/PMMA blend.
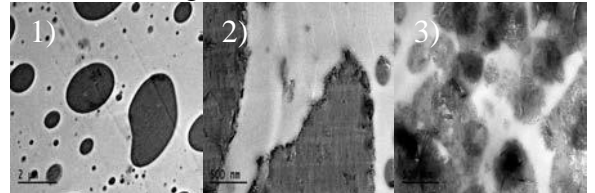

Figure 1: TEM images of PS/PMMA. Image 1 (no graphene) shows clear phase-separation and large domain size. Image 2 (5% graphene) shows that when graphene filler is added, it navigate to the interface of the polymers, resulting in decreased domain size and increased miscibility (evident in image 3, which contains a 15% filler).
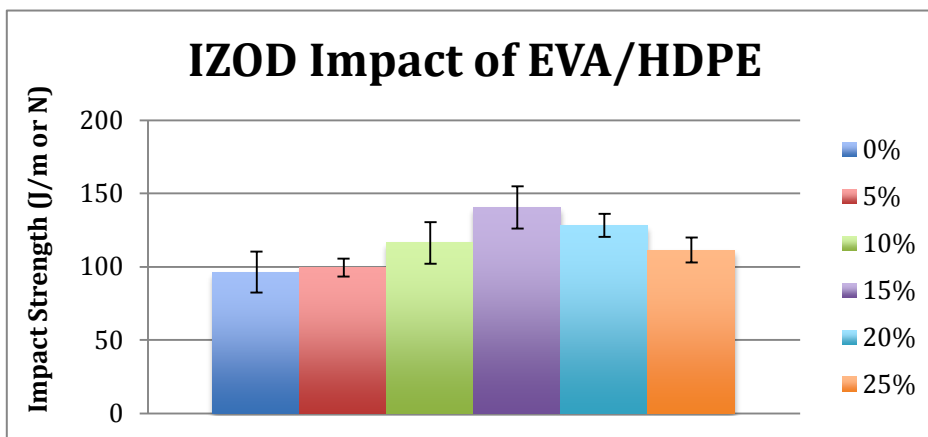

**Figure 2:** Impact strength results for EVA/HDPE with varying graphene concentrations. The impact strength was greater than the control for all blends containing graphene and a maximum impact strength was achieved with a 15% filler.

1. Si, M., Araki, T., Ade, H., Kilcoyne, A. L. D., Fisher, R., Sokolov, J. C., & Rafailovich, M. H. (2006). Compatibilizing bulk polymer blends by using organoclays.Macromolecules, 39(14), 4793-4801.

Session 8:   Nanotoxicology

Yan Xu, Fan Yang : Graduate Supervisors

Briana Friedman, Stern College for Women at Yeshiva University
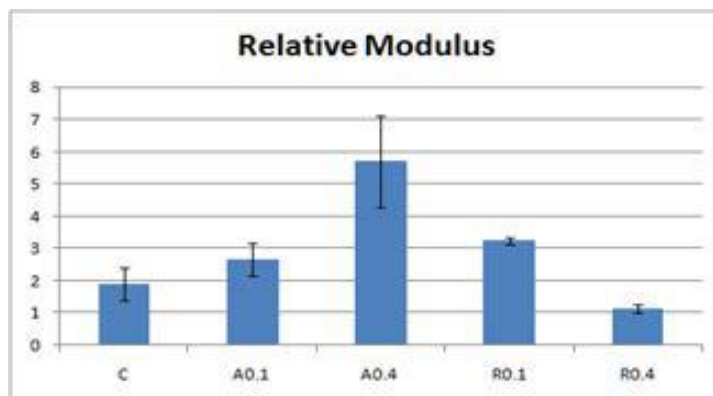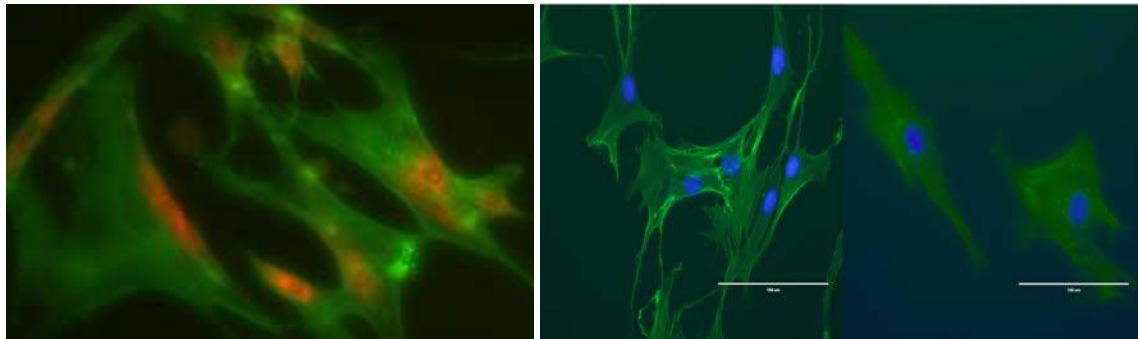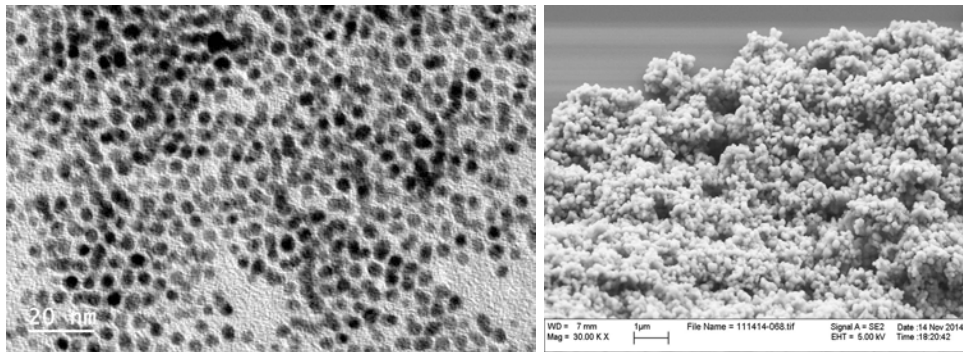
Toxicology of RDP-mixed Polymers on Human Dermal Fibroblast Cells

Walt Leung[1], Jae Yang[2], Fan Yang[2], Tatsiana Mironava[2], Miriam Rafailovich[2]

[1]Piedmont Hills High School, San Jose, CA 95132 [2]Garcia MRSEC, SUNY Stony Brook, NY 11794

Within the past half-century, many flame retardants – most notoriously organohalogenic compounds – have been proven highly toxic to the human body[1]. Consequently, RDP – resorcinol bis(diphenylphosphate) – and other members of the organophosphate family, which have been researched and shown benign by some studies[2], have begun to replace the older models of halogen-based flame retardants. However, with limited research on the organophosphate family, it cannot be said with certainty that they are completely non-toxic.

In this research project, the toxicology of RDP on green fluorescent human dermal fibroblast cells was analyzed through cell counting and fluorescent microscopy. This was accomplished by plating green fluorescent fibroblast cells onto polymer scaffolds of Na+-Clay-PS (Polystyrene) alongside Na+-Clay-RDP-PS and pure PS, as shown in Figure 1. The control sample was an industrial-grade plasma irradiated cell well. In addition, SEM was used to analyze the polymer surfaces.
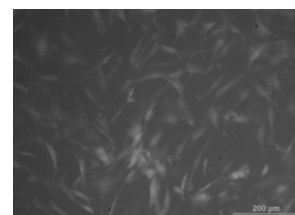

Figure 1 – Fluorescent microscopy showing green fibroblast cells on a polymer scaffold

From the data collected by the daily cell counts shown in Figure 2, the RDP-based samples trended similarly with the control samples from Day 1 to Day 4. Thus, it can be said that the RDP-mixed polymers were non-toxic and can be used as a substitute for the industrial-grade wells for cell culturing. However, in order to further test this hypothesis, other variables would need to be tested, such as differing concentrations of RDP and culturing on different polymers such as PMMA.
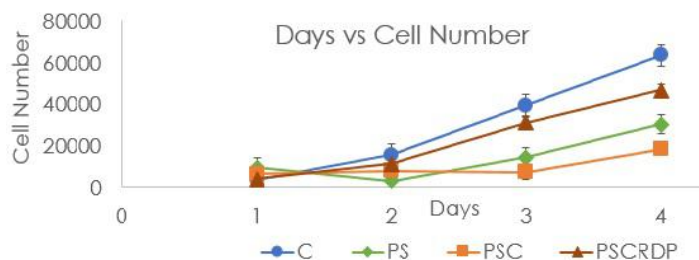
Figure 2 – Cell numbers from Day 1 to Day 4

---

[1] Roze, Elise. "Prenatal Exposure to Organohalogens, Including Brominated Flame Retardants, Influences Motor, Cognitive, and Behavioral Performance at School Age." *Environmental Health Perspectives*117.12 (2009): 1953-958. *JSTOR*. Web. 06 Aug. 2015.

[2] Veen, Ike Van Der, and Jacob De Boer. "Phosphorus Flame Retardants: Properties, Production, Environmental Occurrence, Toxicity and Analysis." *Chemosphere* 88.10 (2012): 1119-153. Web.

Cytotoxic Effects of TiO$_2$ Nanoparticle Exposure on Adipose-derived Stromal Cell Susceptibility to Bacterial Infection

Oliver Xu[1,2], Natalie P. Tan[1,3], Jeremy Silverman[1,4]
Collaborators: Yan Xu[1], Briana Friedman[5], Dr. Tatsiana Mironava[1], Dr. Miriam Rafailovich[1]
[1] Garcia Program, Stony Brook University, 100 Nicolls Road, Stony Brook, NY 11790
[2] Edina High School, 6754 Valley View Road, MN 55439
[3] Herricks High School, 100 Shelter Rock Road, New Hyde Park, NY 11040
[4] South Side High School, 140 Shepherd Street, NY 11570
[5] Stern College for Women, 245 Lexington Avenue, New York, NY 10016

Titanium dioxide (TiO$_2$) nanoparticles form a characteristic white pigment and are found in many consumer products, such as sunscreen, toothpaste, paints, plastics, paper, food coloring, cosmetics, catalysts, drugs, lacquers, and varnishes.[1,2] Due to the extent of its availability, questions have been raised concerning the toxicity of TiO$_2$ nanoparticles. Prior studies have found that nanosized and ultrafine TiO$_2$ particles can generate pulmonary fibrosis and lung tumors in rats, as well as showing cytotoxic effects in rat lung alveolar macrophages.[1] A recent study described the genotoxicity induced by TiO$_2$ nanoparticles in human epidermal cells via DNA damage, micronuclei formation, glutathione decrease, and lipid hydroperoxide and reactive oxygen species increase.[2] However, considering its widespread use and increasing exposure, relatively little is known about the cytotoxic effects of TiO$_2$ nanoparticles on human cells. Adipose-derived stromal cells (ADSCs) are a heterogenous mix of cells found within the stromal vascular fraction of adipose tissue and are capable of differentiating into fat, bone, cartilage, muscle, and nerve tissue.[3] The purpose of this experiment was to determine the effects of anatase and rutile TiO$_2$ nanoparticles on these cells' vulnerability to infection by *Staphylococcus aureus*.

Cells were washed with DPBS and, after trypsinization, were plated in 6-well culture plates using DMEM. After 24 hours of incubation, cells were exposed to 0.1 mg/mL and 0.4 mg/mL of both anatase and rutile TiO$_2$ nanoparticle solution. Cells were originally incubated for 24 hours, but after inconclusive confocal microscopy results, incubation time was increased to 72 hours. *S. aureus* were prepared in brain heart infusion broth, and the solution was added to each culture in a thousand to one bacteria to cell ratio. Nanoparticle exposed-bacteria infected-cells were sent to Dr. Stephen Walker for colony counting. Another sample of nanoparticle-exposed bacteria infected-cells were stained with LIVE/DEAD BacLight Bacterial Viability Kit fluorescent dye to be studied under the confocal microscope. A third sample of cells was stained with LIVE/DEAD dye to be examined under the fluorescent microscope. A fourth batch of cells was fixed with 3.7% formaldehyde and washed with DPBS and 0.4% Triton. Cells were then stained with Alexa Fluor 488 Phalloidin and Propidium Iodide to be examined via fluorescent microscopy. Zeta potential measurements and atomic force microscopy were also conducted.

Our results demonstrated that as the nanoparticle concentration increased, the number of bacteria attached to the cells also increased (Figure 1). Zeta potential results also confirmed our use of medium instead of water to dissolve the TiO$_2$ nanoparticles. Atomic force microscopy, used to measure the cell membranes' modulus, indicated that the cells exposed to rutile TiO$_2$ nanoparticles at a concentration of 0.4 mg/mL had the softest membranes, while those exposed to anatase TiO$_2$ nanoparticles had harder membranes compared to the control. However, due to the large margin of error present in the atomic force microscopy data, it may not be reliable. Similarly, confocal and fluorescent microscopy results were also inconclusive due to lack of incubation time and unhealthy bacteria samples, respectively (Figure 2). In the future, we would like to conduct tests on the adipocyte cells that we differentiated. We would also like to test other nanoparticles such as platinum and see their effects on preadipocytes and other types of cells.
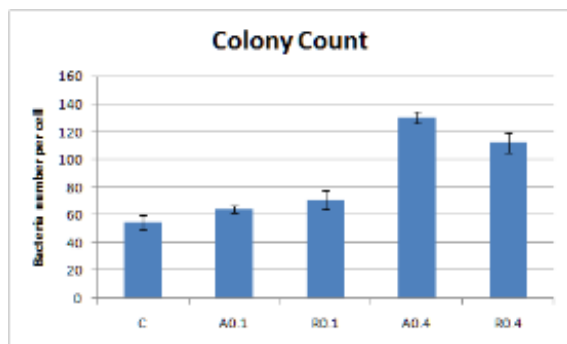

Figure 1 Colony count sent by Dr. Stephen Walker was analyzed to determine the amount of bacteria adhered to each cell.
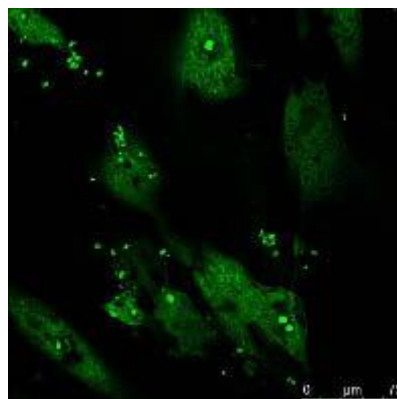

Figure 2 Confocal microscopy of *S. aureus* adhered to ADSC membrane with LIVE/DEAD stain. Cells were incubated with 0.4 mg/mL rutile TiO2 nanoparticles for 24 hours.

[1] Wang, Jing J.; Sanderson, Barbara J.S.; Wang, He. 2007. Cyto- and genotoxicity of ultrafine TiO$_2$ particles in cultured human lymphoblastoid cells. Mutation Research 628:99-106.
[2] Shukla, Ritesh K.; Sharma, Vyom; Pandey, Alok K.; Singh, Shashi; Sultana, Sarwat; Dhawan, Alok. 2011. ROS-mediated genotoxicity induced by titanium dioxide nanoparticles in human epidermal cells. Toxicology in vitro, 25(1):231-241.
[3] Tholpady SS, Llull R, Ogle RC, Rubin JP, Futrell JW, Katz AJ. 2006. Adipose tissue: stem cells and beyond. Clin Plast Surg 33(1):55–62.

Effect of cell donor age on the cellular response to nanoparticle exposure

Hyun Jo Kim[a], Andrew Adelhardt[b], Fan Yang[c], Tatsiana Mironava[c]

a. St. Paul's School, 325 Pleasant Street Concord, New Hampshire 03301
b. Paul D. Schreiber High School, 101 Campus Drive, Port Washington, New York 11050
c. Department of Materials Science and Engineering, Stony Brook University, Stony Brook, NY, 11794

Nanotechnology is an emerging field in consumer items, medical devices and electronics. Studies have shown the size of these particles enable them to penetrate deep into skin and absorb into human cells.[1] Despite these findings, relatively little is known on the long-term effects or immediate toxicity of these particles. Gold nanoparticles (Au NPs) have been introduced in clinical trials as radiosensitizers, NMR contrast enhancers and also drug delivery systems. Since cell characteristics and mechanics alter dramatically as the cell ages, research on the impact of AuNP's on a variety of aged cells is critical.

This study examined human dermal fibroblasts of the neonatal stage, the late twenties or early thirties and in the eighties. This wide disparity between the values was designed to span the majority of cell characteristics of human life. Previous studies revealed the diameter of the particles and concentration affected cell response, thus two different sizes (17 nm and 36 nm), and three different concentrations (50, 100, 150 µL/mL) were used. The nanoparticles were synthesized using the citrate reduction method, and size distribution, stability and diameter were confirmed with DLS, Zeta Potential and TEM, respectively.
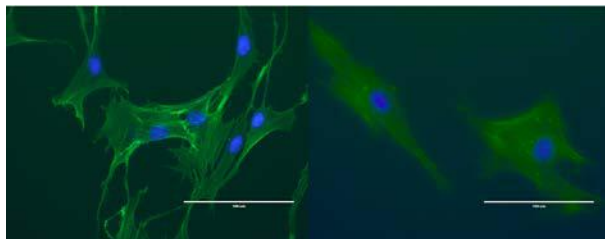

Figure 1: Flourescent microscopy demonstrates the contraction of actin fibers due to nanoparticle exposure. Left image are control cells. Right image are cells exposed to large nanoparticles at 150 µL/mL.

Cell response and mechanical change was measured using proliferation, modulus, uptake and also fibrinogen content. Proliferation revealed in all ages, cell growth was consistently limited as particle size and concentration increased. Cell count also revealed the neonatal was most resistant to the particles, followed by cells in the thirties. This was expected as neonatal cells have a natural growth rate faster than the other two age groups. The higher count of the younger cells also resulted in the dilution of the nanoparticle concentration, likely reducing toxicity. Using proliferation data, the doubling time of each concentration was calculated. In most circumstances, doubling times were lower compared to the control as the concentration and particle size increased. In terms of different ages, the doubling time of the older cells decreased more significantly than younger cells in comparison to their respective controls. Tests under the fluorescent microscope revealed actin contraction and deformation when exposed to increasing concentration and size of the AuNP's, displayed in Figure 1.The control appeared more elongated compared to cells exposed to nanoparticles. Future studies include nanoparticle uptake and cell survival rate analysis. Results show that cell growth is hindered and the mechanics of the cell are altered when exposed to gold nanoparticles. Increasing both the size and concentration of the nanoparticles yields greater toxicity and more dramatic effects on cell functionality.

---

[1] Tatsiana Mironava, Michael Hadjiargyrou, Marcia Simon, Vladimir Jurukovski, Miriam H. Rafailovich. Gold nanoparticles cellular toxicity and recovery: Effect of size, concentration and exposure time. *Nanotoxicology* (2010) 4(1), 120-137

[2] Nadine Pernodet, Xiaohua Fang, Yuan Sun, Asya Bakhtina, Aditi Ramakrishnan, Jonathan Sokolov, Abraham Ulman, and Miriam Rafailovich. Adverse Effects of Citrate/Gold Nanoparticles on Human Dermal Fibroblasts. *Small 2006* (6),766-773

Session 9: DNA

Ke Zhu,Na Hyun Cho: Graduate Supervisors

Alyssa Auerbach, Stern College for Women at Yeshiva **Won Park,** Stony Brook University;
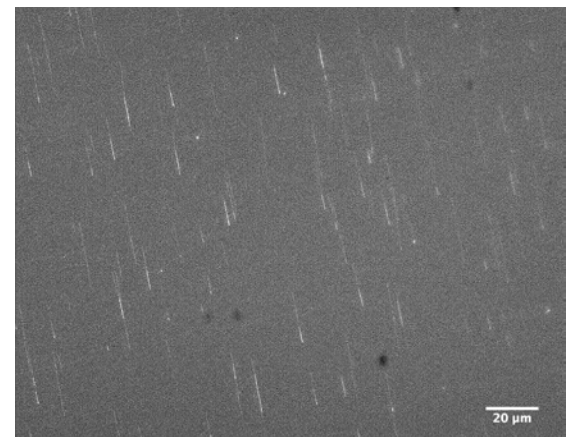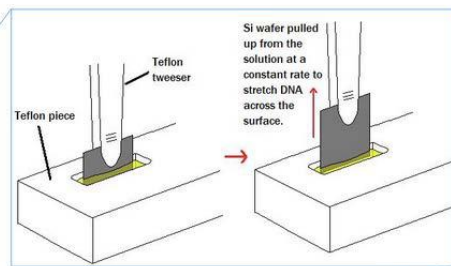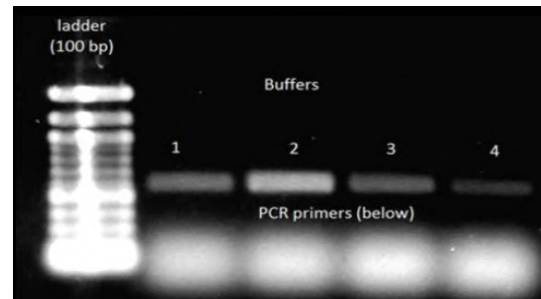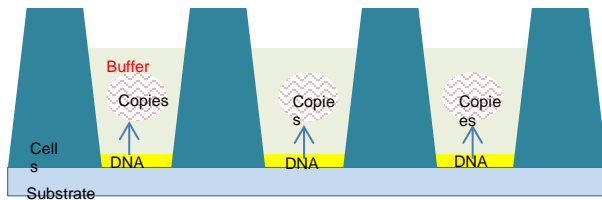
Novel DNA Sequencing: Comparison of 4 types of NEB buffers to desorb DNA molecules from PMMA surfaces

George Yang[1], BASIS Scottsdale High School[1], Scottsdale, AZ 85259
NaHyun Cho,[2] Julia Budassi,[2] Ke Zhu,[2] Dr. Jonathan Sokolov[2]
Stonybrook University[2], Stonybrook, NY 11794

Gene sequencing's various applications include analysis of cancer-causing mutations, examining the malaria genome, and studying epigenetic modifications to the genome (Mardis, 2011, Quail, 2012). Next-generation sequencing, or massively parallel sequencing, analyzes multitudes of DNA strands simultaneously. Each year, it increases in accuracy and efficiency, improving its uniformity of coverage, error rate, and read length (Mardis, 2011, Quail, 2012).

However, Next Generation methods rely on costly data analysis (Mardis, 2011). Currently, DNA is cut randomly, then inserted into the sequencer (Kurosawa & Washizu, 2007). Thus, it depends on processing to assemble the fragments into their original order, adding to the cost and error of sequencing (Kurosawa & Washizu, 2007).

A method of avoiding random-fragments data analysis is by stretching DNA molecules onto a Polymethyl methacrylate (PMMA) surface, cutting the DNA, and removing it in an ordered way. DNA molecules can be adsorbed on the PMMA substrate by "combing" (Nazari & Gurevich, 2012, Liu et. al., 2004). The meniscus force and adhesion force between the DNA molecules and the PMMA surface stretch the DNA linearly onto the PMMA surface (Nazari & Gurevich, 2012). The adsorbed DNA can then be cut in an ordered way with soft lithography technology. In the past, through microcontact printing, DNA molecules have been deposited onto a polymer surface using a polydimethylsiloxane (PDMS) stamp (Lange et. al., 2004). Likewise, a PDMS stamp coated with deoxyribonuclease enzyme (DNAse) as "ink" may be used to cut the DNA in an ordered way.

The motivation of this project was to improve the sequencing method. Holey carbon microarrays have been constructed through microcontact printing (Chester, et al. 2007). To remove the DNA from the surface of the PMMA while maintaining the order of the DNA, such a holey stamp could be put over the PMMA surface that has DNA combed onto it. Thus, DNA could be desorbed into the hole of the microarray stamp. Hence, the main obstacle to orderly removal of DNA from the PMMA surface is finding a buffer that would efficiently desorb the DNA.

The aim of this project was to compare the efficiencies of four standard enzyme digestion buffers from New England Biolabs to remove DNA from a PMMA surface.

The DNA removed is still of such a small quantity that it needs to be amplified for gel electrophoresis, so we amplified it through PCR. The results of the test on these four buffers is shown in Figure 1. In particular, Buffer 2 was around two times more efficient at desorbing the DNA than the other buffers tested.

Likely, the different NaCl concentrations within the buffers caused the different desorption efficiencies. NaCl neutralizes the phosphate backbone of the DNA, reducing the electrostatic interaction between the DNA and the PMMA surface.

We estimate the amount of DNA obtained through PCR was on a nanogram level.
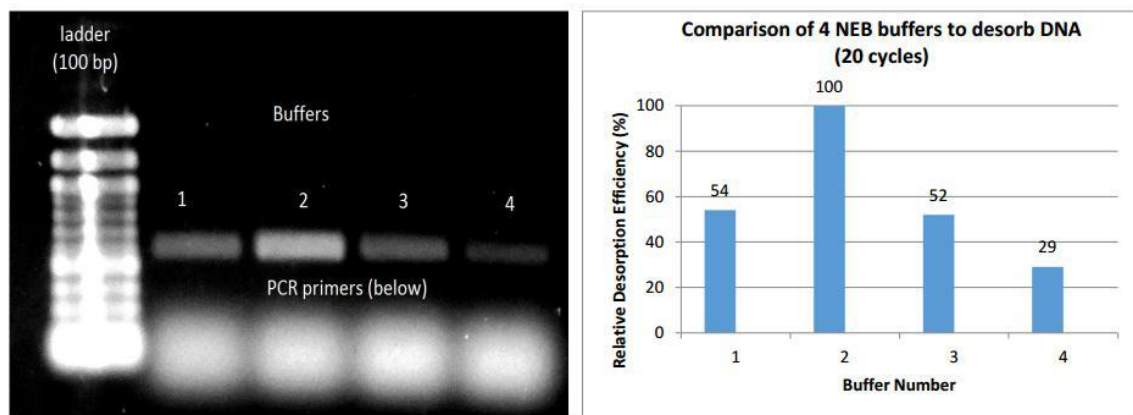

Figure 1. Gel electrophoresis for amplified 600bp lamba DNA with 4 standard NEB Buffers

References

Chester, D. W., Klemic, J. F., Stern, E., Sigworth, F. J., & Klemic, K. G. (2007). Holey carbon micro-arrays for transmission electron microscopy: A microcontact printing approach. *Ultramicroscopy*, *107*(8), 685–691. doi:10.1016/j.ultramic.2007.01.004

Kurosawa, O., & Washizu, M. (2007). Dissection, acquisition and amplification of targeted position of electrostatically stretched DNA. *Journal of Electrostatics*, *65*, 423–430. doi:10.1016/j.elstat.2005.03.094

Liu, Y., Wang, P., Dou, S., Wang, W., Xie, P., Yin, H., . . . Xi, X. G. (2004). Ionic effect on combing of single DNA molecules and observation of their force-induced melting by fluorescence microscopy. *Chemical Physics*, *121*(9), 4302-4309. doi:10.1063/1.1777220

Mardis, E. R. (2011). A decade's perspective on DNA sequencing technology. *Nature*,*470*, 198-203. doi:10.1038/nature09796

Nazari, Z. E., & Gurevich, L. (2013). molecular combing of DNA: methods and applications. *Journal of Self-Assembly and Molecular Electronics*, *1*, 125-148. doi:10.13052/same2245-4551.116

Quail, M. A., Smith, M., Coupland, P., Otto, T. D., Harris, S. R., Connor, T. R., . . . Gu, Y. (2012). A tale of three next generation sequencing platforms: comparison of Ion Torrent, Pacific Biosciences and Illumina MiSeq sequencers. *BMC Genomics*, *13*(341). doi:10.1186/1471-2164-13-341

Synthesis of an Ideal Silane Surface for DNA Adsorption and Desorption

Sean Donnelly, South Side High School
Alyssa Auerbach, Stern College for Women at Yeshiva University
Julia Budassi, Department of Materials Science and Engineering, Stony Brook University
Dr. Jonathan Sokolov, Department of Materials Science and Engineering, Stony Brook University

The goal of this project is to develop a way to cut DNA into segments of known lengths so that DNA sequencing by Next Generation sequencing technologies can be streamlined. DNA sequencing has significant applications in many fields, including personalized medicine and forensics, and improving the process has far-reaching implications. Currently, most methods of DNA sequencing involve cutting the DNA sample randomly by sonication, amplifying the DNA fragments, and using overlaps in the fragments' sequences to determine where the pieces go in the overall sequence.[1] This process is time consuming and requires a great deal of data processing for assembling the sequences, particularly in genomes with long stretches of repeats. Cutting the DNA while preserving the order of cut pieces would resolve this problem, as the origins of the individual pieces could be easily identified. This lab has attempted to do this by combing the DNA onto a surface, cutting it using soft lithography, removing it from the surface, and amplifying the ordered fragments. Our work specifically aims to develop a silane surface onto which DNA can be combed and from which the fragments can be removed easily using distinct buffer solutions for each process.

We varied multiple factors in order to develop an optimal silane surface for adsorption. Silicon wafers were silanized with (3-aminopropyl)triethoxysilane (APTES) in small Teflon® tubs at ambient temperature for varying lengths of time. Phosphate buffered saline (PBS) and toluene were used as solvents with varying concentrations of APTES. Results indicated 0.5% APTES dissolved in PBS silanized for 70 minutes produced the smoothest surfaces. After finding an optimal silanization method, we incubated the surfaces with glutaraldehyde and bovine serum albumin (BSA) in a humidity chamber.[2] DNA was combed onto the surface by withdrawing the surfaces from DNA solution at a constant speed. Both the dye used to observe DNA as well as the concentration of DNA in lanthanum (III) chloride solution were varied.

Fluorescence microscopy results, depicted below in Figure 1, show that DNA can be combed onto a silicon surface silanized for 70 minutes with 0.5% APTES in PBS and incubated with glutaraldehyde and BSA. However, the DNA depicted in the figure (the dimmer bright spots) is not as linear nor as dense as was expected, although it was shown that higher concentrations of DNA in solution led to higher density on the surface. No significant differences were observed between the two dyes used, YOYO-1 and SYBR® Gold.

Future work will include varying the concentration of lanthanum (III) chloride solution used to dissolve the DNA to obtain linearized DNA on the surfaces, and attempting to desorb the DNA from the surface using poly(acrylic acid) (PAA). We speculate the 4mM lanthanum (III) chloride solution used may be too concentrated, leading to shearing of the DNA. Using a less concentrated lanthanum chloride solution, and preparing fresh DNA solutions may resolve this problem. Once the DNA has been linearized on the surface, we will attempt to remove the DNA to determine its viability for usage in cutting DNA using soft lithography.
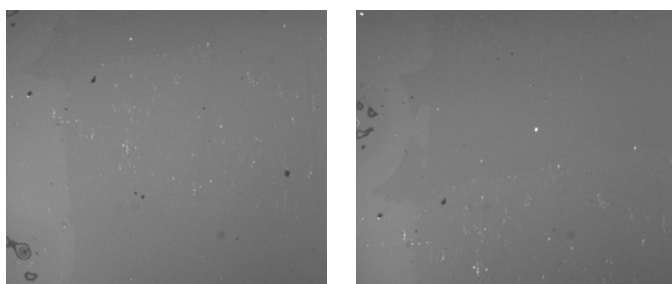

Figure 1: Images of combed DNA on a silanized
surface taken using a confocal microscope

s

[1] Adams, Jill U. "Complex Genomes: Shotgun Sequencing." *Nature.com*. Nature Publishing Group, 2008. Web. 06 Aug. 2015.

[2] Koota, J., I. Seuffert, H. Li, R. Lehner, and T. Gisler. "Reversible, Meniscus-Free Molecular Combing of Long-Chain DNA." *Langmuir*. American Chemical Society, 25 June 2007. Web. 06 Aug. 2015.
Nicholas, M., Rao, L., Gennerich, A. (2014). Covalent immobilization of microtubules on glass surfaces for molecular motor force measurements and other single-molecule assays. National Institutes of Health Public Access. 1136: 137-169.

Combing and removing DNA from Coated Silicon Wafers.

Demian Zuric[1], Jonathan Sokolov[2]

[1]Ward Melville High School, East Setauket NY 11733, [2]Stony Brook University, Stony Brook, NY

Sequencing DNA is a subject with broad application in many fields of research. The current methods of sequencing however, only works for small segments of DNA. The original strand of DNA must be cut small enough for direct sequencing and then the sequenced fragments must be reassembled. This process is very tedious and takes a long time. The goal of our research was to desorb DNA after combing it onto Silicon surfaces, and maintain the order of the DNA segments even after cutting them. We tried two different methods to desorb the DNA: One was to denature DNA on PMMA-coated Silicon surfaces using a formamide solution. The other was using a different buffer, to try to desorb DNA from silane-coated surfaces.

Both processes involved cutting Silicon surfaces into 1cm X 1 cm squares and then cleaning them with deionized water. Next they were cleaned with an Ammonium Hydroxide, Hydrogen Peroxide and Deionized water solution followed by cleaning in a Sulfuric acid, hydrogen peroxide and deionized water solution. Then a PMMA solution is made in toluene (15mg/ml) and it is spin-casted at 2500 rpm onto the silicon surfaces. The PMMA surfaces were then annealed at 130 degrees Celsius for 2 hours. The DNA solution is made, first by heating 10 microliters of YOYO-1 (which allows the DNA to fluoresce), 20 microliters of DNA and 180 microliters of a buffer made of 0.1 molar NaOH and 0.02 MES solution (which we varied the concentrations of to try and improve results) for 1-2 hours at 45 degrees Celsius, and then diluting it with 1790 microliters of the same buffer. The PMMA surfaces are then dipped in this DNA solution. We then visually confirm if the DNA has been combed onto the surface with fluorescent microscopy. We then attempted to desorb the DNA by denaturing it with a Formamide and SSC Buffer solution, with concentrations of 7:3 and 1:1 (by volume) to test which provided better results. We tested various bathing times and temperatures for the silicon surfaces in the formamide solution to find which combination yielded the most efficient desorption.

After the cleaning with deionized water, the surfaces to be coated with silane were heated in Piranha solution (60% Sulfuric acid, 40% Hydrogen Peroxide) for 15 minutes, and then sonicated in chloroform for 15 minutes to clean them. After being rinsed with deionized water again and air dried, they were put in a salinization solution overnight and then cleaned once again with chloroform and deionized water. While it sat in the salinization solution overnight, a DNA solution, similar to the PMMA one but with TE buffer, was made for the Silicon surface to be dipped into. After The dipping and visual confirmation, we used phosphate and sodium buffers to desorb the DNA on the silicon surfaces.

Due to time restraints, we didn't get to test as many variable with the silane-coated surfaces and the process associated with it. Given the opportunity to do further research, I would like to see what results would occur by varying some part of the procedure.
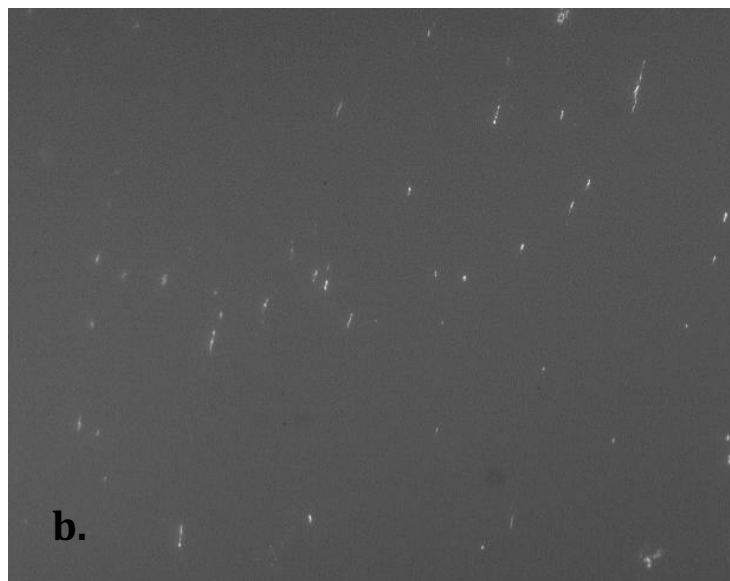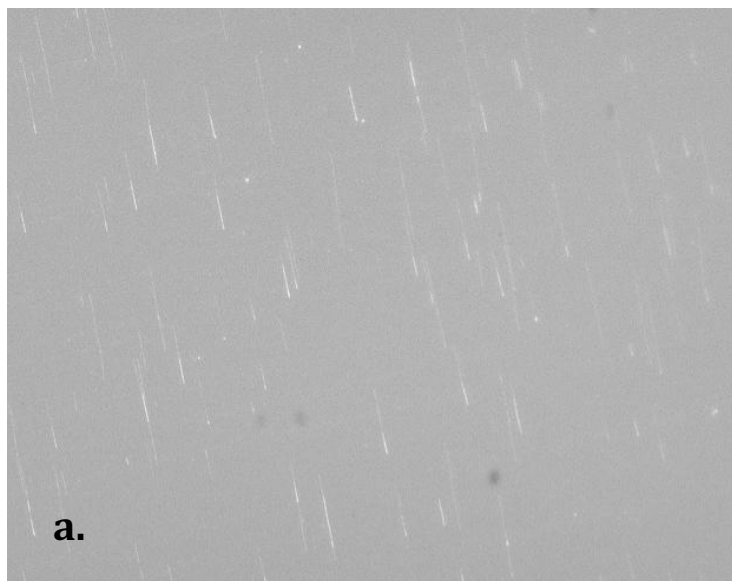

Figure 1: a. DNA on a PMMA coated surface prior to formamide bath (40X lens) b.Left over DNA after formamide treating of PMMA Coated surface (40x lens)
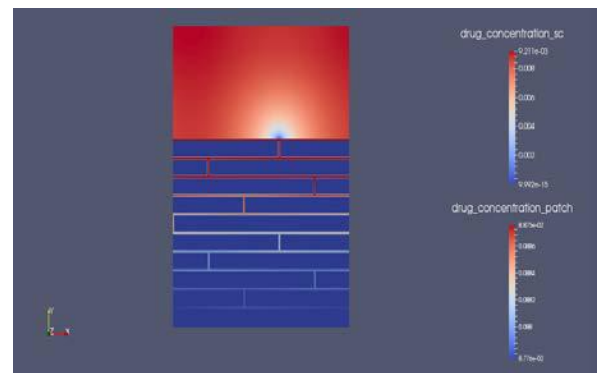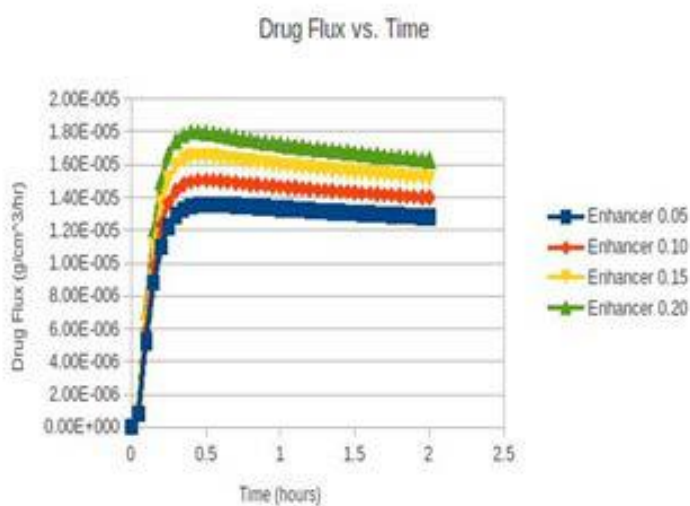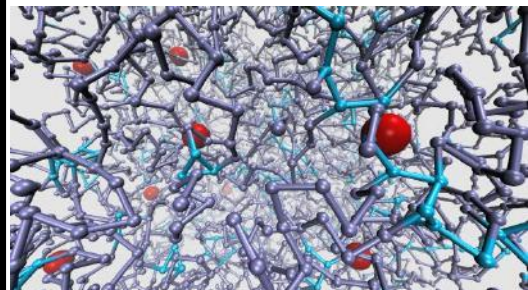
Session 10: Computational Analysis

Di Xu : Graduate Supervisor

Julia Landsberg, CUNY-Queens College

Computer Aided Diagnosis of Breast Lesions from Ultrasound Images

Andrew Zuckerman[1], Alice Wu[2], Allan Tannenbaum[3], Liangjia Zhu[3], Miriam Rafailovich[4]
[1]The Wheatley School, Old Westbury, NY, 1568   [2]Half Hollow Hills West, Dix Hills, NY, 11746
[3]Department of Computer Science, Stony Brook University, Stony Brook, NY, 11794
[4]Department of Materials Science and Engineering, Stony Brook University, Stony Brook, NY, 11794

Breast cancer is the second leading cause of cancer death in women in the United States[1]. However, early detection of breast cancer through screenings has the potential to halt its development. Once a palpable mass or abnormality is found in a routine examination or mammogram, an ultrasound breast image can be taken to more closely examine the lesion. Although ultrasound imaging has increased sensitivity to the detection of cancerous lesions, it also has increased the number of false-positives diagnosed by doctors, which has led to unnecessary biopsies and worry for patients, making some medical doctors question the efficacy of using ultrasounds for breast cancer diagnosis at all[2].

The purpose of this study is to determine if a computer can accurately classify a breast lesion from an ultrasound image as either benign or malignant. A similar goal is thus objectively quantifying the lesion and removing any human subjectivity in diagnosis. Although the machine learning phase of this project has not been conducted yet, the images have already been processed — methodologies and results will be displayed below.

The ultrasound image collection that is being used contains 269 benign lesions and 232 malignant lesions from the Gelderse Vallei Hospital's public, online database. Each image is smoothed with an anisotropic filter, thresholded, and then opened morphologically. The largest object in the image remaining serves as a mask for active contour modeling, which is the chosen technique used to segment the lesion from the ultrasound image. The characteristics that are being targeted from the lesion include: smoothness/irregularity of boundary, homogeneity, eccentricity, and orientation.

This image processing technique has led to clear segmentations and specific metrics which both can be seen to the right. Figure 1 contains the original image while Figure 2 contains the segmented image. L^2/A is the ratio between the square of the perimeter of the region and the region's area. The eccentricity and orientation are derived from an ellipse that has the same second-moments as the segmented region.
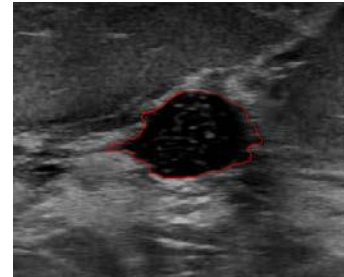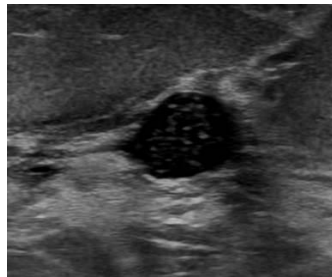

Figure 1: Original Image

Figure 2: Segmented Image

Metrics
L^2/A = 19.5408
Eccentricity = 0.77362   Orientation = 8.5347 degrees
Mean of Lesion Pixels = 0.043924   Standard Deviation of Lesion Pixels = 0.055179

The research conducted thus far suggests that benign and malignant lesions each demonstrate different, measurable physical qualities when imaged through ultrasound. Our technique can thus help doctors more objectively diagnose breast lesions. Once the machine learning aspect of our project is performed, we will be able to assess whether a computer can accurately diagnose breast cancer from ultrasound image.

---

[1]What are the key statistics about breast cancer? (2015, June 10). Retrieved from American Cancer Society website: http://www.cancer.org/cancer/breastcancer/detailedguide/breast-cancer-key-statistics

[2]Berg WA, Blume JD, Cormack JB, et al. Combined Screening With Ultrasound and Mammography vs Mammography Alone in Women at Elevated Risk of Breast Cancer. *JAMA*. 2008;299(18):2151-2163.

Lattice Boltzmann Modeling of Coupled Diffusion in Transdermal Drug Delivery: A Computational Analysis of the Effects of Permeation Enhancers on Drug Diffusion

Jonathan Jow[1], Ning Sun[2], Dr. Dilip Gersappe[2], and Dr. Miriam Rafailovich[2]

[1]Phillips Academy, Andover, MA; [2]Department of Materials Science and Engineering, Stony Brook University, Stony Brook, NY, 11790

Systemic delivery of drugs via transdermal patches offers multiple advantages over the traditional method of oral dosage, most notably in the avoidance of presystemic metabolism in the gastrointestinal tract and liver, a near constant drug release rate that can maintain concentrations of drug in the plasma for days, and increased patient compliance.[1] For development and optimization of these patches, it is important to understand the mechanisms underlying multicomponent nonlinear drug permeation across the skin. The presence of various diffusing components is vital, as many transdermal drug delivery formulations contain permeation enhancers in addition to the drug, which temporarily loosen the crystallized structure of the lipid matrix to increase the diffusivity of the drug.[2] The primary objective of this study is to observe the effects of varying permeation enhancer concentration on the diffusive properties of the system.

The Lattice Boltzmann method is employed to simulate two-dimensional drug diffusion from a reservoir of fentanyl (drug) and oleic acid (enhancer) into the skin's primary defensive barrier and outermost layer, the stratum corneum (SC) (Figure 1). The SC has a biphasic structure composed of impermeable corneocytes that are embedded within an ordered lipid matrix in which drugs can diffuse. The Bhatnagar-Gross-Krook (BGK) operator and Fick's Laws of Diffusion are used to model the fluid dynamics of the system, and solutions to Fick's Laws are approximated through the central finite differences method. The model is then optimized to minimize computational time by decreasing its size while maintaining less than a 1% margin of error.

The drug flux of the system, a measure of the amount of drug diffusing through the base of the SC per time interval, is examined as an indicator of drug transfer rate. Results suggest that increasing the concentration of permeation enhancer raises the peak drug flux value and decreases the time necessary to attain this peak. Further simulations will also be run to test the viability of the existing homogenization method as a means to simulate diffusion through the SC.
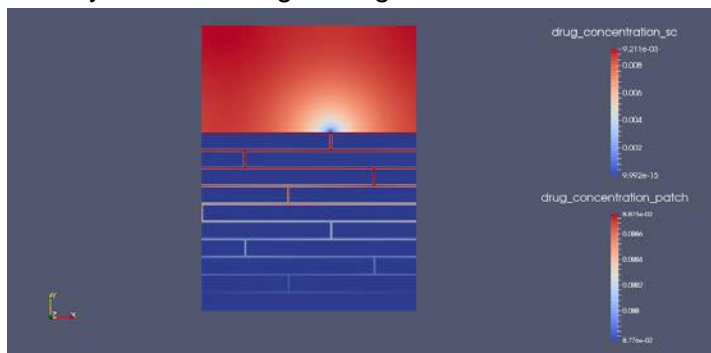
Figure 1: Drug concentration in patch and stratum corneum, 0.1 hours of simulation

1 Rim, J., Pinsky, P., & Osdol, W. (n.d.). Finite Element Modeling of Coupled Diffusion with Partitioning in Transdermal Drug Delivery. *Annals of Biomedical Engineering Ann Biomed Eng,* 1422-1438.

2 Rim, J., Pinsky, P., & Osdol, W. (2009). Multiscale Modeling Framework of Transdermal Drug Delivery. *Annals of Biomedical Engineering Ann Biomed Eng,* 1217-1229.

Molecular Dynamics Simulations of Hydrogels in Drug Delivery

Jonathan Huang[1], Andrew Wang[2], Di Xu[3], Dr. Dilip Gersappe[3], Dr. Miriam Rafailovich[3]

[1]University High School, Irvine, CA

[2]Taipei American School, Taipei, ROC

[3]Dept. of Materials Science and Engineering, Stony Brook University, Stony Brook, NY

Hydrogels have potent uses in biomedical applications, especially as drug carriers, because of their unique properties and biocompatibility. Understanding the kinetics of drug encapsulation and release is essential in improving the performance and applicability of hydrogels in drug delivery. The porous structure of the hydrogels allows for drugs to diffuse to target sites. However, the effectiveness of hydrogels in carrying and releasing solutes heavily depends on their network structures. Molecular dynamics (MD) is a computational technique that calculates the trajectories and motions of atoms using the classical laws of motion. MD allows us to analyze the behavior of a large number of atoms on a molecular level, a task impossible to perform in a conventional laboratory setting. MD also provides information on the overall polymer network structure.

We use LAMMPS (Large-scale Atomic/Molecular Massively Parallel Simulator), a molecular dynamics simulator, to analyze how the frequency of end monomers along the polymer chain and the bond functionality of crosslinking monomers affect the diffusivity of the solute. Each pair of atoms interacts through forces modeled by the 12-6 Lennard-Jones (LJ) function. We vary the size and shape of the solutes with different number of solvent atoms in simulations. Each simulation is run for 10 million timesteps to allow the system to reach equilibrium, as shown in Figure 1. Mean square displacements of the solute atoms are calculated and used to extrapolate the diffusion coefficient for different sets of parameters.

Figure 1: A molecular visualization of a polymer network with 20 solute atoms (red) generated through the VMD (Visual Molecular Dynamics) program. The end monomers (light blue) have bond functionality 3.

We generate a polymer network with 20 solute atoms added into 1000, 3000, or 6000 solvent atoms. The control value for bond functionality is set to 4 and the control for frequency of crosslinking monomers is every 20. Different simulations have bond functionality 3 and 6 and frequency of crosslinking monomers every 5 and every 10. Overall our results support the classical rubber network theory that as crosslinking density increases, the degree of swelling and diffusivity of the solute decreases. The degree of swelling between 3000 and 6000 solvent atoms did not register a significant difference, suggesting that the polymer network is near saturation at 3000 solvent atoms. Networks with bond functionality 6 and frequency of end monomers 5 are also saturated.

The simulations provide information on the effects of different parameters on the network structure and the overall swelling of solute-carrying hydrogels. Understanding the kinetics of swelling can lead to more practical uses of hydrogels in drug delivery therapies.
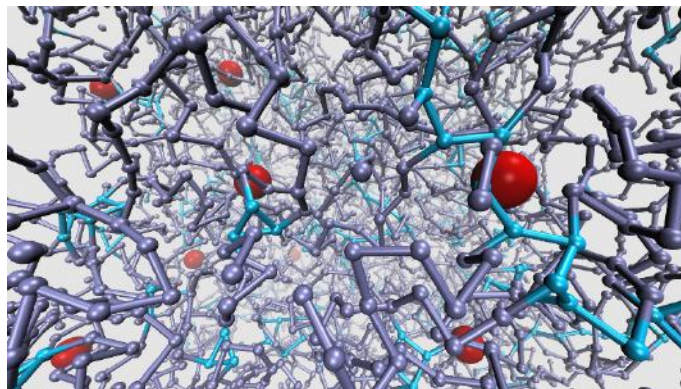
[1] Allen, M. P. Introduction to Molecular Dynamics Simulation. *NIC Series,* **2004**, 23, 1-28.

[2] Hoare, T. R.; Kohane, D. S. Hydrogels in drug delivery: Progress and challenges. *Polymer,* **2008**, 49, 1993-2007.

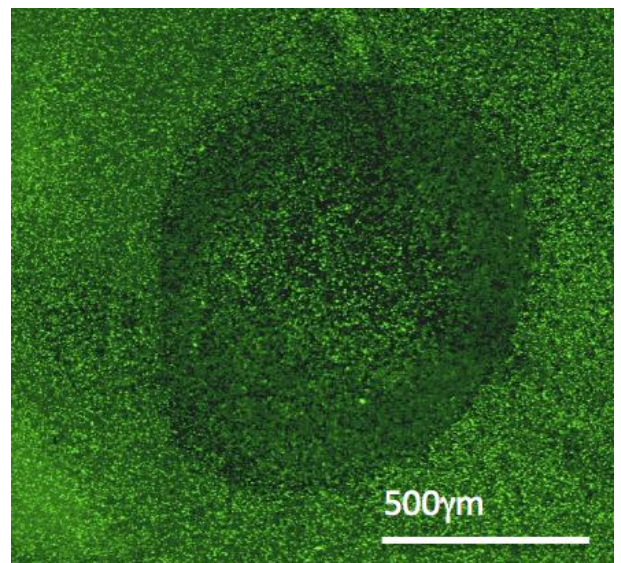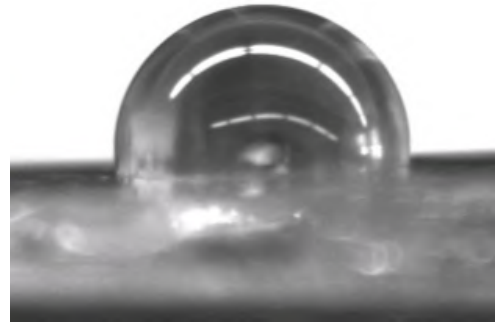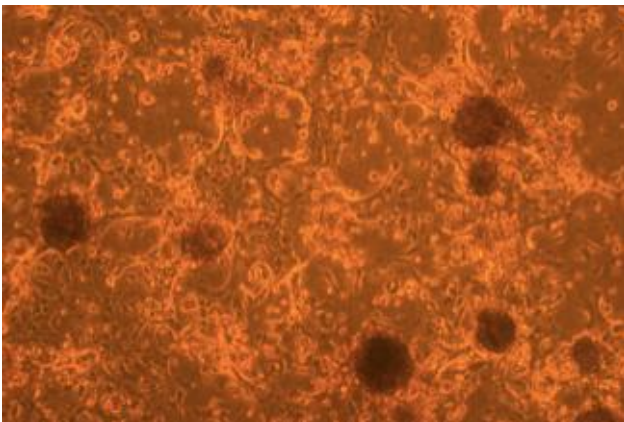[3] Amsden, B. Solute Diffusion within Hydrogels: Mechanisms and Models. *Macromolecules,* **1998**, 31, 8382-8395.

Session 11:   Hydrogels

Clement Marmorat: Graduate Supervisor

Steven Krim, Stony Brook University
Ellyn Anderson, NYU- Poly

"Synthesis and Analysis of novel, Biocompatible, and Biomimetic Nano Graphene-Oxide doped Cross-Linked Hydrogels for Drug Delivery in Squamous Carcinoma"

Arvind Sridhar[1], Clement Marmorat[2], Dr. Marcia Simon[2], Dr. Miriam H. Rafailovich[2]
[1]Bellarmine College Preparatory, San Jose, CA 95126; [2]Stony Brook University, Stony Brook, NY 11794

Tissue engineering and regenerative medicine (TERM) are burgeoning fields which aim to develop novel cures for humanity's most debilitating diseases. In TERM, cells of interest are cultured on scaffolds that promote their attachment, proliferation, and growth, before being implanted into various areas of the human body. Due to the demand for such tissue-engineered constructs, inexpensive, biocompatible, biodegradable, and biomimetic scaffolds are preferable to allow cells to attach and grow into functional tissue. Therefore, natural protein-based scaffold materials are of prime interest compared to artificial, hardly biodegradable synthetic scaffolds. In this study, we engineer and analyze gelatin-based hydrogel nanocomposites doped with nano graphene oxide (nGO) for Skin Tissue Engineering (STE) and further applications. The hydrogels synthesized consist of a gelatin primary component enzymatically cross-linked with Microbial Transglutaminase (MTG) to make them stable at body temperature, as well as additives of nGO to improve the properties of the scaffold. Two different concentrations of MTG (1:25 and 1:125) and 2 different concentrations of nGO (0.01% and 0.001% w/v) were used to synthetized hydrogels. Mechanical properties of the gels were assessed through rheology; highly MTG-concentrated gels (3.6 mg/mL), both with and without nGO, exhibited significantly higher elastic modulus compared to softly-MTG concentrated gels (0.8 mg/ml). Contact angle measurements showed that nGO presence in hard cross-linked gels resulted in significant increase in the scaffolds hydrophilicity and tissue engineering application capability[2]. Differential Scanning Calorimetry (DSC) and Thermogravimetric Analysis (TGA) were also performed and revealed that gels with nGO exhibited a more stable heat release when compared to gels with the same amount of MTG but lacking nGO.
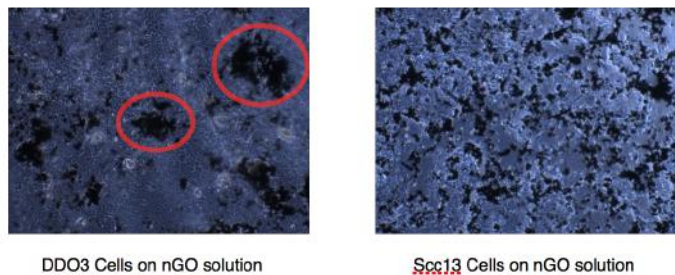

DDO3 Cells on nGO solution   Scc13 Cells on nGO solution

Figure 1. This figure was taken after 24 hours incubation of the cell samples. The red circles in the DDO3 sample (left) encircle large aggregates of nGO particulates in suspension in the media. However, no such aggregates are present in the Scc13 sample (right).

In vitro cell culture of squamous carcinoma keratinocytes (Scc13), normal keratinocytes (DO33), and 3T3 fibroblasts were performed and analyzed on both hard gels and nGO doped hard gels. Preliminary analysis of cells in nGO solution (1 mg/mL) on tissue culture plastic (TCP) after 24 hours of incubation at 37°C revealed that nGO particulates in the media had aggregated in the DO33 culture, but were well dispersed in the Scc13 culture, as shown in **figure 1**. With the Scc13 control culture being confluent, empty spaces in the nGO Scc13 plate indicates cell death. Additionally, 3T3 fibroblasts in the nGO Scc13 co-culture were still attached to the tissue culture plastic, while in the nGO DO33 plate, the keratinocytes had reached confluency, expelled the fibroblasts into the media, caused the fibroblasts to bind to nGO, and therefore cause the nGO to aggregate in the media. Further experimentation proved that nGO binds to and is cytotoxic to human dermal fibroblasts, supporting our hypothesis. These preliminary results suggest that nGO solution inhibits cancerous cell growth while allowing normal cells to proliferate, a finding that can improve the viability of STE from stem cells for clinical applications, as well as drug delivery for squamous carcinoma[1]. Future experimentation involves the optimization of the hydrogel scaffold to reach higher nGO activity and better controlled release kinetics.

[1]Norbert Pallua and Christoph V. Suschek. "Tissue Engineering: From Lab to Clinic." 2011: Berlin, Springer. Page 79.
[2]J. P. Fisher and A. H. Reddi. "Functional Tissue Engineering of Bone: Signals and Scaffolds." 2003: Oulu, Finland, *Topics in Tissue Engineering*. Volume 1, Issue 1. Chapter 5.

Fluorescent Gelatin-based Hydrogels for Analysis of Fibroblast Cell Migration and Cell Traction Forces.

Maho Koga[1], Clement Marmorat[2], Miriam Rafailovich[2]

[1]Ward Melville High School, East Setauket NY 11733, [2]Stony Brook University, Stony Brook NY 11794

Cross-linked gelatin hydrogels are derived from natural proteins which make these gels biocompatible and biodegradable; therefore, an ideal scaffold for tissue engineering. Gelatin natural physical bonds are unstable at body temperature, thus Microbial Transglutaminase (MTG), an enzyme that catalyzes the crosslinking activity of proteins, was used to strengthen and stabilize the gels for physiological conditions applications [1]. As cell migration is an important process affecting a wide range of activities, such as tissue formation during embryonic development, wound healing, development of immune responses, as well as invasion of disease, this process is something that should be studied on scaffolding materials such as hydrogels [2].

In order to study cell migration as well as traction force on these hydrogels, fluorescent particles were homogeneously mixed in with the gelatin. Experimentation was done with beads of particle diameter .03μm and 1μm, and particle concentrations of 25, 40, 50, 90, 100, 150, and 180μL of bead solution were tested. A 25μL of bead solution with beads of 1μm in diameter was found to produce the best image under confocal microscopy (Fig.1a) As a preliminary test, we used a 1% concentration of agarose in DI water gel, and observed the beads movement at the interface between a solidified agarose drop and the hydrogel. We expected that as the agarose 1μL drop on the surface of the hydrogel, stress would be exerted onto the substrate in a circular fashion (Fig.1b and 1c). Previous research has indicated that the cell has localized areas of high stress while attached to functionalized HA substrates [3]. Future research will involve plating fibroblast cells and observing their movement through vectorial mapping analysis (Fig. 1c), as well as assessing cellular migratory and attachment properties on cross-linked gelatin scaffolds.
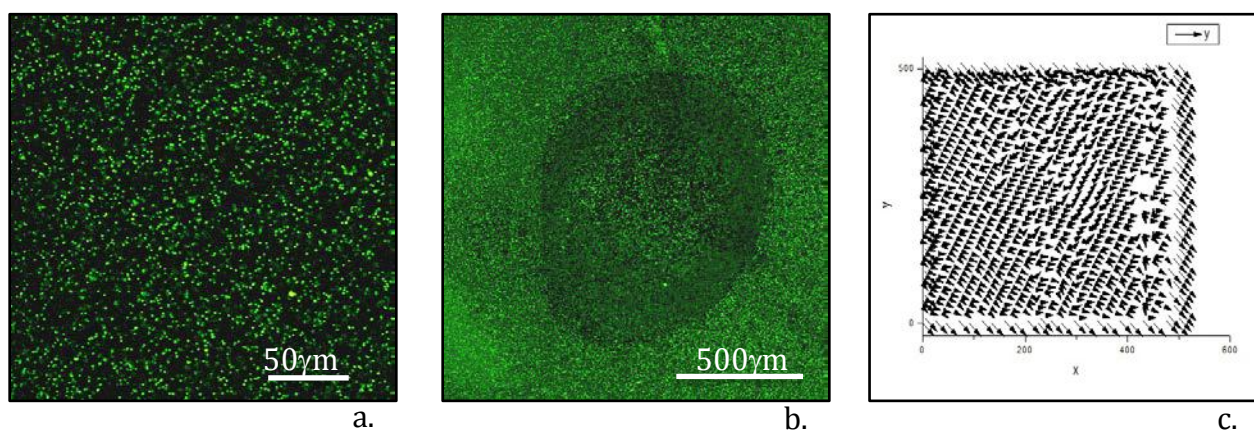

Fig.1. a. 25μL bead concentration gel under 40x confocal microscope. **b.** 2ul Agarose gel drop on 25ul bead solution under 10X magnification **c.** Vector mapping of agarose drop forces between t=0 and t=20minutes on the hydrogel.

[1] Yung, C.W., et al. "Transglutaminase Crosslinked Gelatin as a Tissue Engineering Scaffold." *Journal of Biomedical Materials Research Part A* 83A.4 (2007): 1039-46. *Wiley InterScience*.

[2] Franz, Clemens M., Gareth E. Jones, and Anne J. Ridley. "Cell Migration in Development and Disease." *Developmental Cell* 2.2 (2002): 153-58. *Science Direct*.

[3] Pan, Zhi; Ghosh, Kaustabh; Liu, Yajie; Clark, Richard A.F.; Rafailovich, Miriam H.; "Traction Stresses and Translational Distortion of the Nucleus During Fibroblast Migration on a Physiologically Relevant ECM Mimic." *Biophysical Journal* 96.10(2009): 4286-4298.

"Development of a Hyaluronic Acid Bioink to 3D print Cell Adhesive Scaffolds"

Dessie DiMino[1], Ellyn Anderson[2], Mary Cowman[2], Clement Marmarot[3], Steven Krim[3] and Miriam Rafailovich[3]
[1]Garden City High School, 170 Rockaway Avenue, Garden City, NY 11530
[2]New York University Polytechnic School of Engineering, 6 MetroTech Center, Brooklyn NY 11201
[3]Stony Brook University, Stony Brook NY 11794

Although commonly used in many labs, spin casting fails to generate samples with consistent topographies and porosities. 3D printing is a novel technique that creates more uniform scaffolds. When making scaffolds, synthetic polymers have been favored over natural polymers due to their variability, but natural polymers such as Hyaluronic Acid can aid in cell attachment and differentiation[1]. This experiment aims to generate replicable scaffolds that are naturally better for cell growth. Hyaluronic Acid is a linear polysaccharide found in extracellular matrices (ECM) and intracellularly[2]. In addition, it is found in synovial fluid and aids in tissue differentiation and healing[2]. Due to these characteristics, it is a prime choice for an additive to scaffolds. In this experiment, Hyaluronic Acid (HA) was made into gels in 0.5%, 1% and 1.5% concentrations by weight in water and was methacrylated with DMAEMA and the photoinitiator Igracure 2595. Half of the samples were also tested with 0.01% gelatin to increase cell adhesion.
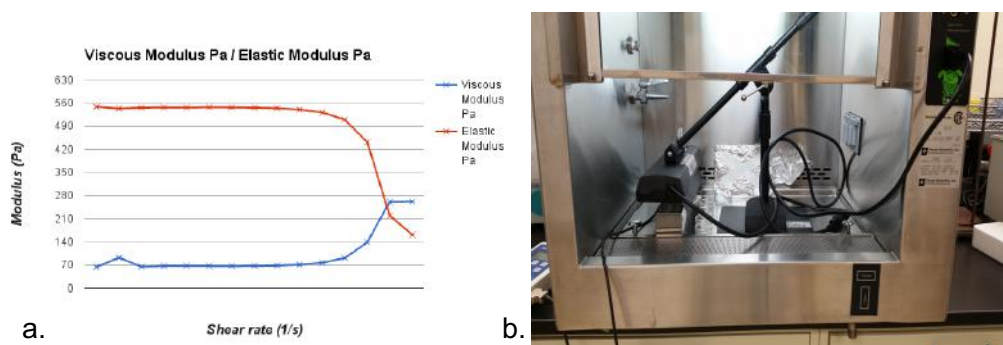

Figure 1.a. Rheogram of a crosslinked 1.5% HA, 1:1 DMAEMA:HA gel, proving gel formation and a stable scaffold. B. Cross-linking setup for the gels with UVB light for 10 min. at 2 mW/cm^2.

It has been observed that the high molecular weight HA (1.7 mDa) creates a much more viscous solution and must be mixed for at least 24 hours at 50 degrees Celsius. After this time the mixture is sufficiently homogeneous and can be crosslinked with a 1:1 ratio of DMAEMA and 2% Igracure. Lower concentrations create less viscous solutions and are also being tested. The 1.7mDa Molecular weight HA creates a solution with a viscosity of 45 cP. DMAEMA was chosen because of its low toxicity, both to cells and the people working with it but it also remains to be seen in a 1:1 ratio is still too toxic for cells to grow. Gels in which HA is mixed homogeneously were tested on the rheometer to determine their elastic modulus and viscous modulus (Figure 1a). Future work includes FTIR analysis to determine the degree of crosslinking after they have dehydrated sufficiently. Gels that are made for plating cells undergo sterilization. The solutions are made and then filtered to remove any bacteria. It was determined that filter size did not affect the success of the crosslinking of the gels. Proper handling of equipment was performed to ensure gels sterility (Figure 1b.) The crosslinked gels were then incubated and swelled in media until ready for cell plating.

In the future, once the viscosity requirements have been met, the samples will be made in a 3D inkjet printer and crosslinked directly on the stage. Additional samples will be tested in the addition of a salt, such as magnesium chloride, to the solution which may decrease the viscosity of the solution. In addition, samples will be plated with dermal fibroblasts, watched for cell growth and judged on their adhesion. Once it has been observed that cells can grow sufficiently on the scaffold, the 3D printer will be used to alter the topography of the scaffold and the various shapes will be monitored for increased growth or differentiation.

[1] Möller, L. (2011). *Preparation and evaluation of hydrogel-composites from methacrylated hyaluronic acid, alginate, and gelatin for tissue engineering* [Scholarly project]. Retrieved July 26, 2015.

[2]Cowman, M. K., & Matuoka, S. (2005, January 10). *Experimental Approach to Hyaluronan Structure*.

Session 12: Sensors

Yingjie Yu: Graduate Supervisor

Matthew Limjoco, Cornell University
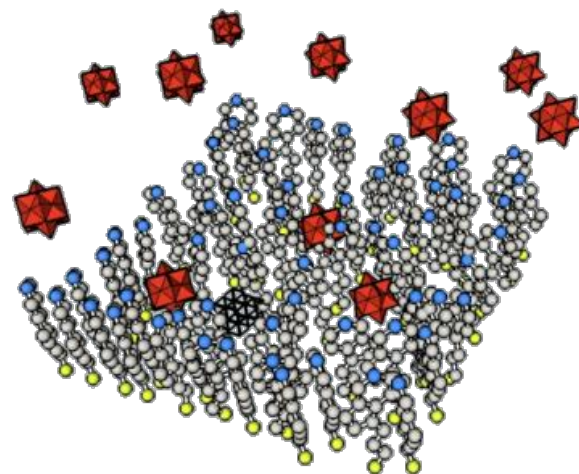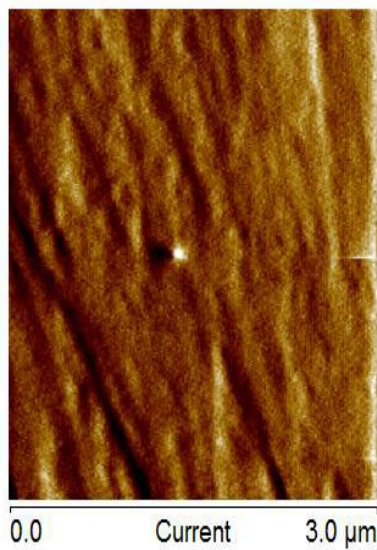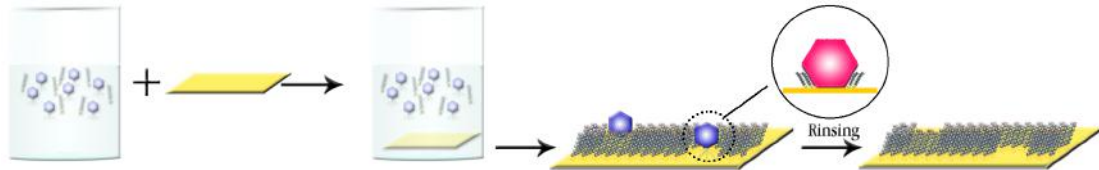
Design of molecularly-imprinted potentiometric sensors for early blood-based detection of liver fibrosis

Yusha Sun[1], Chiho Im[2], Matthew Limjoco[3], Yinjie Yu[4], Miriam Rafailovich[4]

[1] A&M Consolidated High School, College Station, TX 77840, [2] Choate Rosemary Hall, Wallingford, CT 06492
[3] Cornell University, Ithaca, NY 14853, [4] Department of Materials Science and Engineering, Stony Brook University, NY 11794

The discovery of biomarkers for chronic liver disease demands efficient, cost-effective biosensors to predict fibrosis, severe fibrosis, or cirrhosis and assess disease stage. Current methods for disease detection require invasive biopsy and may lead to complications[5]. Even non-invasive, analytical detection of biomarkers such as the use of antibody-based assays are costly and inconvenient. We use self-assembled monolayers (SAMs) in the process of molecular imprinting via a "lock and key" fit between a desired biomolecule and the monolayer surface in the detection of hyaluronic acid, a serum-based glycopolymer which indicates development for liver fibrosis at elevated levels[1, 2]. Previous work has established the sensitivity of molecularly-imprinted surfaces toward proteins such as hemoglobin by imprinting on alkanethiol molecules assembled on a gold-coated silicon surface[1, 2]. Here we demonstrate the effectiveness of the sensor in distinguishing between hyaluronic acid of varying molecular weight and determining solution concentration, which suggests the applicability of the sensor in general detection of polymers as well.

The sensor, consisting of a gold-coated silicon plate in which 11-mercapto-1-undecanol, alkanethiol molecules with hydroxyl groups are bound to the gold through the sulfur-gold bond, produces a SAM with imprinted cavities of HA molecule. The sensor is attached to a potentiometer in solution, which measures a change in sensor potential relative to a reference electrode when HA attaches to the cavities formed.

We evaluated the ability for our sensor to detect HA, specifically HA with molecular weights of 22 kDa and 1.7 MDa. As shown, the potential ΔE changes corresponding to the stepwise additions of different molecular weight HA increased smoothly, then leveled off at a constant value due to saturation of cavities (Figure 1). Due to the nature of the sensor, we model the curve of concentration of substrate molecule versus ΔE with an equation similar to Michaelis-Menten:

$$\Delta E = \frac{E_{\max} [\text{conc}]}{C_M + [\text{conc}]}$$

blue, solid: 22kDa HA
purple, dotted: 22kDa HA, fit
green, solid: 1.7MDa HA
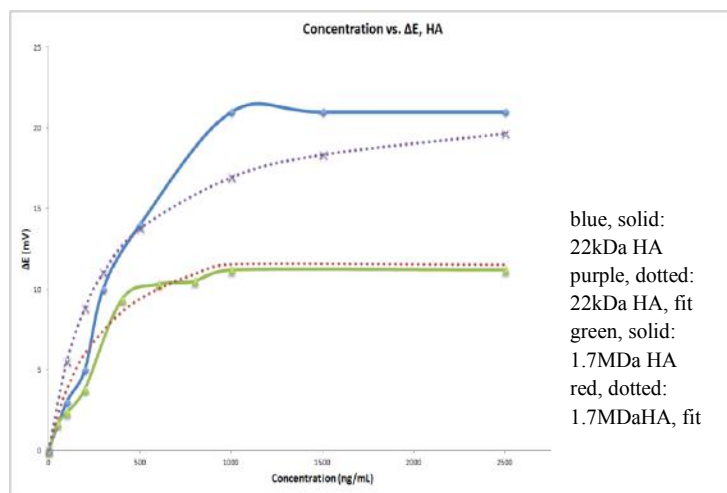red, dotted: 1.7MDaHA, fit

Figure 1. Curves for the concentration of HA in solution versus the ΔE observed. The blue and green curves represent the trials with 22kDa HA and 1.7MDa HA, while the dotted curves represent the rational function fit.

,where Emax represents the maximum ΔE value, C_M represents the concentration at which the ΔE is half of its maximum value, and [conc] is the substrate concentration (Fig. 1). We are then able to predict the concentration of HA in solution given a set change in potential. We also evaluated how specific our response was by cross-incubation of two different HA; the ΔE remained close to 0, which implies that our sensor is able to distinguish between the two weights.

The HA concentration in blood serum of chronic liver fibrosis patients has been shown to be around 2×10^6[3], which fits the high molecular weight sensor we developed[3]. Fibrosis stages 1-5 have HA concentrations of from 17-490 ng/mL, which can conceivably be determined by our sensor[4]. Further work is needed to quantify the detection limit of our HA sensor and to test the sensor on normal and fibrosis patient blood samples.

[1] Y.T. Wang, Y.X. Zhou, J. Sokolov, B. Rigas, K. Levon, M. Rafailovich, A potentiometric protein sensor built with surface molecular imprinting method, Biosensors & Bioelectronics 24 (2008) 162–166.
[2] Yantian Wang, Zhiquan Zhang, Vijay Jain, Jinju Yi, Steffen Mueller, Jonathan Sokolov, Zhenxian Liu, Kalle Levon, Basil Rigas, Miriam H. Rafailovich, Potentiometric sensors based on surface molecular imprinting: Detection of cancer biomarkers and viruses, Sensors and Actuators B 146 (2010) 381-387.
[3] Murawaki Y, et. al, Molecular weight of hyaluronate in the serum of patients with chronic liver disease, Res Commun Mol Pathol Pharmacol. 1998 Feb;99(2):207-16.
[4] V.S. Wong, et. al, Serum hyaluronic acid is a useful marker of liver fibrosis in chronic hepatitis C virus infection, Journal of Viral Hepatitis, 1998, 5, 187–192.
[5]Philippe Halfon, et. al, Accuracy of Hyaluronic Acid Level for Predicting Liver Fibrosis Stages in Patients With Hepatitis C Virus, Comp Hepatol. 2006;5.

Fabrication and Optimization of a Potentiometric Biosensor via pH and Concentration Analysis for the Detection of Hemoglobin

[1]Anthony Zheng, [2]Jeremy Wang
[3]Matthew Dane Limjoco, [4]Yingjie Yu, [5]Dr. Gábor Balázsi, [4]Dr. Miriam Rafailovich,
[1]*Westview High School, OR,* [2]*Syosset High School, NY,* [3]*Cornell University, NY,*
[4]*Department of Materials Science & Engineering, Stony Brook University*
[5]*Department of Biomedical Engineering, Stony Brook University*

In recent decades, research into biosensors has increased due to the biosensors' fast detection and inexpensive components. One type of biosensor is the potentiometric biosensor, which creates an electrical signal by measuring a voltage. In order for a biosensor to be released into the market, its sensitivity and specificity must be confirmed to test the limit of its detection[2]. Current ways of detecting hemoglobin are through mini kits that can cost up to $300.00. Thus, a biosensor for hemoglobin, an essential oxygen transporting protein in vertebrates, was created and optimized. Abnormal formation of hemoglobin have been associated with thalassemia and sickle cell anima, and extreme hemoglobin levels have shown to be related to polycythemia and anemia[1].
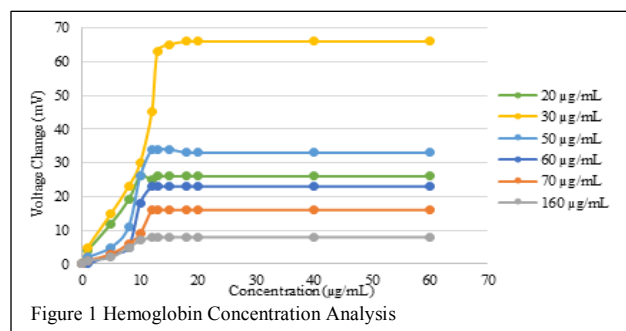

Figure 1 Hemoglobin Concentration Analysis

To create the biosensor, a gold-coated silicon wafer was immersed into a mixed solution of alkanethiol 11-Mercapto-1-undecanol) and the template molecule, hemoglobin in this case. This causes molecular imprinting (MI), where the target molecules create cavities in the thiol self-assembled monolayer (SAM) via hydrophobic interactions and electrostatic forces. The SAM binds to the gold surface via sulfur-metal bonds. After a two to three hours incubation, the template molecules can be washed off the surface of the wafer using deionized water (DI), leaving cavities complementary to Hemoglobin. When the template molecules are injected into a solution of DPBS with the biosensor, an electrochemical signal is created due to the change in voltage between the working and reference electrode. This is measured through a potentiometer.

In order to optimize the biosensor for possible clinical uses, the hemoglobin biosensor was optimized by testing various biosensors at different concentrations and pHs. As seen in Figure 1, the optimal concentration of hemoglobin was determined to be 30 μg/mL. The pH able to perform best was 6.5. In addition, rough and smooth surfaces were tested with Hemoglobin. Smooth gold resulted in better detection. Deviating from the optimal conditions resulted in poor detection of Hemoglobin.

In conclusion, the potentiometric measurements from testing demonstrated that the biosensors were able to detect hemoglobin at the determined optimal pH and concentration. In the future, more research is required to assess the hemoglobin biosensor. This could be done by cross testing the imprinted hemoglobin with misshaped hemoglobin and other proteins. By doing this, the patient would be tested to see if he or she has damaged hemoglobin and lead to further examinations. Future optimization involving optimal imprinting time, optimal thiol concentration, and sensor size could be studied further. Further work includes testing the hemoglobin sensor in human blood serum with living cells.

References

[1] Steinberg, M. H., Forget B. G., Higgs D. R., & Weatherall D. J. (2009). *Disorders of Hemoglobin: Genetics, Pathophysiology, and Clinical Management.* (2nd ed.). Cambridge: Cambridge University Press.

[2] Wang, Y., Zhang, Z., Jain, V., Yid, J., Muellere, S., Sokolov, J., Liuf, Z., Levong, K., Rigash, B., & Rafailovich, M. "Potentiometric Sensors Based on Surface Molecular Imprinting: Detection of Cancer Biomarkers and Viruses." *Sensors and Actuators B: Chemical 146* (2010): 381-87. Print.

Surface Characterization and Engineering of Materials with Electronic Phase Transitions

Eric Chen[1], Aditya Cowsik[2], Mengkun Liu[3], Stephanie Gilbert Corder[3], and John Logan[3]

[1] Aragon High School, San Mateo, CA 94402

[2] Clayton High School, Clayton, MO 63105

[3] Department of Physics, Stony Brook University, Stony Brook, NY 11794

The metal compounds Vanadium Dioxide (VO_2) and Samarium Monosulfide (SmS) undergo an insulator-metal transition (IMT) when a certain degree of heat and pressure respectively are applied. To better understand their properties and possible applications, the materials have been characterized through the use of the Atomic Force Microscope (AFM) and spectroscopy. AFM scans of VO_2 thin films heated to transition temperatures revealed anisotropic, conducting stripes whose width and quantity varied with temperature [1]. Using AFM nanoindentation and lithography techniques [2], we applied intents and scratches to the surfaces of both yttrium doped and undoped SmS samples. Scans and images taken of the experimental regions reveal localized color and conductivity changes where force was applied. Taking the excitation spectrum of a SmS sample in the conductive regime, we discovered a peak at 635nm (Fig 1). These results reveal electrical and optical properties which could lead to the creation of new metamaterials. Other possible applications include pressure/temperature sensors and non-volatile memory systems.
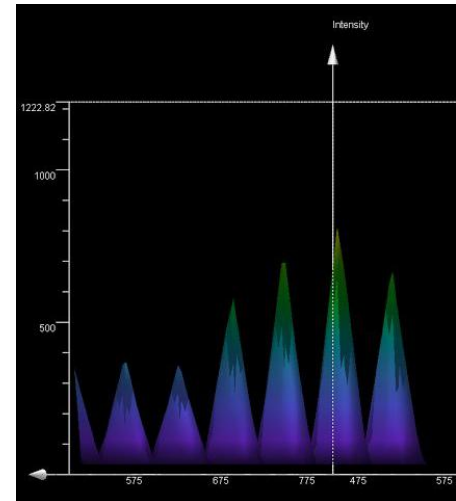

Figure 1: A spectrum of 33% Ytrium doped SmS, revealing peak intensity at a wavelength of 635nm.

[1] M. K. Liu, M. Wagner, E. Abreu, S. Kittiwatanakul, A. McLeod, Z. Fei, M. Goldflam, S. Dai, M. M. Fogler, J. Lu, S. A. Wolf, R. D. Averitt, and D. N. Basov, "Anisotropic electronic State via Spontaneous Phase Separation in Strained Vanadium Dioxide Films." Phys. Rev. Lett. 111, 096602 – Published 29 August 2013

[2] X.N. Xie, H.J. Chung, C.H. Sow, A.T.S. Wee, "Nanoscale materials patterning and engineering by atomic force microscopy nanolithography." Materials Science and Engineering: R: Reports Vol. 54 (1 November 2006): 1-48

Garcia 2k15